

DEVELOPMENT OF A CYCLE DESIGN SOFTWARE
FOR TURBOSHAFT ENGINES

A THESIS SUBMITTED TO
THE GRADUATE SCHOOL OF NATURAL AND APPLIED SCIENCES
OF
MIDDLE EAST TECHNICAL UNIVERSITY

BY

MERT ERK

IN PARTIAL FULFILLMENT OF THE REQUIREMENTS
FOR
THE DEGREE OF MASTER OF SCIENCE
IN
MECHANICAL ENGINEERING

SEPTEMBER 2015

Approval of the thesis:

**DEVELOPMENT OF A CYCLE DESIGN SOFTWARE FOR TURBOSHAFT
ENGINES**

submitted by **MERT ERK** in partial fulfillment of the requirements for the degree of
**Master of Science in Mechanical Engineering Department, Middle East
Technical University** by,

Prof. Dr. Gülbin Dural Ünver
Dean, Graduate School of **Natural and Applied Sciences** _____

Prof. Dr. R. Tuna Balkan
Head of Department, **Mechanical Engineering** _____

Prof. Dr. M. Haluk Aksel
Supervisor, **Mechanical Engineering Dept., METU** _____

Examining Committee Members:

Prof. Dr. Kahraman Albayrak
Mechanical Engineering Dept., METU _____

Prof. Dr. M. Haluk Aksel
Mechanical Engineering Dept., METU _____

Assoc. Prof. Dr. M. Metin Yavuz
Mechanical Engineering Dept., METU _____

Asst. Prof. Dr. Cüneyt Sert
Mechanical Engineering Dept., METU _____

Asst. Prof. Dr. Ö. Uğraş Baran
Mechanical Engineering Dept., TED University _____

Date: 30.09.2015

I hereby declare that all information in this document has been obtained and presented in accordance with academic rules and ethical conduct. I also declare that, as required by these rules and conduct, I have fully cited and referenced all material and results that are not original to this work.

Name, Last Name: Mert Erk

Signature :

ABSTRACT

DEVELOPMENT OF A CYCLE DESIGN SOFTWARE FOR TURBOSHAFT ENGINES

Erk, Mert

M.S., Department of Mechanical Engineering

Supervisor: Prof. Dr. M. Haluk Aksel

September 2015, 98 pages

In this thesis, a computer software for the cycle design of a turboshaft engine is developed. Firstly, a numerical air model was implemented and the model of the turboshaft to be used in the simulation was selected. The first requirement for the software is the capability of performing design point calculations and parametric studies. This feature, which is the initial part of an aircraft engine design, was integrated into the software. At this point, to have a better estimation of the component performances, basic efficiency estimation modules of compressor, combustor and turbines were developed and embedded into the code. After setting the design point of the engine, the software can give insight to the designer about operating at different points from the design point in the operating envelope of the aircraft. In order to accomplish the off-design performance estimations, the map scaling technique was used with the reference maps and matching of the components of the designed turboshaft was programmed with the Newton-Raphson iteration technique. In addition to the off-design performance estimations, the dynamic behavior (transient) estimation module of the software was developed. After all, a GUI (Graphical User Interface) was constructed for the use of each parts of the software in a “user-friendly” environment. The results of the code were compared

with the engine performance data and the commercially available program “GasTurb11” in order to confirm the reliability of the software to perform preliminary engine design studies.

Keywords: Gas Turbine Model, Thermodynamic Matching Model, Turboshaft Simulation, Inlet Distortion Model, Turboshaft Preliminary Design

ÖZ

TURBOŞAFT MOTORLARI İÇİN ÇEVİRİM TASARIM YAZILIMI GELİŞTİRİLMESİ

Erk, Mert

Yüksek Lisans, Makine Mühendisliği Bölümü

Tez Yöneticisi: Prof. Dr. M. Haluk Aksel

Eylül 2015, 98 sayfa

Bu tezde turboşaft motoru çevrim tasarımı için bilgisayar yazılımı geliştirilmiştir. Öncelikle, hava modeli oluşturularak simülasyonlarda kullanılacak turboşaft modeli belirlenmiştir. Daha sonra, yazılımın gereksinimi olan ve hava aracı için ilk ve kritik aşama olan tasarım noktası hesaplamaları ve parametrik çalışma kabiliyetleri programa entegre edilmiştir. Bu noktada, komponent performanslarının olası değerlerine daha iyi yakınsama yapılabilmesi amacıyla, kompresör, yanma odası ve türbinler için temel verimlilik tahmin modülleri geliştirilmiş ve kodun içine eklenmiştir. Tasarım noktası seçildikten sonra yazılımın kullanıcıya, tasarlanan motorun, hava aracının tasarım noktası dışında kalan işletim zarfında nasıl çalışacağı hakkında fikir vermesi gerekmektedir. Bu nedenle, komponent referans haritaları üzerinde harita ölçeklendirme tekniği ile ölçeklendirme özelliği yazılımın içerisine eklenmiştir. Tasarlanan turboşaft motorunun komponentlerin eşleşmesi ise Newton-Raphson iterasyon tekniği ile programlanmıştır. Buna ek olarak, motorun dinamik davranışını tahmin eden ivmelenme modülü geliştirilmiştir. Son olarak, yazılımın her bir modülünden daha “kullanıcı-dostu” bir ortamda faydalanılabilmesi için bir

kullanıcı arayüzü oluşturulmuştur. Yazılımın ön tasarım aracı olarak kullanılabilmesi için gerekli olan güvenilirliği doğrulamak için yazılımın sonuçları da literatürde mevcut motor performans verileri ile ve ticari bir yazılım olan “GasTurb11” ile karşılaştırılmıştır.

Anahtar kelimeler: Gaz Türbin Modeli, Termodinamik Eşleşme Modeli, Turboşaft Simülasyonu, Giriş Akım Bozukluğu, Turboşaft Ön Tasarım, Turboşaft Çevrim Yazılımı

Anneme ve babama ...

ACKNOWLEDGEMENT

First of all, I would like to thank to my family for fully supporting me throughout my educational progress. In addition, special thanks go to my best friend Orhan Ziya for his endless support and encouragement in the difficult times during advancing the educational steps.

I would like to thank my supervisor Prof.Dr. M. Haluk Aksel for his support and guidance throughout this thesis.

I would also like to thank Taylan Ercan and Gökhan Aran for their contribution to have attracted my attention at this part of science and support for understanding key concepts of this thesis topic and guiding me in preliminary design studies and needs of preliminary design tool with their experience in gas turbine industry.

Lastly, thanks also go to my colleagues Emrah Güllü, Mustafa Bilgiç, Ozan Çelik and Burak Gülsaçan for their support, encouragement during this work and aid in the proofreading of this thesis.

TABLE OF CONTENTS

ABSTRACT	v
ÖZ	vii
ACKNOWLEDGEMENT	x
TABLE OF CONTENTS	xi
LIST OF TABLES	xiv
LIST OF FIGURES	xv
LIST OF ABBREVIATIONS	xviii
LIST OF SYMBOLS	xix
CHAPTERS	
1 INTRODUCTION	1
1.1 Gas Turbines and Brayton Cycle	1
1.2 Component Details	10
1.3 Design Methodologies	17
1.4 Modelling of Gas Turbines	18
1.5 Literature Survey	20
1.6 Objectives	24
1.7 Thesis Outline	25
2 ON-DESIGN PERFORMANCE ESTIMATION	27
2.1 Turboshaft Model and Air Stations	27
2.2 Air Model	29
2.3 On-Design Calculations	32
2.4 Parametric Design	37

3	COMPONENT DESIGN PERFORMANCE ESTIMATIONS	41
3.1	Compressor Design Mode.....	41
3.2	Compressor Efficiency Calculation Mode.....	44
3.3	Turbine Efficiency Calculation Mode	48
3.4	Combustor Design Mode	57
4	OFF-DESIGN PERFORMANCE ESTIMATION.....	59
4.1	Map Scaling	59
4.2	Beta-Line Technique.....	61
4.3	Component Matching in Off-Design Calculations	62
4.4	Changing Parameters at Off-Design	64
4.5	Operating Lines.....	65
4.6	Handling Bleed Effects	67
5	SIMULATION OF INLET DISTORTION EFFECTS.....	69
5.1	Methodology	69
5.2	Sample Results and Comparison with GasTurb11	72
6	TRANSIENT PERFORMANCE ESTIMATION.....	75
6.1	Heat Soakage Model	79
7	COMPARISON OF THE DEVELOPED SOFTWARE RESULTS WITH THE LITERATURE.....	81
7.1	Steady – State Performance Comparison.....	81
7.2	Transient Performance Comparison	82
8	CONCLUSIONS AND FUTURE WORK	85
8.1	Conclusion	85
8.2	Future Work.....	86
	REFERENCES.....	89
	APPENDICES	

A. NEWTON-RAPHSON ITERATION METHOD	93
B. SCREENSHOTS OF THE DEVELOPED SOFTWARE	95

LIST OF TABLES

TABLES

Table 2.1 - Air Stations used in the developed software.....	28
Table 2.2 – Dry air property constants	31
Table 2.3 - Kerosene property constants	31
Table 3.1 - Air Stations used in centrifugal compressor efficiency estimation	47
Table 3.2 - Air Stations used in turbine efficiency estimation.....	49
Table 4.1- Comparison of results of the developed software and GasTurb for given sample inputs.....	67
Table 4.2 - Operating line power output comparison of the developed Software and GasTurb11	67
Table 5.1 - Inlet distortion effect on performance	73
Table 7.1 - Comparison of certification data of LHTEC CTS800-4N with model in the developed software.....	82

LIST OF FIGURES

FIGURES

Figure 1.1 - Simple turboshaft engine [1]	1
Figure 1.2 - Air standard Brayton cycle [3]	2
Figure 1.3 - Efficiency versus pressure ratio [2]	4
Figure 1.4 - T - s diagram for compressor [2]	5
Figure 1.5 - Comparison of stage by stage and total temperature rises [2]	7
Figure 1.6 - Forces acting on blades [4]	11
Figure 1.7 - Airfoil angle of attack relative to approaching air [4]	11
Figure 1.8 - Axial compressor velocity triangles [5]	12
Figure 1.9 - Compressor performance map [4]	13
Figure 1.10 - Annular combustor types (forward and reverse flow annular combustors) [5]	14
Figure 1.11 - Combustor parts and sample equivalence ratios [5]	15
Figure 1.12 - Turbine velocity triangles [5]	16
Figure 1.13 – Design sequence of preliminary design [6]	18
Figure 1.14 - Performance simulation models' accuracy versus complexity graph ...	21
Figure 1.15 - Development phase commitments [23]	24
Figure 2.1 - Model of turboshaft engine with power turbine	28
Figure 2.2 - Sample input of design point calculations	33
Figure 2.3 - Sample output of design point calculations with the inputs in Figure 2.2	36
Figure 2.4 - Output of "GasTurb" software with the inputs in Figure 2.2	37

Figure 2.5 - Sample input parameters of parametric design calculation	38
Figure 2.6 - Output of parametric design module with given input in Figure 2.5	38
Figure 2.7 – Results of parametric study example in the same graph.....	39
Figure 3.1 – Main outputs of the developed component performance estimation modules	41
Figure 3.2 - Velocity triangle nomenclature of compressor [3].....	42
Figure 4.1 - Performance characteristics of axial and centrifugal compressors [32].	60
Figure 4.2 - Compressor map and beta lines	62
Figure 4.3 - Off-design matching algorithm	64
Figure 4.4 – Sample output of operating line in compressor map in the developed code	65
Figure 4.5 – Sample output of operating line in HP turbine map in the developed code	66
Figure 4.6 – Sample outputs of operating line in power turbine map in the developed code	66
Figure 4.7 - Handling bleed effect on operating line	68
Figure 5.1- Inlet distortion output of the developed software.....	72
Figure 5.2 - GasTurb11 output with inlet distortion	73
Figure 6.1 - Transient matching algorithm.....	76
Figure 6.2 - Sample output of transient performance on component maps	77
Figure 6.3 - Sample output of transient performance - output figures of Tt4 and Ncorr	78
Figure 6.4 - Comparison of Tt4 and GG spool speed of GasTurb11 and the developed software	78
Figure 7.1 - HP turbine inlet temperature versus time elapsed	83
Figure 7.2 - Power turbine inlet temperature versus time elapsed.....	83
Figure A.1 – Newton-Raphson method.....	93

Figure B.1 - TEImep home page.....	95
Figure B.2 - TEImep turbine module.....	96
Figure B.3 - TEImep parametric study	96
Figure B.4 - TEImep operating line sample result.....	97
Figure B.5 - TEImep transient sample screenshot	97
Figure B.6 - Transient sample map result	98

LIST OF ABBREVIATIONS

CFD	Computational Fluid Dynamics
VIGV	Variable Inlet Guide Vane
NGV	Nozzle Guide Vane
ISA	International Standard Atmosphere
MDO	Multidisciplinary Design Optimization
HPT	High Pressure Turbine
PT	Power Turbine
GUI	Graphical User Interface
SFC	Specific Fuel Consumption
AIP	Aerodynamic Interface Plane
FAA	Federal Aviation Administration
TEImep	Developed Program – TEI Modelling and Estimation of Gas Turbine Performance
OEI	One Engine Inoperative Power Rating
COEI	Continuous One Engine Inoperative Power Rating

LIST OF SYMBOLS

a	Speed of Sound (m/s)
	Distorted Section Angle ($^{\circ}$)
	Absolute Flow Angle ($^{\circ}$)
β	Customer Bleed Air Percentage (%)
γ	Specific Heat Ratio
ϵ_1	High Pressure Turbine Nozzle Guide Vane Cooling Air Percentage (%)
ϵ_2	High Pressure Turbine Rotor Cooling Air Percentage (%)
η	Efficiency (%)
η_c	Cooling Effectiveness
η_{zc}	Isentropic efficiency with zero tip clearance
μ	Dynamic Viscosity (Pa.s)
	Head Coefficient
π_i	Pressure Ratio of Gas Turbine Component i
ρ	Density (kg/m^3)
τ	Fuel Pump Time Constant (s)
τ_i	Enthalpy Ratio of Gas Turbine Component i
ϕ	Temperature Dependent Portion of Entropy (kJ/kgK)
	Stage Flow Coefficient
Ω	Burner Loading ($\text{kg}/(\text{s atm}^{1.8}\text{m}^3)$)
A	Area (m^2)
c_p	Specific Heat Capacity (kJ/kgK)

cer	Compressor Efficiency Decrease Rate with Relative Clearance
DC	Pressure Distortion Coefficient
DT	Temperature Distortion Coefficient
e	Polytropic Efficiency (%)
EPR	Exhaust Pressure Ratio
f	Fuel to Air Ratio
h	Specific Enthalpy (kJ/kg)
h_{HT}	Heat Transfer Coefficient (W/m ² K)
htr	Hub to Tip Radius Ratio
HT_{const}	Heat Transfer Constant (W/K)
$HSTC$	Heat Soakage Time Constant (s)
$(h_i)_{in}$	Enthalpy of the gas entering the component i
$(h_i)_{out}$	Enthalpy of the gas leaving the component i
I	Polar Moment of Inertia of High Pressure Spool (kg.m ²)
	Work Input Coefficient
	Combustion Intensity (kW/atm m ³)
K_{cool}	Cooling Constant
k_{inp}	Loss Correction Factor
L	Combustor Loading ((kg/s) / (atm ^{1.8} m ³))
L_c	Length of the Combustion Chamber (m)
LHV	Lower Heating Value of Fuel (kJ/kg)
\dot{m}	Mass Flow Rate (kg/s)
M	Mach Number
n	Stage Number
N	Rotational Speed (rpm)

P	Pressure (Pa)
PR	Pressure Ratio
pr	Stage Pressure Ratio
Pr	Reduced Pressure
POT	Power Off-take (kW)
$(P_{ti})_{in}$	Total pressure of the gas entering the component i
$(P_{ti})_{out}$	Total pressure of the gas leaving the component i
\dot{Q}	Heat Transfer Rate (kW)
Q_0	Compressor Volumetric Flow Rate (m ³ /s)
R	Gas Constant (kJ/kgK)
	Degree of Reaction
Re	Reynolds Number
rtc	Relative Tip Clearance
swp	Speed-work Parameter
T	Temperature (K)
T^*	Temperature (K) divided by 1000
t	Elapsed Time (s)
t_{res}	Residence time (s)
U	Impeller Speed (m/s)
UP	Unbalanced Power on Shaft (kW)
V	Absolute Flow Velocity (m/s)
V_c	Volume of the Combustor (m ³)
W	Relative Flow Velocity (m/s)
\dot{W}	Power (kW)
w	Mass Flow Rate (lbm/s)

WF Fuel Flow Rate (kg/s)

Subscripts

a Axial Component

θ Whirl Component

b Burner

b1 Customer Bleed Flow

b2 High Pressure Turbine Nozzle Guide Vane Cooling Air

b3 High Pressure Turbine Rotor Cooling Air

c, comp Compressor

corr Corrected to Standard Day Conditions

cool Cooling

d Diffuser

Design value of the engine to be designed

des Design point

e Exhaust

h High Speed Spool

Hub

i Any component of turboshaft engine

md Design value of the reference maps

m Value of the interested point for scaling

Mechanical

Mean-Line

max Maximum

m1 Mixer 1 (High Pressure Turbine Nozzle Guide Vane Cooling)

m2 Mixer 2 (High Pressure Turbine Rotor Cooling)

<i>n</i>	Nozzle
<i>p</i>	Power off take Spool
<i>r</i>	Ram
<i>rel</i>	Relative
<i>ro</i>	Rotor
<i>s</i>	Stage
<i>st</i>	Stator
<i>std</i>	Standard Day Conditions
<i>t</i>	Total Property, Tip
<i>tH</i>	High Pressure Turbine
<i>tL</i>	Power Turbine
<i>turb</i>	Turbine
<i>VD</i>	Vaned diffuser
<i>VLD</i>	Vaneless diffuser
Superscripts	
'	Ideal Process

CHAPTER 1

INTRODUCTION

1.1 Gas Turbines and Brayton Cycle

Gas turbine engines are the engines that are widely employed in aircrafts and industrial plants. It has three main parts which are the compressor, combustion chamber and turbine. The most simplified versions of gas turbines are turbojet and turboshafts. The schematic of a turboshaft is given in Figure 1.1.

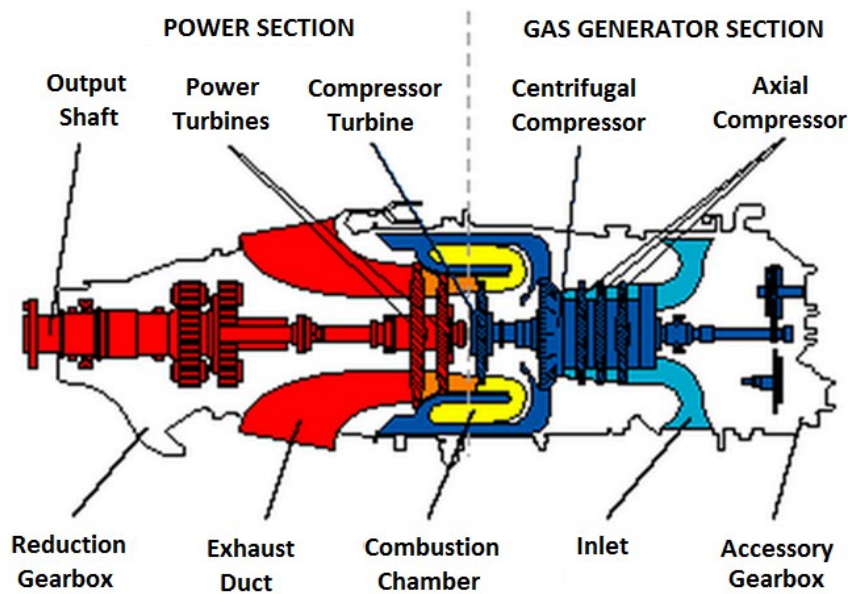


Figure 1.1 - Simple turboshaft engine [1]

Basic operation begins by increasing the air pressure using a compressor towards the combustion chamber. Fuel is then injected into the high pressure air in the combustion chamber where the combustion process occurs. After combustion, acquired high energy flow is converted into mechanical energy by expanding the flow to a lower pressure in a turbine. This drained energy is used to operate the

compressor. There is a remaining energy that is obtained when the fuel is more than required to rotate only the compressor. Since the main purpose of an engine is to produce more power than the amount required just to rotate the compressor, this is a must [2]. This remaining energy of the flow is used to produce thrust by increasing the air velocity in the nozzle. Industrial or helicopter applications differ at this point since there is no need for thrust. In these cases, an additional turbine extracts the remaining energy of the flow and its shaft is connected to the location where the mechanical power is required.

Gas turbine operations can be best modeled by a Brayton cycle. The simplest Brayton cycle approach uses the assumption of an air-standard model and gives an idea about the fundamental operation of this cycle.

1.1.1 Ideal Cycle

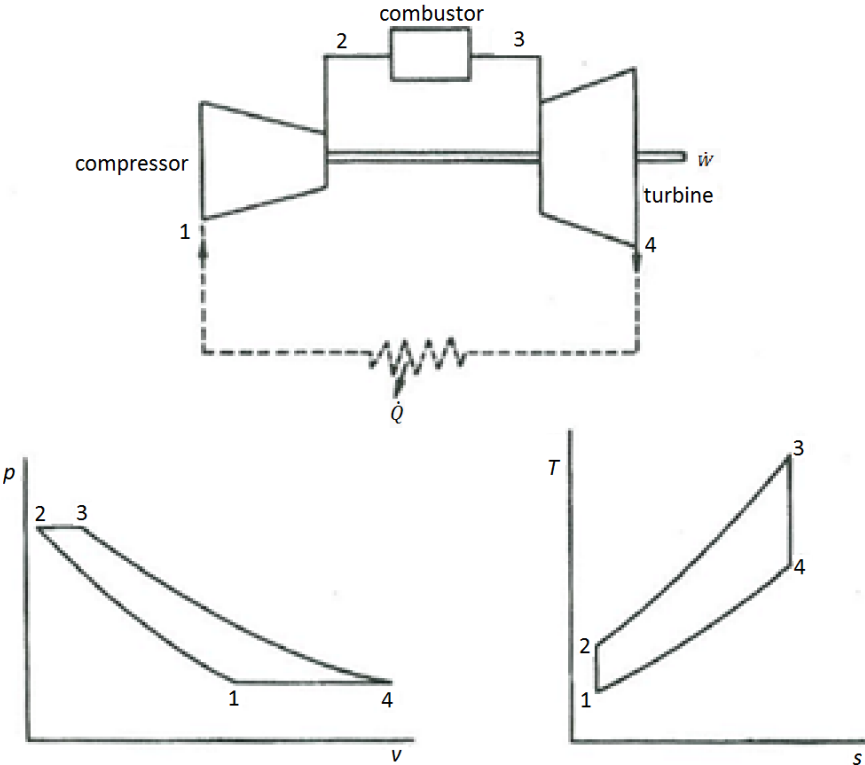


Figure 1.2 - Air standard Brayton cycle [3]

The schematic representation of an air standard cycle of turbojet engine and the corresponding $p-v$ and $T-s$ diagrams are given in Figure 1.2. Assuming that there is no bleed, compressor and turbine powers can be found as [3]

$$\dot{W}_{comp} = \dot{m}_2(h_{t2} - h_{t1}) \quad (1.1)$$

$$\dot{W}_{turb} = (\dot{m}_2 + \dot{m}_f)(h_{t3} - h_{t4}) \quad (1.2)$$

where \dot{W}_{comp} is the compressor power, \dot{W}_{turb} is the turbine power, \dot{m} is the mass flow rate of operating gas, \dot{m}_f is the fuel flow rate and h_t is the total enthalpy of the operating gas. In addition, numbered subscripts denote the corresponding air stations as seen in Figure 1.2.

Net total power output for this type of gas turbine is

$$\dot{W}_{cycle} = \dot{W}_{turb} - \dot{W}_{comp} \quad (1.3)$$

where \dot{W}_{cycle} is the net total power output.

Combustion is modeled in this simple cycle with heat addition and the amount of the heat addition is given by

$$\dot{Q}_{23} = \dot{m}_f LHV = (\dot{m}_2 + \dot{m}_f)h_{t3} - \dot{m}_2 h_{t2} \quad (1.4)$$

where \dot{Q}_{23} is the heat addition rate at combustor whereas LHV is the lower heating value of the fuel.

The resulting efficiency of the cycle can be defined as

$$\eta_{cycle} = \dot{W}_{cycle} / \dot{Q}_{23} \quad (1.5)$$

Furthermore, if the specific heats are assumed to be constant throughout the cycle (gas is calorifically and thermally perfect), if the air flow rate is assumed to be much more than the fuel flow rate and finally if the compressor and turbine efficiencies are assumed to be 100%, the cycle efficiency can be written as [3]

$$\eta_{cycle} = 1 - \frac{1}{PR_{comp}^{\frac{\gamma}{\gamma-1}}} \quad (1.6)$$

where PR_{comp} is the pressure ratio of the compressor and γ is the specific heat ratio of the operating gas.

This formula can be represented in an efficiency versus pressure ratio graph as shown in Figure 1.3.

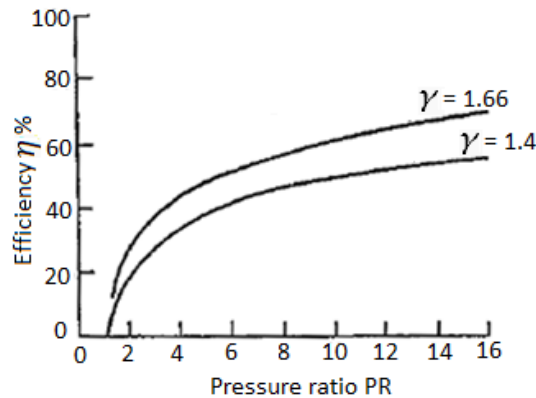


Figure 1.3 - Efficiency versus pressure ratio [2]

Another important parameter for a turboshaft engine is the specific fuel consumption. It is defined by the ratio of the fuel consumption of the engine over the delivered shaft power. Specific fuel consumption, *SFC*, can be expressed in formulation as

$$SFC = \frac{\dot{m}_f}{\dot{W}_{cycle}} \quad (1.7)$$

where \dot{m}_f is the fuel consumption of the turboshaft engine.

Moving on to actual cycles rather than ideal cycles requires the discussion and explanations about efficiency definitions for the fundamental components of gas turbines and pressure losses. This enables the understanding of the actual cycle behavior.

1.1.2 Actual Cycle

In the actual cycles, there are sources of losses that degrade the performance of the gas turbine engine. The irreversible process in compressors and turbines, the pressure losses in the burner and the ducts are the examples of these losses. In order to understand the basics of these losses, it is required to investigate the gas turbine components in detail.

1.1.2.1 Efficiencies of Compressors and Turbines

The ratio of the actual to the ideal work transfers is the efficiency definition for any machine. The ideal process in turbomachines is isentropic since turbomachines essentially operate in an adiabatic way [2].

Taking the stagnation properties into account, the isentropic efficiency for a compressor is defined as

$$\eta_{comp} = \frac{\Delta h'_t}{\Delta h_t} \quad (1.8)$$

where $\Delta h'_t$ is the enthalpy change for ideal compression whereas Δh_t is the change in enthalpy in actual compression.

For a perfect gas,

$$h_t = c_p T_t \quad (1.9)$$

where c_p is the specific heat capacity and T is the temperature and subscript t denotes the total (stagnation) property of the working gas.

Because of the assumption of constant c_p , the Equation (1.8) can be rearranged by using air station numbers, which are defined in Figure 1.2, as

$$\eta_{comp} = \frac{T'_{t2} - T_{t1}}{T_{t2} - T_{t1}} \quad (1.10)$$

where T'_{t2} denotes outlet temperature under ideal compression in compressor and η_{comp} is the isentropic compressor efficiency. The actual and ideal processes for compressor can be shown in T - s graph in Figure 1.4.

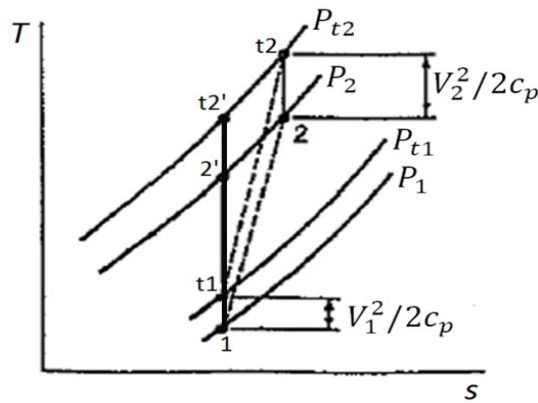


Figure 1.4 - T - s diagram for compressor [2]

Besides, the isentropic turbine efficiency is defined as

$$\eta_{turb} = \frac{\Delta h_t}{\Delta h'_t} \quad (1.11)$$

where η_{turb} is the isentropic turbine efficiency.

It is the reciprocal of η_{comp} given by Equation (1.8) since turbines operate to absorb energy from the operating gas. Rewriting the above equation with the assumption of constant c_p and using the same station numbers given in Figure 1.2, one can obtain

$$\eta_{turb} = \frac{T_{t3} - T_{t4}}{T_{t3} - T'_{t4}} \quad (1.12)$$

where T'_{t4} denotes the outlet stagnation temperature under ideal expansion in turbine.

It should also be noted that, for an isentropic process [2]

$$\frac{P_{t2}}{P_{t1}} = \left(\frac{T_{t2}}{T_{t1}} \right)^{\frac{\gamma}{\gamma-1}} \quad (1.13)$$

where P is the pressure of operating gas. Using Equation (1.13), the exit temperature of a compressor can be obtained in terms of the inlet total temperature, isentropic efficiency and pressure ratio as

$$T_{t2} = T_{t1} \left\{ 1 + \frac{1}{\eta_{comp}} \left[\left(\frac{P_{t2}}{P_{t1}} \right)^{\frac{\gamma-1}{\gamma}} - 1 \right] \right\} \quad (1.14)$$

Similarly, for turbines, the exit temperature can be found by using

$$T_{t4} = T_{t3} \left\{ 1 - \eta_{turb} \left[1 - \left(\frac{P_{t4}}{P_{t3}} \right)^{\frac{\gamma-1}{\gamma}} \right] \right\} \quad (1.15)$$

Another widely used efficiency definition is the polytropic efficiency. In cycle parametric studies with varying pressure ratios, a question arises about whether fixing the values of the compressor and turbine isentropic efficiencies is a logical way or not. Since it is found that the isentropic efficiency of the compressor tends to decrease with increasing pressure ratio whereas the turbine isentropic efficiency tends to increase with it [2]. Therefore, the main reason for defining polytropic efficiency is to remove this controversy.

Assuming that the compressor has a certain number of stages and isentropic efficiency of each stage is constant, the increase in the overall total temperature rise can be given by

$$\Delta T_t = \frac{1}{\eta_s} \sum \Delta T'_{ts} \quad (1.16)$$

where subscript s denotes stage whereas $'$ denotes that the process is an ideal one. Using the definition of the isentropic efficiency for a compressor given in Equation (1.8) with the assumption of constant c_p , the overall total temperature rise is

$$\Delta T_t = \Delta T'_t / \eta_{comp} \quad (1.17)$$

Combining Equations (1.16) and (1.17) yields

$$\frac{\eta_s}{\eta_{comp}} = \frac{\sum \Delta T'_{ts}}{\Delta T'_t} \quad (1.18)$$

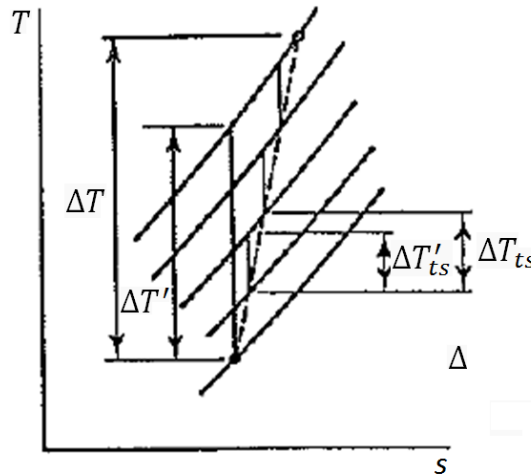


Figure 1.5 - Comparison of stage by stage and total temperature rises [2]

It can be seen from Figure 1.5 that $\sum \Delta T'_{ts}$ is larger than $\Delta T'_t$. This implies that η_s is larger than η_{comp} and the difference between them increases as the pressure ratio increases. The physical interpretation can be given as follows: friction in one stage requires more work in the next stage which can be termed by 'preheat' effect [2]. This approach can be used in turbines and it results in $\eta_{turb} > \eta_s$.

The isentropic efficiency of each stage during the compression process is assumed to be constant and it is defined as the polytropic efficiency. In formulation,

$$e_{comp} = \frac{dT'_t}{dT_t} = constant \quad (1.19)$$

where e_{comp} is the polytropic efficiency of the compressor.

For an isentropic process,

$$\frac{T_t}{P_t^\gamma} = constant \quad (1.20)$$

So that

$$\frac{dT'_t}{T_t} = \frac{\gamma - 1}{\gamma} \frac{dP_t}{P_t} \quad (1.21)$$

Combining Equations (1.20) and (1.21)

$$e_{comp} \frac{dT_t}{T_t} = \frac{\gamma - 1}{\gamma} \frac{dP_t}{P_t} \quad (1.22)$$

Integrating this equation between the inlet and the exit of the compressor results in

$$e_{comp} = \frac{\ln\left(\frac{P_{t2}}{P_{t1}}\right)^{(\gamma-1)/\gamma}}{\ln\left(\frac{T_{t2}}{T_{t1}}\right)} \quad (1.23)$$

This equation can be used for finding the polytropic efficiency by using the measured values of the total pressure and temperature at the inlet and the exit of the compressor. The polytropic efficiency can be related to the isentropic efficiency using Equations (1.10) and (1.23) as

$$\eta_{comp} = \frac{\left(\frac{P_{t2}}{P_{t1}}\right)^{(\gamma-1)/\gamma} - 1}{\left(\frac{P_{t2}}{P_{t1}}\right)^{(\gamma-1)/\gamma e_{comp}} - 1} \quad (1.24)$$

A similar procedure can be applied for the expansion process in turbines and the resulting equation relating the isentropic efficiency of the turbine to the turbine polytropic efficiency can be obtained as

$$\eta_{turb} = \frac{1 - \left(\frac{P_{t4}}{P_{t3}}\right)^{e_{turb}(\gamma-1)/\gamma}}{1 - \left(\frac{P_{t4}}{P_{t3}}\right)^{(\gamma-1)/\gamma}} \quad (1.25)$$

where e_{turb} is the polytropic efficiency of the turbine.

1.1.2.2 Pressure Losses

Pressure losses in ducts and inlet sections of engines should be introduced for actual cycles. These losses are mainly due to friction and curvatures along the path of operating gases which significantly affect the engine performance. In addition, burner pressure losses should be accommodated in the actual cycle modelling due to the aerodynamic resistance of flame stabilizing- mixing devices and momentum changes produced by exothermic reaction [2].

1.1.2.3 Mechanical Losses

Friction and windage in bearings are the main source of mechanical losses in a gas turbine. A mechanical efficiency of 98 to 99 percent can be used for the estimation of the performance of actual cycles.

1.1.2.4 Variation of Specific Heat

For real gases in normal operation conditions, the specific heat value can be approximated to be dependent only on temperature. The assumption of constant specific heat results in some error in cycle calculations which degrades the performance estimation. In order to overcome this issue, a gas model, which will be explained in next chapter, is introduced into the developed code and the air properties are updated with respect to the temperature of working gas at each station.

1.1.2.5 Bleeds

In gas turbines, an increase in the exit temperature of the combustion chamber results in higher thermal efficiency and lower specific fuel consumption. However, limitations in materials because of metallurgical reasons direct the engine manufacturers to cool the materials. Besides, state of the art coatings or metallurgical improvements in materials are used in turbine blades. The turbine cooling air bleed is extracted from the compressor discharge air due to its high pressure which enables a

cooling operation without external power requirements. Mixing of the cooling air with the main stream air is modeled with no pressure loss in the developed software and the temperature calculations will be given in detail in the next chapter.

Another bleed usage is termed as customer bleed extraction and it may be used for aircraft cabin pressurization. Usually discharge air at the exit of the compressor is used as modeled in the developed software.

In addition, handling bleed may also be needed in the gas turbine applications. Handling bleeds can be extracted from the interstage or the discharge air passing through the compressor depending on needs. Briefly, it is used to ease the concerns on the phenomenon of surge in compressors.

1.2 Component Details

In order to have a broader understanding of how the engine behaves in different conditions, a deeper investigation of the gas turbine components is needed. With this aim, details of the main components will be introduced in this section.

1.2.1 Compressors

The high pressure air in gas turbines are provided by the compressor and its performance is generally presented by plotting the pressure ratio against the corrected airflow. These plots are used in the cycle off-design calculations and will be mentioned in detail later. Mainly, two types of compressors are used which are centrifugal and axial compressors. The axial compressor is used at medium and high power applications whereas the centrifugal compressors are used in low powered gas turbines. The compressor operation in both types is limited due to the phenomena of ‘stall’ (or surge) and ‘choking’ (or Stone Wall) at certain conditions of airflow, pressure ratio and rotational speed [4].

Airflow over airfoil exerts forces on blades and they can be separated into components as in Figure 1.6.

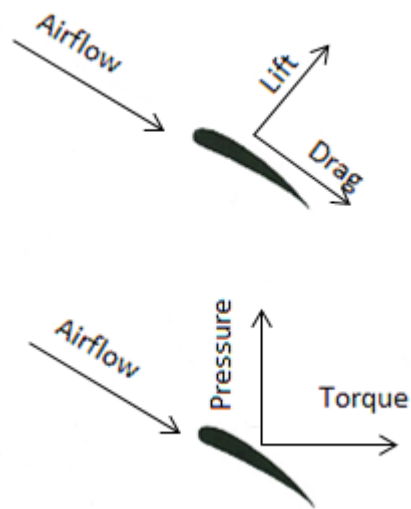


Figure 1.6 - Forces acting on blades [4]

Looking from the aerodynamic perspective, two important parameters strongly affect the successful operation of a compressor which are the angle of attack of the airfoil and the speed of the airfoil relative to the approaching air.

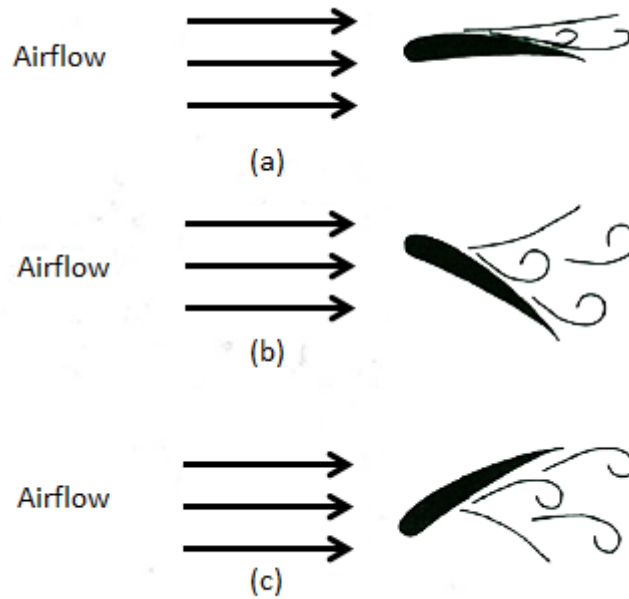


Figure 1.7 - Airfoil angle of attack relative to approaching air [4]

It can be seen in Figure 1.7b that, for large positive angle of attacks may result in the flow not following the convex surface of the airfoil. In another case (Figure 1.7c), large negative values of the angle of attack may result in separation from concave

surface of the airfoil. The drag increases for both of these cases. Furthermore, excessive speeds may result in shock waves and increase in drag force on blade as well [4].

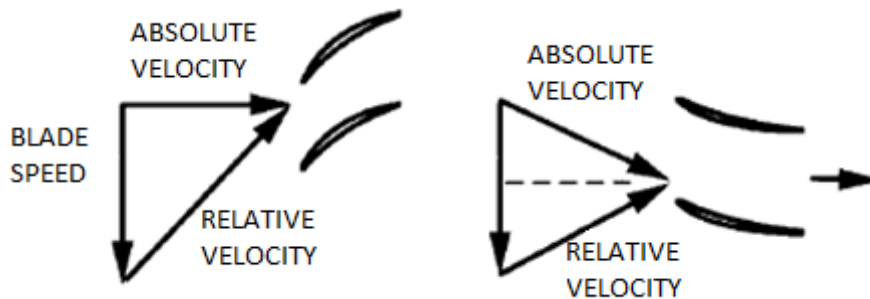


Figure 1.8 - Axial compressor velocity triangles [5]

In Figure 1.8, it is possible to see how the velocity components are defined. The power required to operate the compressor can be estimated via these triangles with the help of Euler turbine equation, which will be illustrated in the component efficiency estimation section.

The point of stall is defined as the incidence at which the airfoil loss coefficient doubles its minimum value. In multistage compressors, stalled operation is acceptable up to a certain degree. To illustrate, front stages of the compressor may stall at low speeds whereas steady state operation is possible at rear stages. Moreover, if stall increases its intensity, compression operation may result in surge phenomenon, which is the point that blades cannot support the adverse pressure gradient and instantaneous breakdowns in the flow. A sudden action such as opening the bleed valves or reducing the fuel flow should be applied to prevent the breakdown of the engine and/or flameouts [5].

As the flow is increased in the compressor at constant speed, no dynamic impact such as stall occurs but the operation is very inefficient at these points. In addition, the operation at these points will result in high temperatures in the turbine.

With these limitations, the compressor performance can be presented by plotting the pressure ratio against corrected airflow for a number of corrected speed lines and efficiency islands as shown in Figure 1.9.

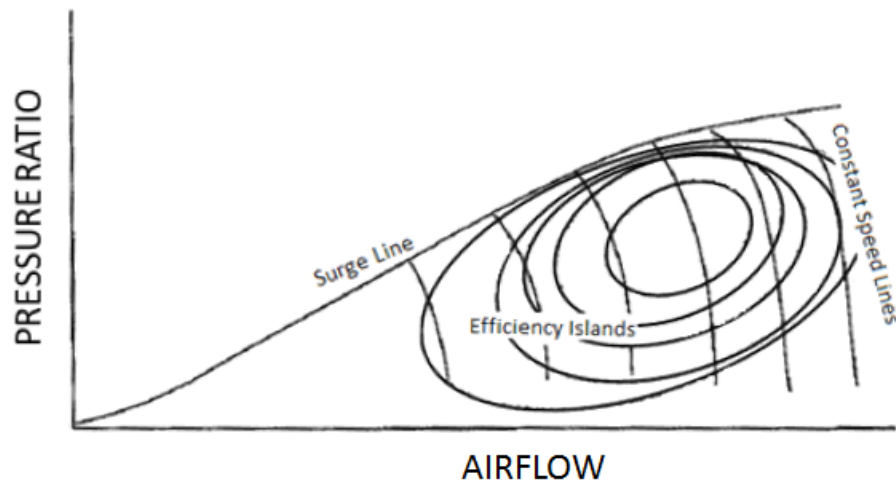


Figure 1.9 - Compressor performance map [4]

The main reason lying under the usage of the pressure ratio versus corrected airflow plots is explained in reference [2] in detail. To briefly explain, the main parameters that affect the operation of the compressor are diameter, speed, airflow, total pressure and temperature at the inlet and the exit of the compressor. After applying Buckingham-Pi theorem, the resulting non-dimensional parameters are the total pressure ratio, total temperature ratio, corrected airflow and corrected speed. Total temperature ratio can be related to total pressure ratio by the isentropic efficiency definition. Therefore, the resulting four parameters are completed by using the isentropic efficiency rather than using the temperature ratio. The total pressure ratio and the corrected airflow are selected as the vertical and horizontal axis respectively whereas the numbers of corrected speeds are plotted on the compressor performance map. Isentropic efficiency contours are also placed on the plot to finalize the presentation of the compressor performance. Furthermore, it should be noted that the turbine maps are generated in the same way that the compressor maps are generated.

1.2.2 Combustion Chamber

Combustion chamber (or burner) is the component in which the chemical energy of the fuel is converted into thermal energy in gas turbines. With the increasing usage of Computational Fluid Dynamics (CFD) in the design of the combustion chamber, the complex flow in these components can be optimised to obtain the maximum efficiency. Different of types of combustors exist and the most widely used ones in

aircraft applications are the forward and the reverse flow annular combustors. The can-annular type combustor can be seen schematically in Figure 1.10.

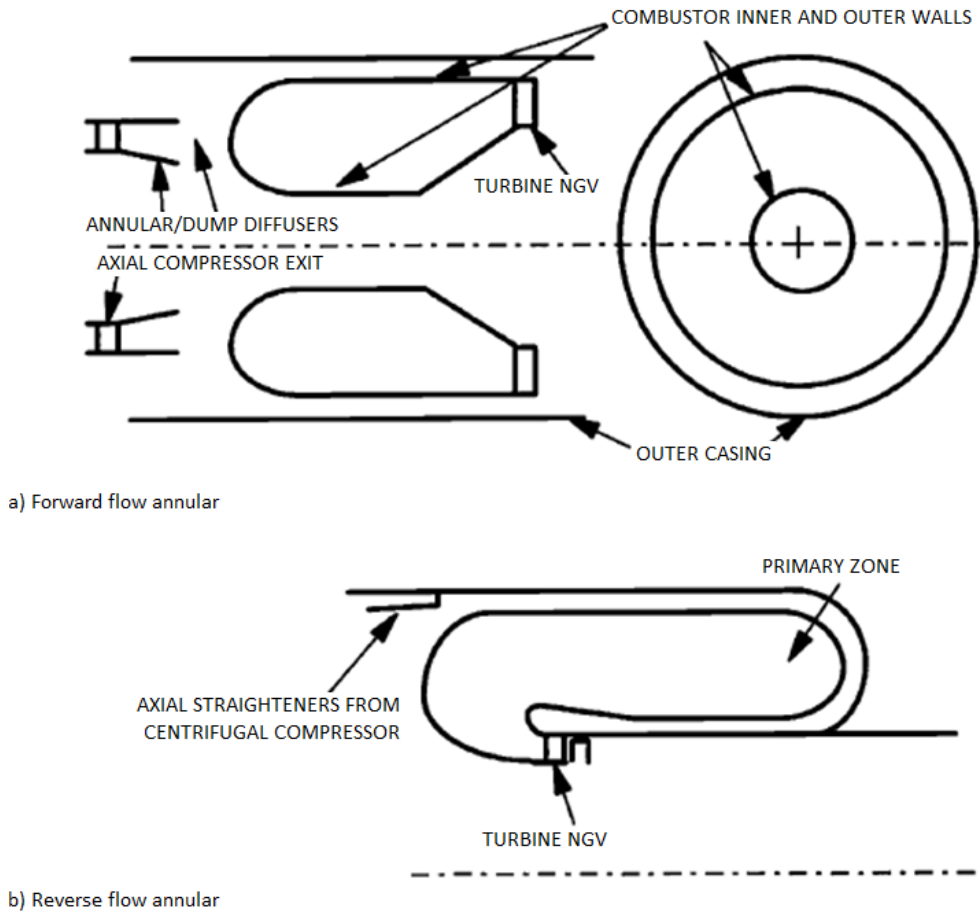


Figure 1.10 - Annular combustor types (forward and reverse flow annular combustors) [5]

Before examining how the combustion occurs in gas turbines, it is helpful to investigate the main sections of the combustion chamber. Mainly, the combustion chamber is divided into three parts which are primary, secondary and tertiary zones. These zones are shown in Figure 1.11.

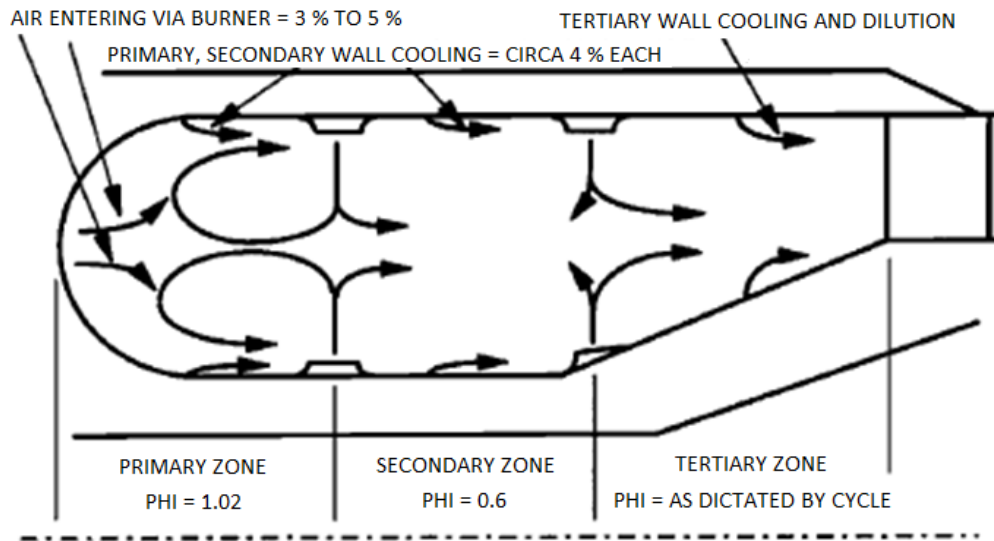


Figure 1.11 - Combustor parts and sample equivalence ratios [5]

Operation of the combustor needs airflow with a low velocity so that the burning operation continues steadily and sufficient time exists for the combustion process. Since the core (primary zone) temperatures are extremely hot to be directed to the turbine, nearly half of the main flow of air is used only for cooling this hot core. In the secondary zone there is some combustion process as well but with the help of the fresh air, equivalence ratio decreases rapidly. In the tertiary zone, there is no combustion and the only process is cooling of the air for turbine operation.

There are combustor parameters that affect the cycle performance strongly, namely the combustion efficiency and the combustion pressure loss. Combustion efficiency is the ratio of the fuel burnt to the total fuel input [5]. The latter one is generally presented in percentage loss and is a result of mixing of flows and friction. For small gas turbines like turboshafts, the combustion efficiency of 99.5 - 99.9% and the pressure loss of 3-4% can be taken as standard values.

On the other hand, there are also parameters that are important in the basic sizing of the combustion chamber. These are the combustor loading, the combustion intensity, the residence time, the local Mach numbers, equivalence ratios and outlet temperature distributions. The loading gives the idea about the difference between the expected work and the work capability of the designed chamber whereas the

intensity shows the rate of heat release per unit volume of the combustor. Finally, the residence time is the time required for air to pass through the combustion chamber.

1.2.3 Turbines

Turbines are one of the turbomachines that extract power from working fluid by expanding it from higher to lower pressures. Similar to the compressors, two types of turbines are common, namely axial and radial turbines. However, radial turbines are rather inefficient with respect to the axial ones. In addition, since the pressure ratio of the inlet and the exit is favorable and not adverse as in the compressor, it is possible to reach much higher pressure ratios in one stage. Due to these reasons, the axial ones are widely used.

Generally, turbines are designed for choked operation in design condition for ease of control of the gas turbine operation. The affecting parameters are the same as the compressors and the parameters of the performance map of the turbines are the same as the compressor namely pressure ratio, isentropic efficiency, corrected flow and corrected speed. However, because of the choked operation in the turbine, the corrected mass flow in the turbine maps are very close to each other throughout the most of the operating envelope. To detect where the turbine operates from the turbine map easier, the horizontal axis is selected as the corrected speed multiplied by the corrected mass flow rather than the corrected mass flow. Furthermore, the velocity triangles can be drawn in a manner similar to the compressors as shown in Figure 1.12.

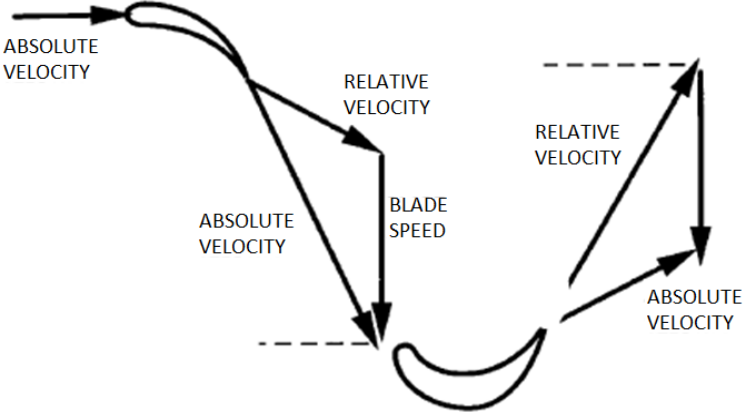


Figure 1.12 - Turbine velocity triangles [5]

1.3 Design Methodologies

The aircraft engine design process starts with the constraint analysis in which the forces on the aircraft such as weight, lift, drag and thrust are examined. The next step is to determine and define the mission profile of the aircraft. Then, it is time to start the design of the specific engine that the aircraft can accomplish the missions that are defined in mission profiles and the engine is capable of overcoming the forces that are examined in the constraint analysis. The objective of this step is to estimate the performance parameters in terms of design limitations, flight conditions and design choices. This is achieved by assuming 1-D flow of a perfect gas with non-ideal efficiencies of engine components. To find an optimum engine for a particular application, the operating point is selected within this step of design process by comparing several numbers of operating points. After this point, the off-design analysis of an engine should be made in order to estimate the engine performance in the flight envelope [6]. From now on, sizing of the determined engine should be made with the aim of estimating the installed performance of the engine. Lastly, the components of the engine such as inlet, exhaust, compressor, turbine and burner must be designed in order to provide the desired power from the engine. This part is known as the engine component design. The design sequence of preliminary design of an engine is shown in Figure 1.13.

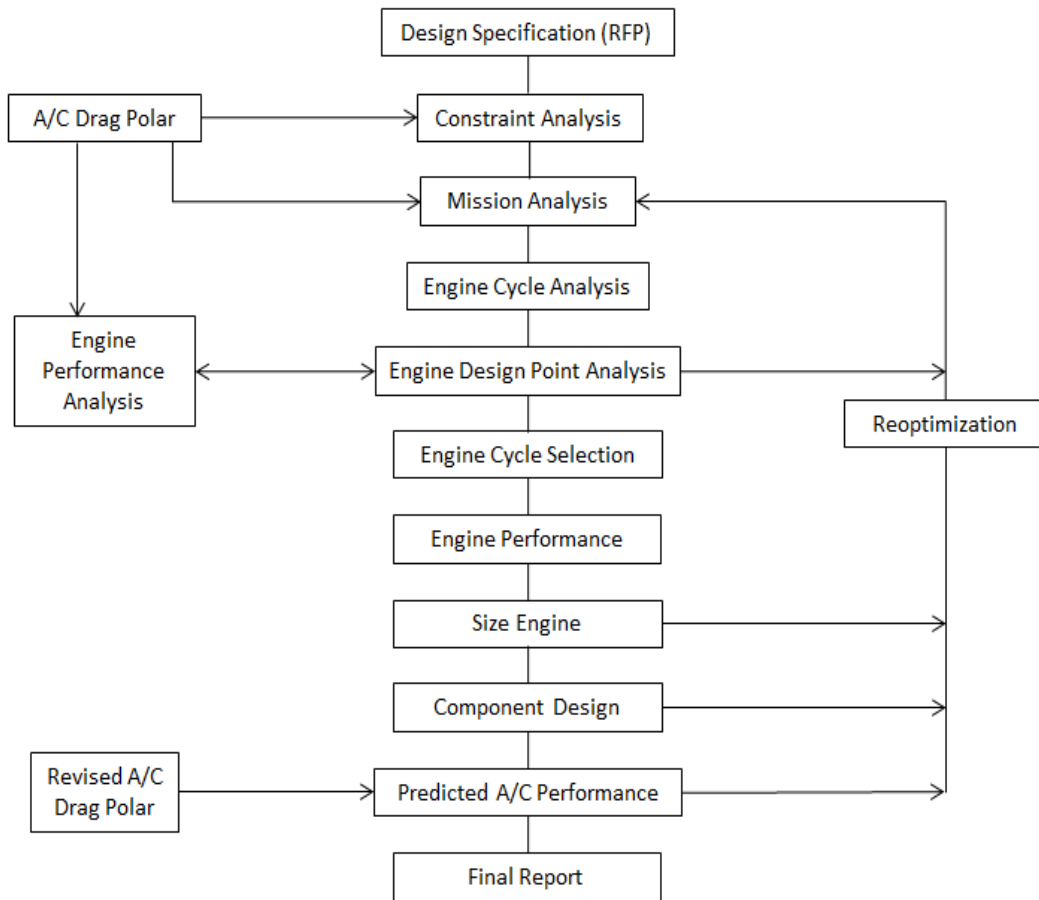


Figure 1.13 – Design sequence of preliminary design [6]

The tool to be developed aims to be capable of performing cycle analysis, parametric analysis for cycle selection and engine steady/unsteady behavior estimations.

1.4 Modelling of Gas Turbines

There are four main matching models according to reference [5] and a brief introduction will be given in this section about these models.

1.4.1 Thermodynamic matching transient performance model

Steady-state matching equations (work and flow compatibility equations) for matching the components are used in this model. The difference that turns the model into transient is the application of an unbalanced power onto the shafts. Fuel flow value, which is provided by the user or the control system of the engine, will be compared with the fuel value coming out from the model with

the specified corrected speed. After matching these two values, next time step calculation is done until the unbalanced power reaches zero. Heat soakage, volume and/or combustor dynamics, which will be mentioned later in this thesis, may be included in order to improve the quality of the simulation. This type of model is the most accurate representation of the transient simulations of engine performance according to reference [5] and the used in:

- Engine control design philosophy
- Control schedule design such as fuel flow, variable inlet guide vanes (VIGVs) etc. in order to maintain safe operation of engine
- Engine transient performance examination during design phase
- Engine performance prediction in some points of operating envelope that it is not practical to test the engine
- Examination of maneuvers that may be expensive or not practical to test

Due to the need of iterations inside the model, rarely the model of this type can achieve real time simulation of the engine performance. Hence, in order to combine with hardware control system of engines, real time models are developed.

1.4.2 Real time aerothermal transient performance model

For matching, a steady state point is run and then the model switches into the transient mode where the model continuously run at points at the intervals of time corresponding to the digital controller update frame. The volumes between the turbomachinery parts of the engine are important in this model and the values at time t is found by previously found dP/dt 's at time $t-1$ calculated by volume dynamics. To explain, the time rate of change of pressure at some sections of the engine are related to the temperature with some constants that are defined specifically for the interested engine. Speeds are also updated with the unbalanced power on the shafts by considering the spool inertias. Component maps are used in order to calculate temperatures. After completing the calculations, the code passes to the next time step and

so, one step of the transient performance is completed. Compared with the thermodynamic matching model, it has significant improvement in execution time; however, the accuracy is lower than that model since no iteration is done during the simulation. This model is often used for the engine control system hardware and flight simulators. To have detailed information about this method, reference [5] can be used as a guide.

1.4.3 Real time transfer function transient performance model

The key performance parameters are related to the fuel flow in this type of model and the time constants to be used must be derived from the outputs of the transient matching model or the engine test data. This model is mostly used in flight simulators due to its simplicity and fast solution capability. Generally, the accuracy is lower than the real time aerothermal transient performance model. In addition, auxiliary system parameters such as oil or starter system can be modelled with this approach in an engine performance simulation.

1.4.4 Real time lumped parameter transient performance model

From test data or aerothermal models of the engine, the matrix of the steady state and the transient performance parameters are generated in this type of model and partial derivatives are obtained with respect to all other parameters. These obtained matrices are used for the simulation of the transients of the engine. This type of model is more favorable to be used in flight simulators but less commonly encountered than the previous model.

1.5 Literature Survey

With the aim of modelling the gas turbine engines, there are a number of studies in the literature. As mentioned in the previous part, the highest accuracy can be reached with the thermodynamic matching transient performance model and the main interest of this thesis is this type of modelling. In reference [7], there is an overview of the performance simulation methods with respect to their complexity and accuracy which can be seen in Figure 1.14.

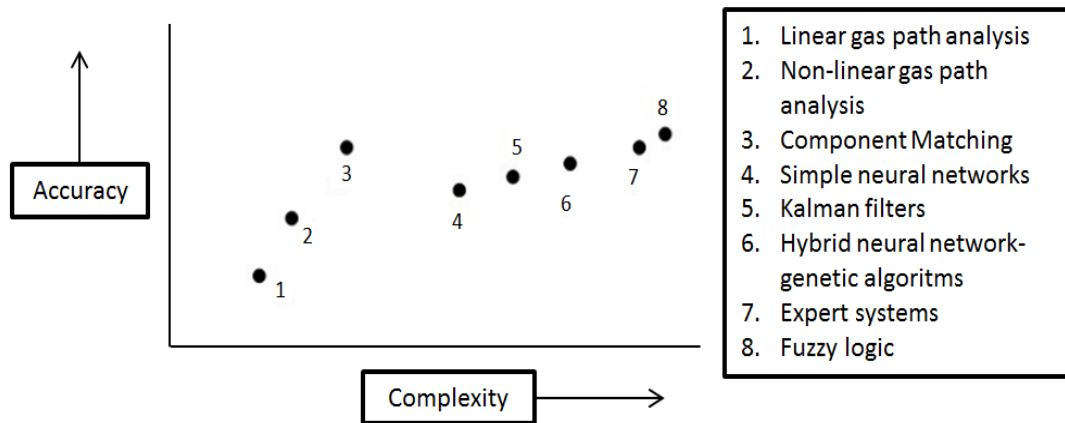


Figure 1.14 - Performance simulation models' accuracy versus complexity graph

Figure 14 illustrates the choice of using component matching model in this thesis and the available sources in the literature about this method will be mentioned at first. In the same reference, gas turbine model is developed with the component map matching and the model is validated by comparison of the results with available literature data. In addition, the interaction between the gas turbine operation and the electrical-thermal systems is investigated with the developed model.

Mostly referenced studies in the thermodynamic matching type of model are executed by, Kurzke, Saravanamuttoo, Walsh and Fletcher. The fundamental equations and approaches are explained at References [5], [8], [9] and [2]. The main idea underlying these references is the same and they concluded that the use of this method is the most practical and accurate way for estimating the gas turbine performance. Furthermore, Kurzke developed a commercial product named as GasTurb which is available for both educational and commercial use. In reference [8], the introduction of this program is mentioned and typical helicopter cycle optimization is stated as the illustration of the usage of GasTurb. It is stated that the code covers all significant aspects of cycle design point selection, off-design and transient operation estimations with reasonably short simulation times.

There are a number of studies which compares the results of GasTurb with experimental data or models of their own such as in references [10], [11], and [12]. In the first one, Kong et al. (2001) developed a performance simulation program for KT-1 turboprop engine. Scaled maps of a similar engine are used in the off-design

and transient simulations and the results are validated by comparing the results with GasTurb and the performance data provided by the engine manufacturer. In the next study, Wemming (2010) conducted a master thesis about the prediction of aircraft performance by using the rubber engine performance model. GasTurb is used for the simulation models and the conclusion is that GasTurb can be used to make accurate engine performance model and can be incorporated to multidisciplinary design optimization (MDO) environment. Lastly, Martinjako (2014) mentioned in his thesis that GasTurb is validated for predicting the performance of LM2500 and Garrett GTCP85-98D.

For the usage in previously mentioned aims such as engine transient performance examination during the design phase, the accuracy is the most important feature of the software instead of the speed of the model. In the case of real time simulation models which is needed by the engine control system, one of the most interested and referenced studies is Ballin's work [13] . This reference paper can be used for the purpose of developing a real-time controller for gas turbine engines. In this study, real-time simulation of T700-GE-700 turboshaft engine is developed with a model of control system based on UH-60A Black Hawk Helicopter. Validation of this study is demonstrated by the comparison of the results with analysis-oriented simulations developed by the manufacturer. In addition to this work, Koçer (2000) developed a real-time model for a small turbojet and investigated the hot-gas ingestion scenario using aerothermal model of T800-LHT-800 turboshaft model [14]. In Novikov's master's thesis (2012) [15], after the development of real-time T700 model, inlet distortion and engine deterioration simulations were demonstrated.

In reference [16], Alexio et al. (2005) described the modelling of a turbofan engine using an object-oriented simulation tool named as EcosimPro. The results are then compared with those models that are accepted by industry and the possible adaptivity feature of the model is demonstrated.

In reference [17], Lazzaretto et al (2001) created gas turbine design and off-design models. In this study, off-design maps were generated with map scaling technique and analytical model was implemented via a commercial equation solver. In addition, the Neural Network Model is presented as an alternative way to analytical modelling.

In reference [18], Shahroudi (1994) participated in a study that aims to obtain a tool in preliminary design phase of a gas turbine based aircraft engine. The software was named as Computer Aided General Engine Design (CAGED) and multivariate Newton-Raphson method is used in obtaining high speed in iterations. Engine models were generated for any engine configuration and variables can be changed in the software with developed graphical user interface (GUI).

In reference [19], Panov (2009) stated that a new Simulink library called GasTurboLib is developed. Using the prepared blocks, the user can create any type of the engine configuration and carry out steady state and transient performance analyses in Simulink. In addition, a control method is developed for full simulation of the engine. To illustrate, engine can be started, operated and shut down in simulations via a governor model. In this referenced paper, demonstration of modeled single and twin shaft engine is available with developed Simulink GasTurboLib library blocks and validated by comparison with the available engine test data.

In reference [20], Garrard (1995) presented his study which is a time dependent simulation of gas turbine engine, named as ATEC (Aerodynamic Turbine Engine Code). The engine operation is simulated by solving conservation equations expressed as one dimensional time dependent Euler equations with additional turbomachinery source terms. Furthermore, the transients can be simulated by combining both implicit and explicit equation solvers inside the program that have the capability of simulating the possible stall in the compressor.

In reference [21], Visser (2014) synthesized the gas turbine performance modelling and simulation available in literature and explained the development of commercial software GSP from beginning to the current version of GSP. Starting from gas turbine performance models, the author introduced the modellings used in GSP and illustrated the applications of the program. In addition, the author stated that this study can be used for an insight for further developments in gas turbine performance modelling.

In reference [22], Janikovič (2010) mentioned that estimation of the life of the engine parts (required due to calculation of operating costs) has become an essential part in

the airline industry due to the growth in competitiveness. The author conducted this study with the aim of developing the needed tool. He added that high fidelity engine models are needed to accurately predict the variations of thermodynamic parameters of engine. Two transient methods, namely rapid transient performance method and thermodynamic matching method are tested in this study. As a conclusion, due to the greater stability and robustness of the thermodynamic matching method, this method is adopted and used in the performance analysis of a gas turbine engine which is needed for estimation of the operating costs.

1.6 Objectives

It should be noted that very important decisions are made during the preliminary design phase of a gas turbine engine. Based on the available technology level, the flow annulus and the bearing arrangement are selected. Hence, most of the necessary resources are committed on completion of the preliminary design phase [23] and the commitments in development phase can be seen in Figure 1.15.

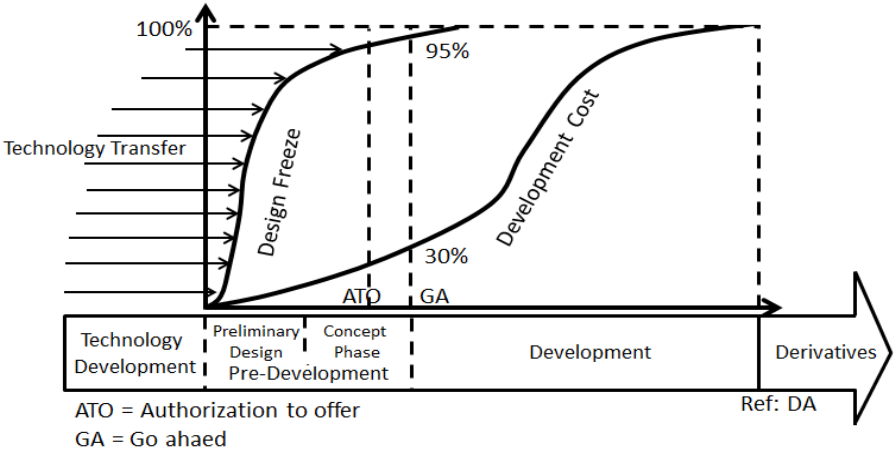


Figure 1.15 - Development phase commitments [23]

The pre-development stage determines the success of the project, since there is no way to return back and change the initial parameters after a certain time. As quick as possible, a good estimation of what the engine will look like and how heavy it will be should be determined.

Making a competitive engine requires high thermal efficiency which results in low specific fuel consumption. The basis of this criterion is strongly dependent on

thermodynamic cycle selection [23]. Therefore, cycle studies have a crucial importance on engine design.

In order to perform cycle studies, a cycle performance estimation program should be used. In this thesis, a computer software is developed in order to achieve a good estimation of turboshaft engine performance in different operating points.

1.7 Thesis Outline

In Chapter 2, the design point analysis mode of the developed software is explained in detail. The turboshaft model used and the numbering of air stations are stated. The developed air model that is used in all of the modules of the software is mentioned in detail. Then, on-design calculations are explained with the definitions before going into details of the parametric design.

In Chapter 3, component performance estimation modules in the software are investigated and detailed calculations are presented. Compressor, turbine and combustor parameters can be calculated via references given in this chapter and these modules lead the designer to set realistic expectations from the main components of the turboshaft and model the cycle by keeping these expectations in mind.

In Chapter 4, off design performance estimation of the modeled turboshaft is discussed. Map scaling and beta line techniques are explained in detail to approximate the off-design behavior of the turbomachinery parts of the engine. After setting the performance maps for the compressors and turbines, the components of the turboshaft engine are matched. The matching procedure is explained in this chapter with using the Newton-Raphson iteration method. Sample results of off-design estimations are then compared with GasTurb11.

In Chapter 5, simulation of inlet distortion effects is discussed and modelling of this phenomenon is explained. Modelling results are then validated with the results of GasTurb11.

In Chapter 6, transient performance estimation methodology is mentioned. After explaining the model used with built-in algorithm, comparison of the results of the software with GasTurb11 is presented.

In Chapter 7, comparison of literature results with the models that are constructed in the developed software is presented. Dividing into two parts, off-design and transient, some of the key parameters are compared with the available data in the literature and the differences between these parameters are stated in a tabulated form.

In Chapter 8, the summary of what has been done in this thesis, their causes and the possible improvements about this study are discussed.

CHAPTER 2

ON-DESIGN PERFORMANCE ESTIMATION

For the design point calculations, the fundamental equations of references [5], [8], [9] and [2] are widely used throughout this chapter. This chapter begins with a turboshaft model and the air station numbering used throughout the chapter and the thesis are indicated in Figure 2.1.

2.1 Turboshaft Model and Air Stations

The model used as a turboshaft engine is a twin-spool configuration with a free power turbine and can be seen in Figure 2.1. The operation begins by sucking ambient air from station 0 to station 1. Through the inlet portion, there are some losses such as friction losses so that the properties of air may change (station 1 to station 2). Then the compressor increases the air pressure towards the combustion chamber (station 2 to station 3). Some bleed air is taken out at the burner exit for turbine cooling and customer usage. Fuel is then injected into the high pressure air in the combustion chamber where the combustion process occurs (station 3.1 to station 4). After combustion, some cooling is required to cool down the nozzle vanes with coolant mixer 1 (station 4 to station 4.1). Then, the high energy flow is converted into mechanical energy by expanding the flow to a lower pressure in a turbine (station 4.1 to station 4.4). This drained energy is used to operate the compressor. Turbine rotor also requires cooling and it is modeled with a coolant mixer 2 (station 4.4 to station 4.5). There is a remaining energy that is obtained when the fuel is more than required to rotate only the compressor. Since the main purpose of an engine is to produce more power than the amount required just to rotate the compressor, this is a must [2]. This remaining energy of the flow is extracted with an additional turbine

(station 4.5 to station 5) and its shaft is connected to the location where the mechanical power is required. At last, the operating gas is thrown out at the station 8.

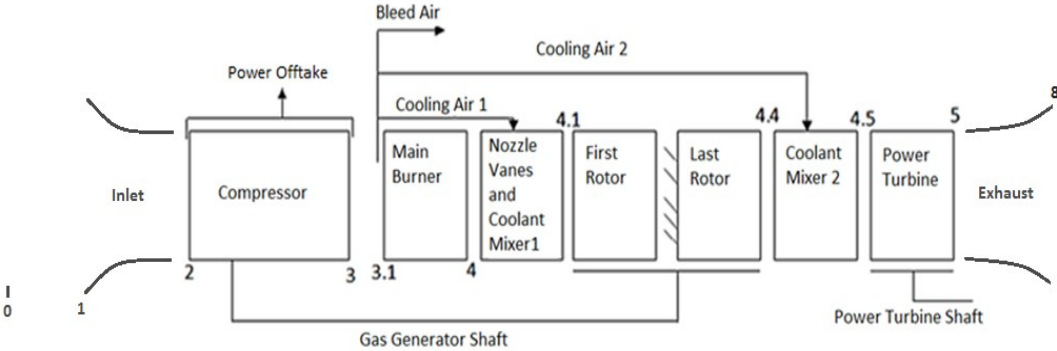


Figure 2.1 - Model of turboshaft engine with power turbine

Stations and locations can be shown in Table 2.1.

Table 2.1 - Air Stations used in the developed software

Station	Location
0	Freestream
1	Inlet or diffuser entry
2	Inlet or Diffuser exit - Compressor inlet
3	Compressor exit
3.1	Burner entry
4	Burner exit - Nozzle vanes entry - Coolant mixer entry
4.1	Nozzle vanes exit - Coolant mixer 1 exit - High pressure turbine entry
4.4	High Pressure Turbine exit - Coolant Mixer 2 entry
4.5	Coolant mixer 2 exit - Power Turbine inlet
5	Power Turbine Exit
8	Nozzle exit

2.2 Air Model

The air model is embedded into software by using formulations of reference [5]. By definition,

$$T^* = T/1000 \quad (2.1)$$

By using temperature (K) and fuel to air ratio, the calculation of the required parameters of the working fluid can be calculated via formulas (2.1) to (2.10).

The specific enthalpy (kJ/kg), h , of the operating gas is calculated by

$$\begin{aligned} h = 1000 & \left(A_0 T^* + \left(\frac{A_1}{2} \right) (T^*)^2 + \left(\frac{A_2}{3} \right) (T^*)^3 + \left(\frac{A_3}{4} \right) (T^*)^4 \right. \\ & + \left(\frac{A_4}{5} \right) (T^*)^5 + \left(\frac{A_5}{6} \right) (T^*)^6 + \left(\frac{A_6}{7} \right) (T^*)^7 + \left(\frac{A_7}{8} \right) (T^*)^8 \\ & + \left(\frac{A_8}{9} \right) (T^*)^9 + A_9 \\ & + \left(\frac{f}{1+f} \right) \left(B_0 T^* + \left(\frac{B_1}{2} \right) (T^*)^2 + \left(\frac{B_2}{3} \right) (T^*)^3 \right. \\ & + \left(\frac{B_3}{4} \right) (T^*)^4 + \left(\frac{B_4}{5} \right) (T^*)^5 + \left(\frac{B_5}{6} \right) (T^*)^6 + \left(\frac{B_6}{7} \right) (T^*)^7 \\ & \left. \left. + \left(\frac{B_7}{8} \right) (T^*)^8 + B_8 \right) \right) \quad (2.2) \end{aligned}$$

The temperature dependent portion of entropy (kJ/kgK), φ , is calculated by

$$\varphi = \int_{T_{ref}}^T c_p \left(\frac{dT}{T} \right) \quad (2.3)$$

Assuming that reference temperature is equal to 0K, the formula for calculation of the temperature dependent portion of entropy is reduced to

$$\begin{aligned}
\varphi = & \left(A_0 \log (T) + A_1 T^* + \left(\frac{A_2}{2}\right) (T^*)^2 + \left(\frac{A_3}{3}\right) (T^*)^3 + \left(\frac{A_4}{4}\right) (T^*)^4 \right. \\
& + \left(\frac{A_5}{5}\right) (T^*)^5 + \left(\frac{A_6}{6}\right) (T^*)^6 + \left(\frac{A_7}{7}\right) (T^*)^7 + \left(\frac{A_8}{8}\right) (T^*)^8 \\
& + A_{10} \\
& + \left(\frac{f}{1+f}\right) \left(B_0 \log (T) + \left(\frac{B_1}{1}\right) T^* + \left(\frac{B_2}{2}\right) (T^*)^2 \right. \\
& + \left(\frac{B_3}{3}\right) (T^*)^3 + \left(\frac{B_4}{4}\right) (T^*)^4 + \left(\frac{B_5}{5}\right) (T^*)^5 + \left(\frac{B_6}{6}\right) (T^*)^6 \\
& \left. \left. + \left(\frac{B_7}{7}\right) (T^*)^7 + B_9 \right) \right) \quad (2.4)
\end{aligned}$$

The specific heat capacity (kJ/kgK), c_p , of the operating gas is calculated by

$$\begin{aligned}
c_p = & \left(A_0 + A_1 T^* + (A_2) (T^*)^2 + (A_3) (T^*)^3 + (A_4) (T^*)^4 + (A_5)(T^*)^5 \right. \\
& + (A_6) (T^*)^6 + (A_7) (T^*)^7 + (A_8) (T^*)^8 \\
& + \left(\frac{f}{1+f}\right) (B_0 + (B_1) T^* + (B_2) (T^*)^2 + (B_3) (T^*)^3 \\
& \left. + (B_4) (T^*)^4 + (B_5) (T^*)^5 + (B_6) (T^*)^6 + (B_7) (T^*)^7) \right) \quad (2.5)
\end{aligned}$$

The gas constant (kJ/kgK), R , of the operating gas is calculated by

$$R = (287.05 - 0.00990f + 10^{-7}f^2)10^3 \quad (2.6)$$

where f is the fuel to air ratio.

The specific heat ratio (kJ/kgK), γ , of the operating gas is calculated by

$$\gamma = \frac{c_p}{c_p - R} \quad (2.7)$$

The reduced pressure, Pr , of the operating gas is calculated by [6]

$$Pr = \exp\left(\frac{\varphi - \varphi_0}{R}\right) \quad (2.8)$$

where $\varphi_0 = 4.810138 \text{ kJ/kgK}$ (2.9)

Lastly, the speed of sound (m/s), a , of the operating gas is calculated by

$$a = \sqrt{\gamma RT} \quad (2.10)$$

There are some cases that input T is not available for these formulas. In this case, Newton-Raphson iteration is performed with an initial guess of the temperature to find the temperature that matches with the input of enthalpy or reduced pressure. Newton-Raphson iteration technique will be explained in Appendix A.

In Ref [5], the defined constants for the calculation of the air model are shown in Table 2.2.

Table 2.2 – Dry air property constants

A_0	0.992313	A_5	7.097112
A_1	0.236688	A_6	-3.234725
A_2	-1.852148	A_7	0.794571
A_3	6.083152	A_8	-0.081873
A_4	-8.893933	A_9	0.422178
		A_{10}	0.001053

In this thesis, kerosene is used as the fuel and the constants related to this fuel are shown in Table 2.3.

Table 2.3 - Kerosene property constants

B_0	-0.718874	B_5	3.081778
B_1	8.747481	B_6	-0.361112
B_2	-15.863157	B_7	-0.003919
B_3	17.254096	B_8	0.0555930

B_4	-10.233795
-------	------------

B_9	-0.0016079
-------	------------

2.3 On-Design Calculations

After creating the sub-functions for calculating the air properties, design point calculations can be made.

Input parameters of the design point mode are as follows:

- Altitude
- Deviation from International Standard Atmosphere (ISA) temperature
- Inlet Mach number,
- Power off-take,
- Customer bleed air percentage,
- High pressure turbine (HPT) nozzle guide vane (NGV) cooling air percentage,
- HPT rotor cooling air percentage,
- Intake pressure ratio,
- Free stream recovery pressure ratio,
- Compressor polytropic efficiency,
- Compressor pressure ratio,
- Burner efficiency,
- Burner pressure percentage loss,
- Lower heating value of fuel,
- HPT inlet total temperature,
- HPT polytropic efficiency,
- Power turbine (PT) polytropic efficiency,
- Exit duct pressure ratio,
- Exhaust pressure ratio,
- Mechanical efficiencies of each shafts in turboshaft model namely offtake, high pressure (HP) and power turbine spools,
- HP spool speed,
- Power turbine spool speed.

The graphical user interface (GUI) of design point calculation inputs can be seen in Figure 2.2.

Inputs					
Altitude :	<input type="text" value="2000"/>	ft	Burner Efficiency :	<input type="text" value="0.99"/>	%
Delta ISA :	<input type="text" value="12"/>	K	Burner Pressure Loss :	<input type="text" value="4"/>	
Inlet Mach No :	<input type="text" value="0.2"/>		Lower Heating Value :	<input type="text" value="43124"/>	kJ/kg
Corrected Air Flow :	<input type="text" value="3.5"/>	kg/s	HP Turbine Inlet Temperature:	<input type="text" value="1450"/>	K
Power Offtake :	<input type="text" value="30"/>	kW	HP Turbine Polytropic Efficiency :	<input type="text" value="0.85"/>	%
Bleed Air Percentage :	<input type="text" value="3"/>	%	Power Turbine Polytropic Efficiency	<input type="text" value="0.87"/>	%
Cooling Air Percentage 1 :	<input type="text" value="0"/>	%	Nozzle Efficiency :	<input type="text" value="1"/>	
Cooling Air Percentage 2 :	<input type="text" value="0"/>	%	Exhaust Pressure Ratio :	<input type="text" value="1.03"/>	
Intake Pressure Ratio :	<input type="text" value="0.99"/>		Offtake Shaft Mech. Efficiency :	<input type="text" value="1"/>	
Free Stream Recovery PR :	<input type="text" value="1"/>		GG Mechanical Efficiency :	<input type="text" value="1"/>	
Compressor Polytropic Efficiency :	<input type="text" value="0.82"/>	%	PT Spool Mechanical Efficiency :	<input type="text" value="0.98"/>	
Compressor Pressure Ratio :	<input type="text" value="13"/>				

Figure 2.2 - Sample input of design point calculations

The link between the temperature and the pressure at the inlet with the altitude is achieved by the formulas of ISA [24] given by

$$T_0 = 288.15 - 6.5 \text{ Altitude}(km) + \Delta T(\text{deviation from ISA}) \quad (2.11)$$

$$P_0 = 101.325 \left(1 - \frac{6.5 \text{ Altitude}(km)}{288.15} \right)^{\frac{(9.80665 * 0.0289644)}{(8.31447 * 0.0065)}} \quad (2.12)$$

The ratio of the total stagnation pressures and the total temperatures between the inlet and the exit of the engine component i are defined as [6]

$$\pi_i = \frac{(P_{ti})_{out}}{(P_{ti})_{in}} \quad (2.13)$$

$$\tau_i = \frac{(h_i)_{out}}{(h_i)_{in}} \quad (2.14)$$

One additional definition is needed for the design point calculations specifically for the turboshaft engine, namely the exhaust pressure ratio

$$\pi_e = \frac{P_{t8}}{P_0} \quad (2.15)$$

It represents the ratio of the total pressure at exhaust to ambient pressure and it is selected by the designer. Mostly, the value of this parameter is in between 1.02 and 1.04. Therefore, it is an input for the developed software since it changes from engine to engine.

Besides, mass flows throughout the engine are

$$\dot{m}_0 = \dot{m}_2 = \dot{m}_3 \quad (2.16)$$

$$\dot{m}_{3.1} = \dot{m}_0(1 - \beta - \varepsilon_1 - \varepsilon_2) \quad (2.17)$$

$$\dot{m}_4 = \dot{m}_0(1 - \beta - \varepsilon_1 - \varepsilon_2) * (1 + f) \quad (2.18)$$

$$\dot{m}_{4.1} = \dot{m}_0((1 - \beta - \varepsilon_1 - \varepsilon_2) * (1 + f) + \varepsilon_1) \quad (2.19)$$

$$\dot{m}_{4.5} = \dot{m}_0((1 - \beta - \varepsilon_1 - \varepsilon_2) * (1 + f) + \varepsilon_1 + \varepsilon_2) \quad (2.20)$$

where β is the customer bleed air percentage, ε_1 is the high pressure turbine (HPT) nozzle guide vane (NGV) cooling air percentage and ε_2 is the HPT rotor cooling air percentage.

The fuel-to-air ratio and the bleed percentages are defined as

$$f = \frac{\text{Burner Fuel Flow}}{\text{Burner Inlet Airflow}} = \frac{\dot{m}_f}{\dot{m}_{3.1}} \quad (2.21)$$

$$\beta = \frac{\text{Customer Bleed Flow}}{\text{Compressor Exit Air Flow}} = \frac{\dot{m}_{b1}}{\dot{m}_{3.1}} \quad (2.22)$$

$$\varepsilon_1 = \frac{\text{HPT NGV Cooling Air Flow}}{\text{Compressor Exit Air Flow}} = \frac{\dot{m}_{b2}}{\dot{m}_{3.1}} \quad (2.23)$$

$$\varepsilon_2 = \frac{\text{HPT Rotor Cooling Air Flow}}{\text{Compressor Exit Air Flow}} = \frac{\dot{m}_{b3}}{\dot{m}_{3.1}} \quad (2.24)$$

The corrected mass flow at any station is calculated by

$$\dot{m}_{corr} = \dot{m} \frac{\sqrt{\frac{T_t}{T_{std}}}}{\frac{P_t}{P_{std}}} \quad (2.25)$$

where \dot{m}_{corr} is the mass flow rate corrected to standard day conditions, T_{std} is the standard temperature 298.15K and P_{std} is the standard pressure 101.325 kPa of a standard day conditions.

The stagnation pressure ratios of the compressor, high pressure and low pressure turbines are dependent on the polytropic efficiencies as

$$\pi_c = \frac{P_{t3}}{P_{t2}} = \left(\frac{Pr_{t3}}{Pr_{t2}}\right)^{e_c} \quad (2.26)$$

$$\pi_{tH} = \frac{P_{t4.4}}{P_{t4.1}} = \left(\frac{Pr_{t4.4}}{Pr_{t4.1}}\right)^{1/e_{tH}} \quad (2.27)$$

$$\pi_{tL} = \frac{P_{t5}}{P_{t4.5}} = \left(\frac{Pr_{t5}}{Pr_{t4.5}}\right)^{1/e_{tL}} \quad (2.28)$$

respectively. Furthermore, as explained in the introduction part, the isentropic efficiency of the compressor and the turbine components are linked with their polytropic efficiencies and the total pressure ratios by using the following formula [2]

$$\eta = \frac{\pi^{\left(\frac{\gamma-1}{\gamma}\right)} - 1}{\pi^{\left(\frac{\gamma-1}{\gamma e}\right)} - 1} \quad (2.29)$$

For burner modelling, the following burner energy balance equation is used,

$$(1 + f) (h_4 - h_{4ref}) + (h_{3ref} - h_3) = f \eta_b LHV \quad (2.30)$$

where *ref* subscript denotes fuel reference temperature which is assumed to be 298.15 K. There would be one additional term if the fuel reference temperature is different than the reference temperature.

There are some important points during the construction of the software that should be kept in mind in order to estimate the design point of a turboshaft engine correctly.

- i. HPT pressure ratio can be found by ensuring energy balance between HPT and compressor as

$$m_2(h_{t3} - h_{t2}) + \frac{POT}{\eta_{mp}} = m_{41}(h_{t41} - h_{t44})\eta_{mh} \quad (2.31)$$

where POT is the power off-take from high pressure spool, η_{mp} is the power off-take shaft mechanical efficiency and η_{mh} is the mechanical efficiency of the spool of the gas generator section of the turboshaft engine.

This formula sets h_{t44} which is needed for the HPT pressure ratio calculation. After finding this value, $Pr_{t4.1}$ and π_{tH} can be obtained. Then, the total pressure at the inlet of the power turbine is calculated by

$$P_{t4.4} = P_{t4.1}(Pr_{t4.4}/Pr_{t4.1}) \quad (2.32)$$

- ii. PT Pressure ratio can be found as

$$\pi_{tL} = \pi_c \pi_{tH} \pi_r \pi_d \pi_b \pi_n \pi_{m1} \pi_{m2} \left(\frac{1}{\pi_e}\right) \quad (2.33)$$

After gathering the formulas and definitions mentioned before together, the design mode of the developed software is generated.

A sample output of design point mode is shown in Figure 2.3.

	m (kg/s)	Tt (K)	Pt (kPa)	mcorr				
amb	3.2547	296.19	94.213	0	Power :	818.768		kW
1	3.2547	298.56	96.879	0	SFC :	0.294403		kg/(kW*h)
2	3.2547	298.56	95.910	3.5000	Fuel Flow Rate :	0.0691899		kg/s
3	3.2547	714.66	1246.8	0	Exit Area :	0.0696641		m^2
31	3.1497	714.66	1246.8	0	Thermal Efficiency :	28.3557		%
4	3.2166	1450	1197.0	0				
41	3.2166	1450.0	1197.0	0.6108				
44	3.2166	1087.9	282.28	0				
45	3.2166	1087.9	282.28	2.2435				
5	3.2166	866.97	97.039	0				
8	3.2166	866.97	97.039	0				
bleed	0.1050	714.66	1246.8	0				
						isentropic eff	polytropic eff	P/P
					Compressor	0.7510	0.8200	13
					Burner	0.9990	0.9990	0.9600
					HP Turbine	0.8709	0.8500	4.2403
					LP Turbine	0.8844	0.8700	2.9089

Figure 2.3 - Sample output of design point calculations with the inputs in Figure 2.2

With the same inputs, the commercially available product “GasTurb” results are shown in Figure 2.4. In this figure, $WRstd$ is the corrected mass flow rate, $PWSD$ is the shaft power, WF is the fuel flow rate, W is the actual mass flow rate, $A\delta$ is the exit area and $Therm\ Eff$ is the thermodynamic efficiency of the designed turboshaft.

Station	W kg/s	T K	P kPa	WRstd kg/s			
amb		296,19	94,215		PWSD	=	818,6 kW
1	3,255	298,56	96,881		PSFC	=	0,2945 kg/(kW*h)
2	3,255	298,56	95,912	3,500	WF	=	0,06695 kg/s
3	3,255	714,30	1246,856	0,416	Therm Eff	=	0,28351
31	3,150	714,30	1246,856		A8	=	0,06964 m²
4	3,217	1450,00	1196,981	0,611			
41	3,217	1450,00	1196,981	0,611			
43	3,217	1087,53	282,330				
44	3,217	1087,53	282,330				
45	3,217	1087,53	282,330	2,243			
49	3,217	866,15	97,042				
5	3,217	866,15	97,042	5,823			
6	3,217	866,15	97,042				
8	3,217	866,15	97,042	5,823			
Bleed	0,105	714,30	1246,856				

Efficiencies:	isentr	polytr	RNI	F/P			
Compressor	0,7509	0,8200	0,908	13,000			
Burner	0,9990			0,960			
HP Turbine	0,8709	0,8500	1,787	4,240			
LP Turbine	0,8845	0,8700	0,586	2,909			
Generator	1,0000						

Figure 2.4 - Output of "GasTurb" software with the inputs in Figure 2.2

When the results are compared, the largest difference is approximately 0.1%, which is a negligible value.

2.4 Parametric Design

In order to select a design point, comparison of different operating points is necessary. As mentioned before, the design point of the engine has to be selected carefully in order not to waste the engine capability by not operating it at its optimum point. Design phase of the components starts immediately after the selection of the design point. As soon as it is selected, large changes in the design point will definitely result in delay in the due date of the engine program and additional costs due to this delay may put the program at a risk of losing lots of money. Therefore, lots of points should be examined in order to fit the design point in the most beneficial way for the user in the operating envelope of the air vehicle. The restrictions are the contractual values which must be provided by the airframer.

In the developed software, there is a possibility of varying any of the two design point inputs by determining the initial value, final value and steps of iteration. Corresponding cycle result in each step will be shown in a carpet plot. The default output graph is the specific fuel consumption versus the shaft power and the parameters represented by the axes can be altered by the user of the software. In addition, it is possible to use the design modes of the rotating components, which gives the user a much more realistic approach than assuming constant component

efficiencies. Sample screenshots of the parametric design mode in the developed software is presented in the Appendix B.

Sample input parameters of the parametric design calculation are shown in Figure 2.5.



Figure 2.5 - Sample input parameters of parametric design calculation

The related output is shown in Figure 2.6.

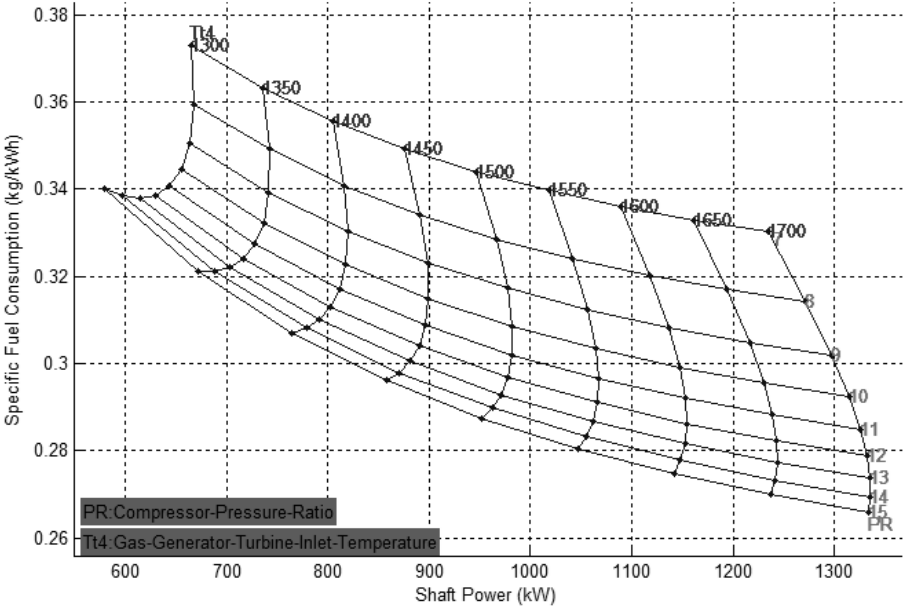


Figure 2.6 - Output of parametric design module with given input in Figure 2.5

There are very small differences between the results of the developed software with “GasTurb” which can be seen in Figure 2.7.

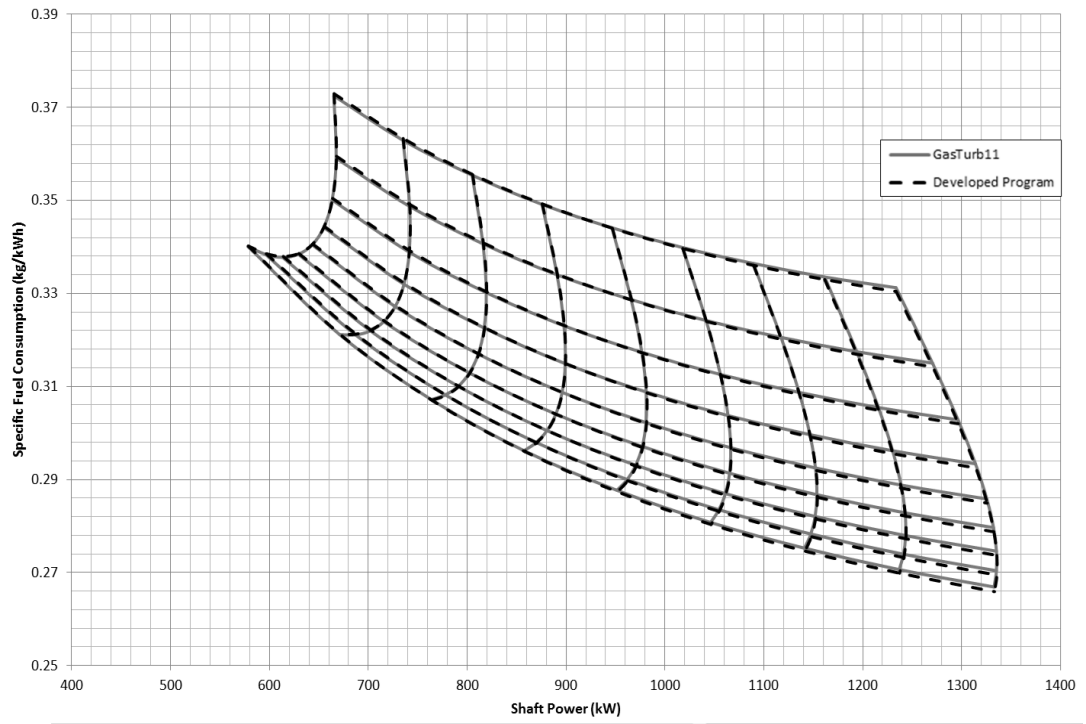


Figure 2.7 – Results of parametric study example in the same graph

CHAPTER 3

COMPONENT DESIGN PERFORMANCE ESTIMATIONS

Component performance estimation is a required feature of a preliminary design tool. The reason is that the component efficiencies should be estimated properly in order to start from a suitable cycle. In this chapter, how the component performances are estimated is explained starting from the compressor. The main outputs of the developed component performance estimation modules can be seen in Figure 3.1.

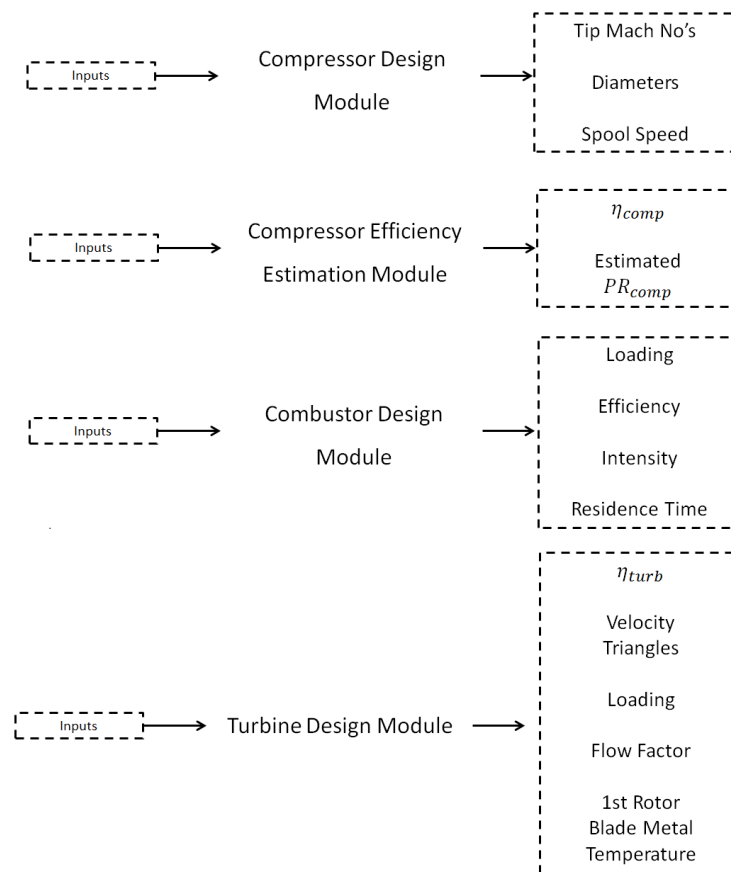


Figure 3.1 – Main outputs of the developed component performance estimation modules

3.1 Compressor Design Mode

Reference [2] is used for the calculation of the compressor design parameters with the velocity triangle nomenclature stated in Figure 3.2.

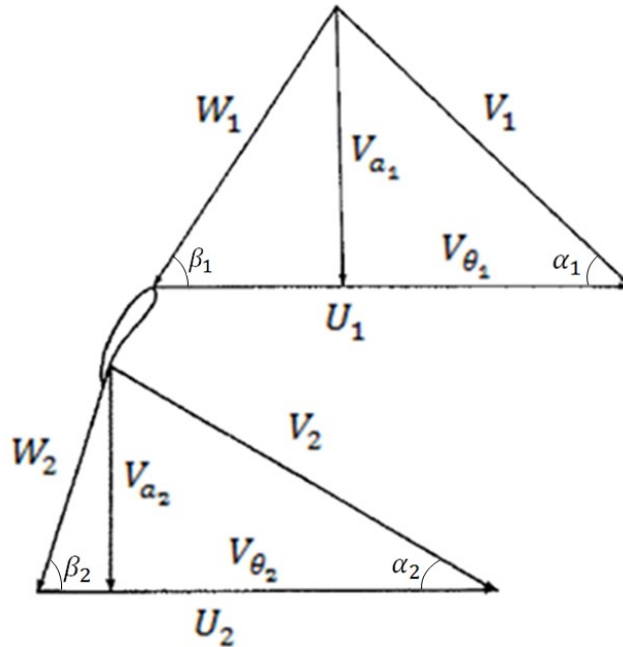


Figure 3.2 - Velocity triangle nomenclature of compressor [3]

3.1.1.1 Inputs

Inputs of the compressor design module are as follows:

- i) Total pressure
- ii) Total temperature
- iii) Tip speed
- iv) Radius ratio
- v) Mach number

3.1.1.2 Calculation procedure

The static temperature at the inlet of the compressor can be found as

$$T_2 = \frac{T_{t2}}{1 + \frac{(\gamma_2 - 1)}{2} M_2^2} \quad (3.1)$$

where M is the Mach number of the working fluid. Similarly, the static pressure at the inlet of the compressor is

$$P_2 = P_{t2} \left(\frac{T_2}{T_{t2}} \right)^{\frac{\gamma_2}{(\gamma_2-1)}} \quad (3.2)$$

While the density of air can be calculated by using the equation of state for a perfect gas,

$$\rho_2 = \frac{P_2}{R_2 T_2} \quad (3.3)$$

where ρ is the density of the working fluid. Corresponding inlet area of the compressor is then:

$$A_2 = \frac{m_2}{\rho_2 V_{a2}} \quad (3.4)$$

and the required tip diameter of the inlet of the compressor is

$$r_{2t} = \sqrt{\frac{m_2}{\pi \rho_2 V_{a2} (1 - htr_2)^2}} \quad (3.5)$$

where r_t is the tip diameter, V_a is the axial velocity and htr is the hub to tip ratio.

Resulting rotational speed with these parameters can be found by

$$N = \frac{60}{2\pi} \frac{U_{2t}}{r_{2t}} \quad (3.6)$$

where U_t is the impeller speed at the tip.

The main output of this mode, which is the rotational speed of the HP Spool, is finally found by applying the above calculations via Equations (3.1) to (3.6). Furthermore, with assuming that there are no inlet guide vanes and the flow enters axially into the compressor, inlet blade height and relative Mach number at the tip can be calculated at the inlet of the compressor by using the following equations. The axial velocity is assumed to be constant everywhere at the inlet. Its value can be found by:

$$V_{a2} = M_2 \sqrt{\rho_2 R_2 T_2} \quad (3.7)$$

Then, the relative velocity at the tip of the inlet of the compressor can be calculated by

$$W_{2t} = \sqrt{V_{a2}^2 + U_{2t}^2} \quad (3.8)$$

where W_t is the relative velocity at the tip. Finally, Mach number at the tip of the compressor inlet is

$$M_{2t} = \frac{W_{2t}}{\sqrt{\rho_2 R_2 T_2}} \quad (3.9)$$

Resulting rotational speed is used in other calculations in the design module of the software if this mode is on.

3.2 Compressor Efficiency Calculation Mode

In the developed software, there are two types of efficiency estimation modes, which are for axial and radial compressors. It is a design choice to construct a turboshaft engine with axial or radial compressors or combining both. Different methods are used in the calculation of these types of compressors.

3.2.1 Axial Compressor

Axial compressor efficiency estimation is presented in reference [25]. Additionally, tip clearance effect is simulated by inputting the percentage change in compressor efficiency with the clearance at last stage. Default value for this change is given as 2% in reference [9] and it is a user defined value.

3.2.1.1 Inputs

Inputs of this module are the followings:

- i) Total to total pressure ratio of compressor
- ii) Corrected air flow at inlet of compressor
- iii) Number of stages
- iv) Loss correction factor : Depending on technology level
- v) Mach number at exit of compressor
- vi) Compressor exit hub to tip radius ratio
- vii) Last stage tip clearance

viii) % Compressor Change for % Clearance

3.2.1.2 Calculation procedure

The unit of the corrected air flow that is used in this module is British units and denoted by w_{corr} . Pressure ratio of each compressor stage is

$$pr = \pi_c^{\frac{1}{n_c}} \quad (3.10)$$

where pr is the pressure ratio of each compressor stage. Polytropic efficiency is given by

$$\eta_p^* = 0.047322 (pr)^2 - 0.21668 pr + 1.1241 \quad \text{for } pr \leq 2 \quad (3.11.a)$$

$$\eta_p^* = -0.027392 pr + 0.93478 \quad \text{for } pr > 2 \quad (3.11.b)$$

where η_p^* is the polytropic efficiency which is not modified with respect to size and tip clearance.

If the tip clearance input is '0', the software does not consider the tip clearance losses with the additional modification explained above and uses the experimental correlation in reference [25]. The sizing of the compressor can be taken into account by using

$$\Delta\eta_p = 0.56826 (10^{-3}) w_{corr} - 0.62224 (10^{-3}) - \left(\frac{0.05603}{w_{corr}}\right) \quad (3.12.a)$$

for $w_{corr} < 10$ or $w_{corr} \geq 1.5$

$$\Delta\eta_p = 0.01767 w_{corr} - 0.06 \quad \text{for } w_{corr} < 1.5 \quad (3.12.b)$$

$$\Delta\eta_p = 0 \quad \text{for } w_{corr} > 10 \quad (3.12.c)$$

where $\Delta\eta_p$ is the modification of polytropic efficiency with the effect of size. If the tip clearance is not equal to zero, then

$$\Delta\eta_p = 0 \quad (3.13)$$

By definition,

$$\eta = \eta_p^* + \Delta\eta_p \quad (3.14)$$

$$\eta_p = 1 - k_{inp} (1 - \eta) \quad (3.15)$$

where η_p is the polytropic efficiency of the compressor and k_{inp} is the loss correction factor.

After the polytropic efficiency is found, it is a straightforward procedure to find the isentropic efficiency of the compressor by using the Equation (2.29). The tip clearance effect is included by the following formula,

$$\eta_{comp} = \eta_{zc} - (cer) (rtc) \quad (3.16)$$

where cer is compressor efficiency decrease rate with clearance, rtc is relative tip clearance (the tip clearance divided by the last stage blade height) and η_{zc} is the isentropic efficiency of the compressor without including the effect of tip clearance. Validation of this study with the experimental data is available in reference [25].

3.2.2 Centrifugal Compressor

Centrifugal compressor efficiency estimation is from reference [26] and the software gives an additional output of the expected pressure ratio for the designed centrifugal compressor from the inputted fundamental geometric parameters. It is the user's option to update input pressure ratio or not.

3.2.2.1 Inputs

The inputs required for the calculation of the centrifugal compressor efficiency can be given as follows:

- i) Actual mass flow rate of air at inlet of compressor
- ii) Total temperature and pressure at inlet of compressor
- iii) Stage number (One or two stages)
- iv) Type of diffuser (Vaned or vaneless)
- v) Impeller tip radius
- vi) Second compressor impeller tip radius (If available)

Air station numbers for only this sub-function is stated at Table 3.1.

Table 3.1 - Air Stations used in centrifugal compressor efficiency estimation

Station	Location
0	Compressor Inlet
1	First Centrifugal Compressor Exit
2	Second Centrifugal Compressor Exit (If available)

3.2.2.2 Calculation procedure

The density, volumetric flow rate and the compressor blade exit tip speed with the assumption of constant tip height is calculated by using

$$\rho_{t0} = \frac{P_{t0}}{R_0 T_{t0}} \quad (3.17)$$

$$Q_0 = \frac{\dot{m}}{\rho_{t0}} \quad (3.18)$$

And

$$U_1 = \frac{2\pi}{60} r_1 N \quad (3.19)$$

respectively. In the above equations, Q is the volumetric flow rate and N is the rotational speed of impeller in revolution per minutes.

After calculating the stage flow coefficient by using

$$\varphi_1 = \frac{Q_0}{\pi r_1^2 N} \quad (3.20)$$

the work input coefficient and the head coefficient of stage are calculated by empirical formulas given in reference [26] as

$$I_1 = 0.68 - \left(\frac{\varphi_1}{0.37}\right)^3 + \frac{0.002}{\varphi_1} \quad (3.21)$$

and

$$\mu_{pVD1} = 0.59 + 0.7 \varphi_1 - 7.5 \varphi_1^2 - \frac{0.00025}{\varphi_1} \quad (3.22)$$

Respectively. In the above equations, φ is the stage flow coefficient, I is the work input coefficient and μ is the head coefficient of stage. In addition, the subscript VD denotes vaned diffuser.

For a compressor with vaned diffuser, polytropic efficiency is calculated by

$$e_{VD} = \frac{\mu_{pVD1}}{I_1} \quad (3.23)$$

For a compressor with vaneless diffuser, polytropic efficiency is calculated by

$$e_{VLD} = e_{VD} - \frac{0.017}{0.04 + 5 \varphi_1 + e_{VD}^3} \quad (3.24)$$

whereas subscript VLD denotes the vaneless diffuser.

For vaned diffuser type, the enthalpy rise can be calculated by

$$\Delta h_{tp} = \mu_{pVD1} U_1^2 \quad (3.25)$$

Similarly, the enthalpy rise for vaneless diffuser type compressor can be calculated by

$$\Delta h_{tp} = \mu_{pVLD1} U_1^2 \quad (3.26)$$

Finally, the estimation of the pressure ratio of the compressor is found by

$$PressureRatio1 = \left(1 + \frac{\Delta h_{tp}}{c_p T_{t0}} \right)^{\frac{\gamma}{\gamma-1}} \quad (3.27)$$

If available, the same procedure is applied for the second compressor. The inputs of the second compressor are determined from the results of the first compressor. These formulations are obtained from a number of experiments carried out as mentioned in reference [26].

3.3 Turbine Efficiency Calculation Mode

The developed software gives an idea about the velocity triangles in the turbine stages by assuming symmetrical triangles (Turbine reaction ratio=0.5) and it estimates the efficiency by using these triangles as in reference [27]. Stage loading, flow factor, exit angles and exit Mach numbers are also calculated for the detailed analysis of the turbine section. This provides the designer an estimation of the stage

number, which is a very important parameter with regards to cost and weight of the turbine design. Furthermore, cooling feature is embedded into the code from reference [28] and this leads user to have an idea about the first rotor mean metal temperature. It should be noted that this temperature is one of the essential considerations in gas turbine design since the determination of the cooling air is completely dependent on this value and the cycle calculations considerably changes with the amount of cooling air for HP turbine. Velocity triangle nomenclature is the same as the one in Figure 3.2.

Air station numbers for only section 3 are stated at Table 3.2.

Table 3.2 - Air Stations used in turbine efficiency estimation

Station	Location
1	Turbine First Stage Stator Inlet
2	Turbine First Stage Rotor Inlet (Stator Exit)
3	Turbine First Stage Rotor Exit
4	Turbine Last Stage Stator Exit (Rotor Inlet)
5	Turbine Last Stage Rotor Exit

3.3.1 HP Turbine Efficiency Calculations

3.3.1.1 Inputs

In order to estimate the HP turbine efficiency, the following input parameters are required:

- i) Total temperature and pressure at station 41
- ii) Required turbine power
- iii) Mass flow rate of bleed air
- iv) Total temperature of bleed air
- v) Rotational speed of high speed spool
- vi) Fuel to air ratio
- vii) Actual mass flow rate of working gas at station 41
- viii) Number of stages

- ix) First HPT rotor inlet diameter
- x) Last HPT rotor inlet diameter (For more than one stage of HPT)
- xi) Exit radius ratio
- xii) $(V_a)_{\text{exit}}/\bar{V}_a$
- xiii) Loss factor (0.3-0.4)
- xiv) First rotor cooling constant

3.3.1.2 Calculation procedure

3.3.1.2.1 Velocity Triangles

First of all, the expected turbine power should be known in order to calculate the velocity triangles. This can be calculated by

$$(\dot{m}_2 (h_{t3} - h_{t2}) + \frac{POT}{\eta_{mp}}) / \eta_{mp} = \dot{W}_{turb} \quad (3.28)$$

It should be noted that, HP turbine efficiency estimation is an iterative process. Initially, the efficiency of the turbine is assumed and the pressure ratio of the turbine corresponding to that efficiency is found. After calculations, the efficiency is updated and this process continues up to a point where the difference between the guessed and calculated efficiencies is less than 0.001. Additionally, the tangential component of the exit velocity is assumed at first and compared with the calculated value by the Euler turbine equation. This requires another iterative process and continues until the velocity difference of 0.01.

Calculating the exit tangential speed of the turbine last stage at mean radius as

$$U_5 = N \frac{2\pi}{60} r_{m5} \quad (3.29)$$

The pressure ratio of each stage is

$$PR_s = \pi^{\frac{1}{n}} \quad (3.30)$$

where PR_s is the pressure ratio of each stage and n is the number of axial stages in HPT.

Calculating the exit tangential speed of the turbine first stage at the mean radius as

$$U_3 = N \frac{2\pi}{60} r_{m3} \quad (3.31)$$

Updating the reduced pressures at station 3 and 5 of the turbines can be updated as

$$Pr_{t5} = Pr_{t1} \pi_{th} \quad (3.32)$$

$$Pr_{t3} = Pr_{t5} PR_s \quad (3.33)$$

The properties of the gas at station 3 can now be updated by using the reduced pressure.

The tip radius of the last stage exit can be found by

$$r_{t5} = 2 \frac{r_{m5}}{1 + htr_5} \quad (3.34)$$

So that the hub radius is

$$r_{h5} = r_{t5} htr_5 \quad (3.35)$$

The exit area can be found by

$$A_5 = \pi (r_{t5}^2 - r_{h5}^2) \quad (3.36)$$

The axial velocity at the last rotor of the turbine can be found by continuity equation as follows,

$$V_{a5} = \frac{\dot{m}_{turb}}{A_5 \frac{P_5}{R_5 T_5}} \quad (3.37)$$

where \dot{m}_{turb} is the mass flow rate through HPT.

An iterative process should be carried out by using Equations (3.29) to (3.37) to evaluate the static temperature of stations until the calculated turbine mass flow rate value is equal to the input mass flow rate value. With this iteration, static temperature of station 5 is found.

The absolute velocity at station 5 can be found by

$$V_5 = \sqrt{V_{a5}^2 + V_{\theta 5}^2} \quad (3.38)$$

The corresponding Mach number and the static temperature can be found with this obtained velocity by formulas,

$$M_5 = \frac{V_5}{\sqrt{\gamma_5 R_5 T_5}} \quad (3.39)$$

$$T_5 = \frac{T_{t5}}{\left(1 + \frac{\gamma_5 - 1}{2} M_5^2\right)} \quad (3.40)$$

After finding T_5 , the static pressure can be found by

$$P_5 = \left(\frac{T_5}{T_{t5}}\right)^{\left(\frac{\gamma_5}{\gamma_5 - 1}\right)} \quad (3.41)$$

Now, it is possible to find the density of the gas at station 5 as

$$\rho_5 = \frac{P_5}{R_5 T_5} \quad (3.42)$$

Finally, the gas flow rate can be found by

$$\dot{m}_{turb} = V_{a5} A_5 \rho_5 \quad (3.43)$$

Since V_{a5} and U_5 are known, now it is possible to construct the velocity triangle at station 5 by using the following relations,

$$W_{\theta 5} = U_5 + V_{\theta 5} \quad (3.44)$$

$$W_5 = \sqrt{W_{\theta 5}^2 + V_{a5}^2} \quad (3.45)$$

$$\alpha_5 = \arcsin\left(\frac{V_{\theta 5}}{V_5}\right) \quad (3.46)$$

$$\beta_5 = \arcsin\left(\frac{W_{\theta 5}}{W_5}\right) \quad (3.47)$$

where α is the absolute flow angle, β is the relative flow angle and subscript θ denotes the whirl component of the corresponding velocity.

After these calculations, there is sufficient information to calculate to the parameters at station 4. The calculation of enthalpy at turbine station 4 is done by

$$h_4 = R_t (h_{t3} - h_{t5}) + h_5 \quad (3.48)$$

where R_t is the degree of reaction of turbine to be designed. The gas properties are then evaluated by using the evaluated enthalpy.

The velocity triangles, may now be calculated as follows,

$$V_{a4} = V_{a5}/V_{aR} \quad (3.49)$$

$$V_{\theta4} = U_4 + W_{\theta4} \quad (3.50)$$

$$W_4 = \sqrt{V_{a4}^2 + W_{\theta4}^2} \quad (3.51)$$

$$V_4 = \sqrt{V_{a4}^2 + V_{\theta4}^2} \quad (3.52)$$

where V_{aR} is the ratio of the exit axial velocity to the average axial velocity of the stage.

Since velocity and air properties are known, it is possible to calculate the Mach number and the pressure at station 4 as

$$M_4 = V_4/a_4 \quad (3.53)$$

$$P_{t4} = P_{t5} \left(\frac{Pr_{t4}}{Pr_{t5}} \right) \quad (3.54)$$

With the available values, it is possible to construct the velocity triangle at station 3 as

$$V_3 = \frac{V_5}{U_5} U_3 \quad (3.55)$$

$$W_3 = \frac{W_5}{U_5} U_3 \quad (3.56)$$

$$V_{\theta3} = V_{\theta5} \frac{U_3}{U_5} \quad (3.57)$$

$$P_{t3} = P_{t1}/PR_s \quad (3.58)$$

With the assumption of symmetrical velocity triangles, all the necessary parameters are found in order to be used in the Euler turbine equation for updating the tangential velocity as iteratively until the difference between its successive values is 0.01.

$$\begin{aligned}
\dot{W}_{turb} = \dot{m}_{turb} [(2 V_{\theta 3} + U_3) U_3 \\
+ (n - 2) \frac{(2 V_{\theta 3} + U_3) U_3 + U_5 (2 V_{\theta 5} + U_5)}{2} \\
+ U_5 (2 V_{\theta 5} + U_5)]
\end{aligned} \tag{3.59}$$

The parameters of station 2 are calculated by the values of station 3 similar to the calculation of station 4 from the values of station 5.

3.3.1.2.2 Cooling Effects

Cooling effectiveness is calculated by using reference [28] as

$$\eta_{cool} = \frac{\dot{m}_{b3}}{\dot{m}_{b3} + K_{cool}} \tag{3.60}$$

where η_{cool} is the cooling effectiveness and K_{cool} is the rotor cooling constant. The resulting metal temperature is then,

$$T_{metal} = T_{trel} - \eta_{cool} (T_{trel} - T_{cool}) \tag{3.61}$$

where T_{cool} is the cooling air temperature which is equal to the compressor exit total temperature. T_{trel} is the HPT First rotor inlet relative total temperature and calculated by using

$$T_{trel} = T_1 \left(1 + \frac{\gamma_2 - 1}{2} M_{2rel}^2\right) \tag{3.62}$$

The next step is the calculation of the outputs of interest which are the HPT first rotor inlet relative temperature, the HPT first stage flow factor (V_{x3}/U_3), the HPT first stage loading ($\Delta h_t/U_3^2$), the HPT exit Mach number (M_5), the HPT exit flow angle (α_3), the HPT cooling effectiveness (η_{cool}) and the HPT first rotor blade metal temperature (T_{metal}).

3.3.1.2.3 Efficiency Estimation

This efficiency estimation is provided by Ref [27] with the inputs of HPT velocity triangles. The isentropic efficiency of the stage is

$$\eta_{stage} = \frac{swp}{swp + \frac{A}{2}} \tag{3.63}$$

where η_{stage} is the isentropic efficiency of the stage, swp is the speed-work parameter and A is a constant to be calculated. The swp is defined as

$$swp = \frac{U}{V_{\theta i} - V_{\theta e}} \quad (3.64)$$

where the subscript i represents the inlet station of the considered rotor and the subscript e specifies the exit station of the considered rotor. The constant A can be calculated as

$$A = K * \frac{Re^{-0.2}}{\cot(\alpha_2)} (f_{st} C + f_{ro} D) \quad (3.65)$$

where K is the loss factor, Re is Reynolds number at the rotor and C and D are the defined constants in order to calculate the turbine efficiency. The constants f_{st} and f_{ro} are calculated as

For the rotor

$$f_{ro} = 2 \quad \text{for } 0 \leq swp \leq 1 \quad (3.66)$$

For the stator

i) For single or first stage

$$f_{st} = 1 \quad \text{for } 0 \leq swp \leq 1 \quad (3.67)$$

ii) For intermediate stages

$$f_{st} = 2 (1 - swp) \quad \text{for } 0 \leq swp \leq 0.5 \quad (3.68a)$$

and

$$f_{st} = 1 \quad \text{for } 0.5 \leq swp \leq 1 \quad (3.68b)$$

The constant C is calculated for both the rotor and the stator as

For Single or First Stages

$$C = (1 + 2 (\cot(\alpha_2))^2 (swp + 0.5))^2 \quad \text{for } 0 \leq swp \leq 0.5 \quad (3.69a)$$

$$C = 1 + 2 (\cot(\alpha_2))^2 \quad \text{for } 0 \leq swp \leq 0.5 \quad (3.69b)$$

For Intermediate or Last Stages

$$C = \frac{(1 + 2 (\cot(\alpha_2))^2 (\text{swp} + 0.5)^2 + (\text{swp} - 0.5)^2)}{0.5} \quad \text{for } 0 \leq \text{swp} \leq 0.5 \quad (3.70a)$$

$$C = 1 + 2 (\cot(\alpha_2))^2 \quad \text{for } 0.5 \leq \text{swp} \leq 1 \quad (3.70b)$$

Similarly, the constant D is calculated for both the rotor and the stator as

$$D = 2 (\cot(\alpha_2))^2 (\text{swp} + 0.5)^2 + 0.5 \quad \text{for } 0 \leq \text{swp} \leq 0.5 \quad (3.71a)$$

$$D = 2 (\cot(\alpha_2))^2 + (1 - \text{swp})^2 + \text{swp}^2 \quad \text{for } 0.5 \leq \text{swp} \leq 1 \quad (3.71b)$$

The dynamic viscosity (Pa·s) is calculated by using the Sutherland's relation [5] at the turbine inlet with the following formula,

$$\mu = 1.5105 * 10^{-6} \left(\frac{T^{1.5}}{T + 120} \right) \quad (3.72)$$

where μ is the dynamic viscosity. Calculating the Reynolds Number at the rotor by

$$Re = \frac{\dot{m}_{turb}}{\mu r_{mean}} \quad (3.73)$$

where r_{mean} is the mean radius of the first stage of the interested turbine.

Finally, the total turbine stage isentropic efficiency can be calculated via following formula,

$$\eta_{turb} = \frac{n}{\frac{1}{\eta_{firststage}} + \frac{n-2}{\eta_{intermediate}} + \frac{1}{\eta_{laststage}}} \quad (3.74)$$

As mentioned before, this is an iterative process and continues until the efficiency found gets very close to the guessed value (previous result). The resulting stage flow factor and the stage loading is plotted in Smith chart [29] to give an insight to the designer that is whether the designed turbine is feasible and efficient or not for the designed configuration of the cycle.

Validation of this study with the experimental data is available in reference [27]. Sample turbine efficiency mode output GUI is presented in Appendix B.

3.3.2 Power Turbine Efficiency Calculations

All of the calculations are similar to the HP Turbine calculations except that the pressure ratio of the power turbine is evaluated by using Equation (2.33).

3.4 Combustor Design Mode

The combustor efficiency estimation is from reference [5] and the software gives an idea about the combustor design parameters such as loading, intensity and residence time. In addition, with the parameters found in this mode, the software updates the burner efficiency in the design calculations for better approximation of the cycle towards reality.

3.4.1.1 Inputs

For the estimation of the combustion efficiency,

- 1) Actual mass flow rate at station 3.1,
- 2) Total temperature and total pressure at station 3.1,
- 3) Combustor mean radius,
- 4) Combustor height,
- 5) Combustor length,
- 6) Combustor average Mach number and
- 7) Fuel to air ratio are required.

3.4.1.1.1 Combustion Efficiency

3.4.1.2 Calculation Procedure

The radius of the tip and hub of the combustion chamber can be calculated by

$$r_t = r_m + \frac{\text{height}}{2} \quad (3.75)$$

and

$$r_h = r_m - \frac{\text{height}}{2} \quad (3.76)$$

respectively. Then the volume V_c of the combustor is

$$V_c = \pi L_c (r_t^2 - r_h^2) \quad (3.77)$$

where L_c is the length of the combustion chamber. The loading, intensity and residence time for the combustor can be evaluated as

$$L = \frac{m_{3.1}}{V_c \left(\frac{P_{t3.1}}{101.325} \right)^{1.8} (10^{(0.00145 (T_{t3.1} - 400))})} \quad (3.78)$$

$$I = m_{3.1} f \eta_b \left(\frac{LHV}{\left(\frac{P_{t3.1}}{101.325} \right) V_c} \right) \quad (3.79)$$

$$t_{res} = L_c / V_c \quad (3.80)$$

Where L is the loading of the combustor, I is the combustion intensity and t_{res} is the residence time. The resulting combustion efficiency can be found by

$$\eta_b = (-5.46974 (10^{-11}) L^5 + 3.97923 (10^{-8}) L^4 - 8.73718 (10^{-6}) L^3 + 0.0003000007 L^2 - 0.004568246 L + 99.7) / 100 \quad (3.81)$$

where η_b is the combustion efficiency. It should be noted that, since η_b and therefore fuel to air ratio (f) changes, combustion calculations are repeated three times. In the software, these calculations are performed three times for this purpose and the values are updated accordingly.

CHAPTER 4

OFF-DESIGN PERFORMANCE ESTIMATION

After determining the design point of the turboshaft engine, it is important to estimate and examine how the engine behaves at different operating points within the aircraft operating envelope. This is a must since the capability of the engine to cope with the defined missions should be examined by the engine manufacturer while developing the cycle of the engine in the preliminary design phase. In the actual case, compressor and turbine maps are not determined at this point of the engine design phase. In order to estimate the performance, there are some techniques to estimate the maps of the components which can be used to determine the performance at the desired operating point. One of these techniques, namely map scaling, is used in this thesis.

4.1 Map Scaling

In the map scaling method, reference maps are used and scaled for off-design calculations. The pressure ratio, efficiency and mass flow values of the maps should be scaled to the design values of the engine to be designed.

The scaling factor used in the pressure ratio is [30]

$$PR = \frac{PR_d - 1}{PR_{md} - 1} (PR_m - 1) + 1 \quad (4.1)$$

For mass flow and efficiency, the following scales are used,

$$\dot{m} = \frac{\dot{m}_d}{\dot{m}_{md}} \dot{m}_m \quad (4.2)$$

$$\eta = \frac{\eta_d}{\eta_{md}} \eta_m \quad (4.3)$$

where subscript d denotes the design value of the engine to be designed, md denotes the design value of the reference maps and m denotes the value of interested point for scaling at the reference maps.

Reference maps for the components are selected as the ones in reference [9]. As the compressor reference map, NASA TM 101433 compressor map is used. For the HPT reference map, high work low aspect ratio turbine of NASA TM83655 is used. Finally, AGARD two stage turbine map is used for the power turbine.

Furthermore, the reference map for the compressor changes to a different map when the centrifugal compressor type is selected in the software. For this reason, a two-stage centrifugal sample engine map is digitized and embedded into the software from reference [31]. This conversion of maps is necessary because although the same process is carried out thermodynamically for both types, each type has different operating characteristics which lead to very different engine parameters in the off-design matching. To illustrate the difference, characteristics of both types are as shown in Figure 4.1.

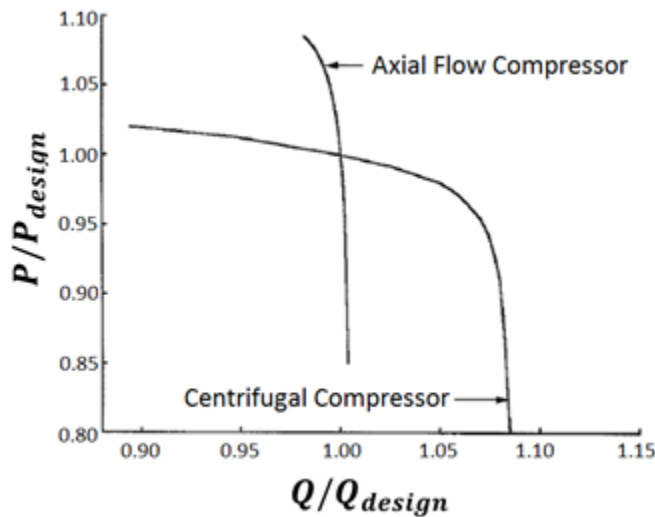


Figure 4.1 - Performance characteristics of axial and centrifugal compressors [32]

Centrifugal compressor characteristics are flatter than axial flow compressor characteristics at constant speed in the pressure ratio versus flow graph. Hence, in centrifugal compressors, the flow can be decreased much more with respect to axial

ones without reaching the surge line. Furthermore, the efficiency of an axial compressor is higher than a centrifugal compressor in an operation within the normal range of designs [4].

After determining the rotating component maps, it is then required to match these components. The engine operates at one point for the given fuel input and the determination of the ‘non-dimensional thermodynamic’ operating point is fully dependent on these component maps. Constraints that force the engine to operate at this single point for the given fuel are work and flow compatibility equations. To illustrate, the flow that passes through the compressor and the turbine is strongly connected to each other whereas the power required to drive the compressor is provided by the extracted power from the working fluid at the turbine.

4.2 Beta-Line Technique

Before matching, new maps, formed for the components, are tabulated for the usage in the developed computer software. To provide a precise reading, “beta-line” technique is used in which mass flow, efficiency and pressure ratios for the specified speeds are tabulated with respect to their betas. Beta lines are arbitrary lines which are placed nearly equally spaced and parallel to surge line in the compressor map. After this point, created maps are tabulated as three matrices carrying corrected mass flow, total pressure ratio and isentropic efficiency data to be used in the developed software [5]. The surge line beta value is equal to 1 whereas the lowest line beta value is equal to 0. The region in between these two lines are divided into equal sections (the mostly preferred section number is 20) and named as their respective beta value that is interpolated linearly between 1 and 0. The map presentation and the respective tabulation of the data can be seen in Figure 4.2.

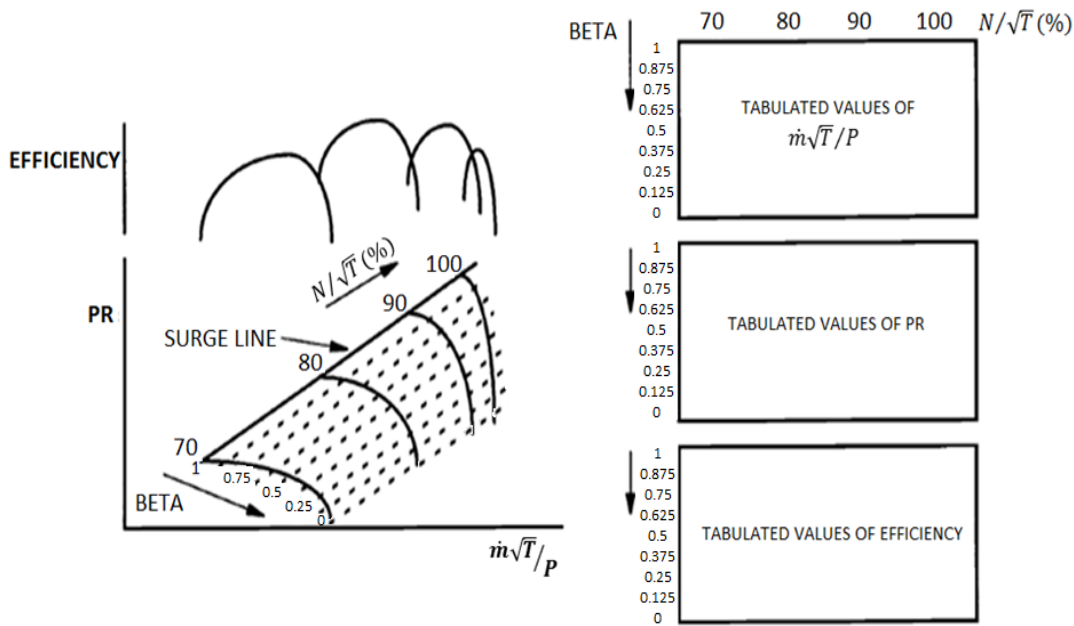


Figure 4.2 - Compressor map and beta lines

In turbine maps, linear interpolation between the map points is used. The beta value is determined by setting the upper most point at that speed equal to 1 whereas the lower most point beta value is set to zero. Interpolation for the interested point is done between these three points.

4.3 Component Matching in Off-Design Calculations

The thermodynamic matching type model is used in the software. This is a universal form of the steady state design models and is commonly referred to as a deck. Once the maps of the components are fixed by setting the geometrical specifications of the components, it is possible to represent the performance of the engine at all on and off design conditions. For a given engine operating condition, the operating point at each map is also unique for the designed components [5]. In other words, unique maps of the unique components are matched to each other for a unique operating point of the engine.

In the component matching, there are four independent variables and four errors that can arise from mismatching of the rotating components. These variables are the compressor beta value, the turbine inlet temperature, the high pressure turbine beta value and the power turbine beta value. Errors that have to be minimized are the high pressure turbine flow difference (should be equal to the expected flow rate through

the compressor), the high pressure turbine work difference (should be equal to the expected work required to rotate the compressor), the power turbine flow difference (should be equal to the expected flow rate through HPT) and lastly the exhaust pressure ratio. A certain total pressure is required to force the exit mass flow with the exit total temperature through the given exit area while the back pressure is equal to ambient pressure [9]. Hence, the last error is the difference between the required pressure ratio and the actual one in the iteration. It should be noted that the power turbine speed is set as constant in off-design (i.e. in a helicopter application it is a requisite). As the main input for the off-design calculations, the relative high pressure spool speed is selected. For the given spool speed, the operating point is fixed at the compressor map with the input of beta value of the compressor. In addition, the corrected speed (N/\sqrt{T}) is fixed for the HP turbine with the knowledge of the turbine inlet temperature. After setting the beta value of the HP turbine in the map, the operating point of the HP turbine is fixed as well. With the determination of this operating condition, the power turbine inlet temperature is fixed which results in the fixed corrected speed of the power turbine. Lastly, the beta value for the power turbine is put into the code to fix the power turbine operating point. At this point, the problem is how to reach a solution. Iterations begin with initial guesses of the four independent parameters mentioned above and iterations are updated with the Newton-Raphson iteration method. This method calculates the Jacobians and updates these parameters accordingly. This process goes on until the square of the sum of the errors decreases up to 10^{-8} .

The algorithm for the off-design calculations are presented in Figure 4.3.

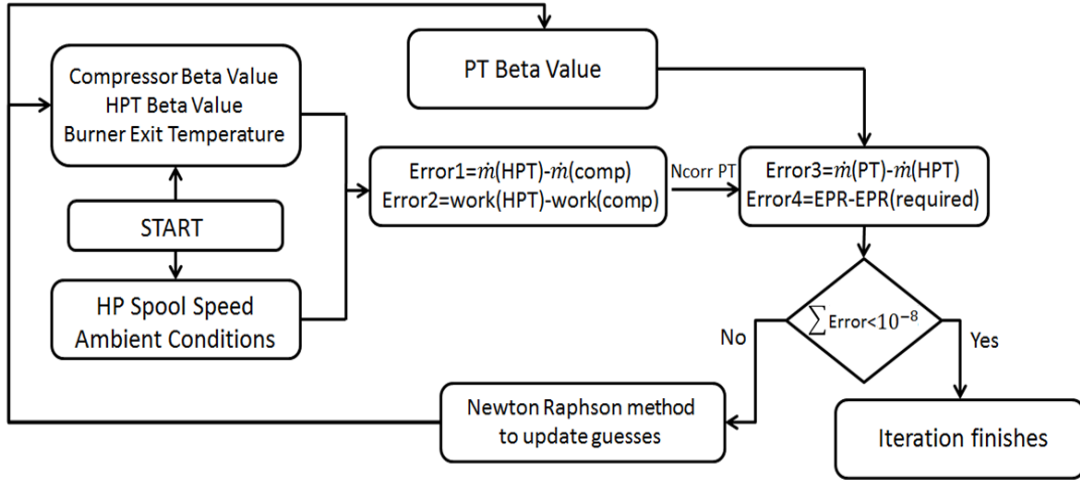


Figure 4.3 - Off-design matching algorithm

4.4 Changing Parameters at Off-Design

Some of the design point input parameters should be modified since the engine is operating in various mass flows in its operating envelope. In order to apply this necessary modification, pressure losses in the burner and the exit duct are assumed to be changing proportional to the corrected mass flow rate such as in reference [9]. In addition, the burner efficiency is also updated with the comparison of the burner loadings of the design and the interested off-design point is obtained in the same way as in reference [9].

The burner loading is defined as

$$\Omega = \frac{W_{3,1}}{P_{3,1}^{1.8} V_c \exp\left(\frac{T_{3,1}}{300}\right)} \quad (4.4)$$

Where $W_{3,1}$ is the air mass flow in the combustor, $P_{3,1}$ is the pressure at the inlet of the combustor in bars, $T_{3,1}$ is the combustor inlet temperature in K and V_c is the combustor volume in m^3 . The burner efficiency can be estimated by the formula from reference [28],

$$\log(1 - \eta) = a + b \log\left(\frac{\Omega}{\Omega_d}\right) \quad (4.5)$$

where $a = \log(1 - \eta_d)$ and b is the burner part load constant. In the developed software, the burner part load constant is taken as 1.6 which is the default value Ref [9].

4.5 Operating Lines

Solving numbers of spool speed operation at off-design will result in operating points for steady state operation in each of the component maps. Linking these points to each other gives the operating line of the components of the engine.

Some samples of off design operation results of the developed code are shown in Figure 4.4 to Figure 4.6.

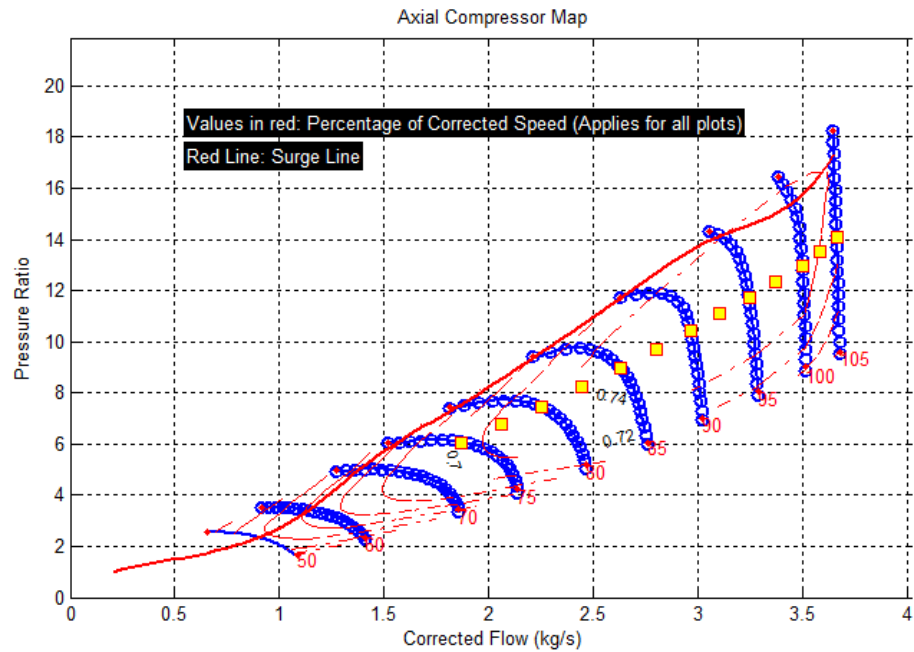


Figure 4.4 – Sample output of operating line in compressor map in the developed code

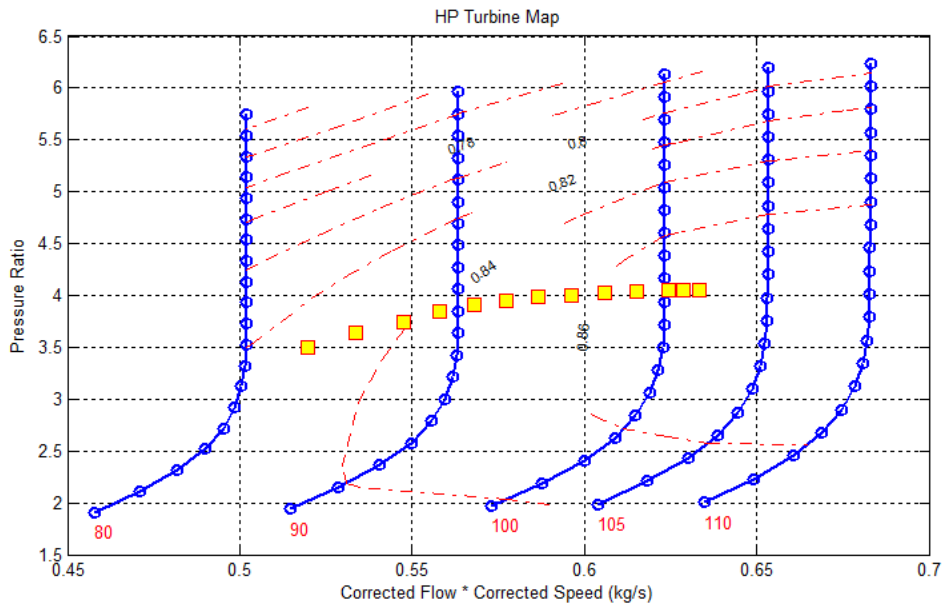


Figure 4.5 – Sample output of operating line in HP turbine map in the developed code

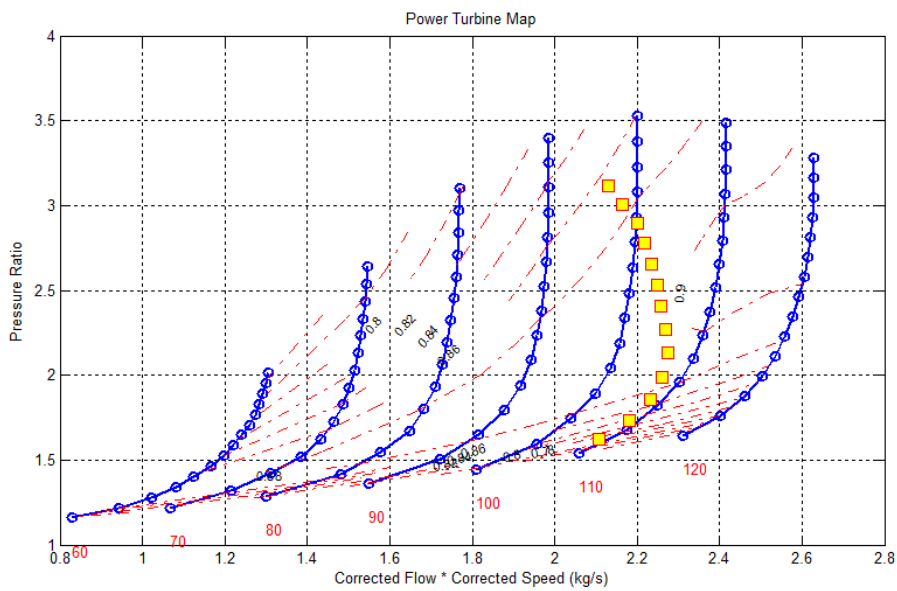


Figure 4.6 – Sample outputs of operating line in power turbine map in the developed code

In Table 4.1, the sample outputs of the operating lines of the developed software and GasTurb are compared while resulting power outputs are presented in Table 4.2. It can be seen that the results are nearly matched with each other.

Table 4.1- Comparison of results of the developed software and GasTurb for given sample inputs

Relative Speed	Developed Code			Gasturb			Absolute % Diff		
	m	PRc	Tt4	m	PRc	Tt4	m	PRc	Tt4
0.75	1.87	6.05	1190	1.8800	6.07	1187	0.53	0.41	0.23
0.8	2.25	7.46	1217	2.2540	7.46	1214	0.18	0.00	0.22
0.85	2.63	8.99	1270	2.6310	8.99	1272	0.04	0.08	0.16
0.9	2.97	10.45	1333	2.9650	10.44	1331	0.17	0.04	0.16
0.95	3.25	11.74	1387	3.2450	11.72	1384	0.15	0.16	0.27
1	3.50	12.99	1445	3.5000	13.00	1450	0.00	0.08	0.33
1.05	3.66	14.12	1545	3.6630	14.09	1544	0.08	0.23	0.08
MEAN							0.16	0.14	0.21

Table 4.2 - Operating line power output comparison of the developed Software and GasTurb11

Relative Speed	Developed Code	Gasturb	Absolute Difference
	POWER (kW)		%
0.75	151.2	153.2	1.2
0.8	259.4	259.2	0.1
0.85	395.1	396.0	0.2
0.9	541.6	540.5	0.2
0.95	677.8	673.8	0.5
1	815.6	818.5	0.4
1.05	957.4	955.7	0.2
MEAN			0.4

To sum up, after using the same reference maps with GasTurb, the results of the developed code are in close agreement with the results of GasTurb, which shows that the written code is operating correctly and ready to be used in engine on and off design (steady operation) performance estimations.

4.6 Handling Bleed Effects

The handling bleed effect is introduced into the developed software and can be switched on in the off-design and transient calculations. It is modeled as the air flow which is taken from the discharge air at the compressor without affecting the main flow. Required inputs for scheduling the handling bleed module are:

- i) Closed above the corrected speed
- ii) Open below the corrected speed
- iii) Maximum handling bleed (kg/s)
- iv) Minimum handling bleed (kg/s)

The handling bleed is widely used in the gas turbine applications due to its beneficial effects over the compressor surge phenomenon. Using the handling bleed valves in

low speed operation is necessary since it moves the operating line down in the compressor performance maps. The reason is that the mass flow rate is increased when the valves are opened and hence the surge margin is increased. To illustrate, the sample operating lines with and without handling bleeds are shown in Figure 4.7 (the darker operating line is the one that the handling bleed effect is active):

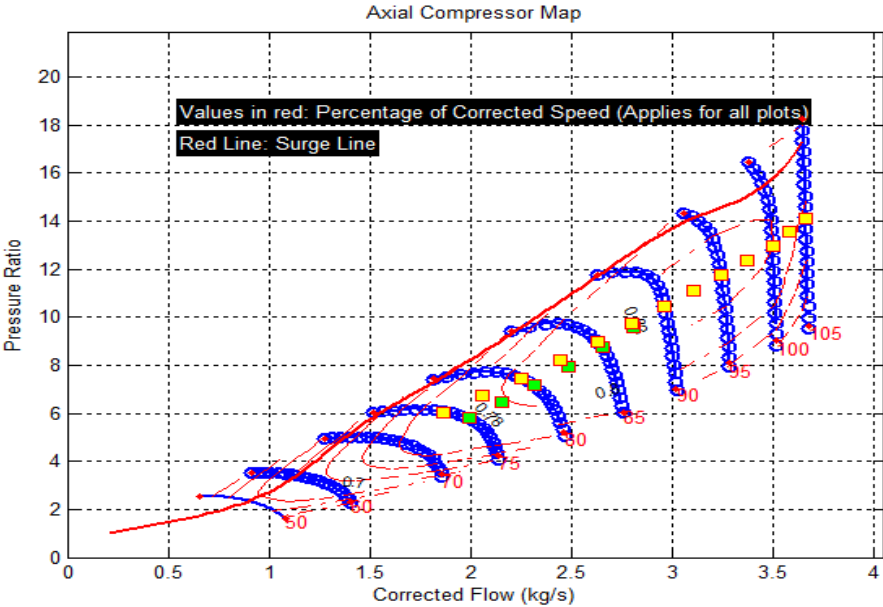


Figure 4.7 - Handling bleed effect on operating line

CHAPTER 5

SIMULATION OF INLET DISTORTION EFFECTS

The two main influences of the inlet distortion in gas turbines are on the stability of the compression system and propulsion system performance due to the compressor efficiency degradation and the control system action in the engine [33]. The effects of the control system, in order not to stall the compressor, are widely investigated in the literature such as in reference [34]. However, since the main interest of the software is not the control system, the compressor efficiency degradation and the resulting performance changes in the turboshaft engine are considered in the software.

Methodology of the inlet distortion part of the software follows mainly reference [33] and the results then will be compared with the commercially available tool GasTurb11. It should be noted that, the coupling factor is not considered in this thesis since the main interest is the turboshaft engine. Because these engines are small gas turbines, there are no serially connected low and high pressure compressors in general.

5.1 Methodology

The parallel compressor theory was first proposed by Pearson [35] and it is the common method in modelling the inlet distortion. The main idea of this theory is that two different streams in the compressor is assumed to be working at the same time and matched with each other to have the same exit static pressures. Inlet properties of the each flow can be modeled by the definitions in reference [36].

The compressor map is divided into parts for the parallel compressor operation and new maps are required for each section of the compressor. In order to create new

maps, same maps with the only difference of corrected mass flows are used for each section. The design point corrected mass flow rate of the distorted part is calculated by the user input angle divided by 360 degrees and multiplied with the whole design point mass flow rate of the compressor. The remaining corrected mass flow is the design point of clean section of the compressor used. New betas are defined in each map and the Newton- Raphson iteration is performed with five parameters and five constraints. The new constraint is that the static pressures at each compressor section exit must be the same. In the developed software, Mach number of 0.2 is the default value at the exit of the compressor and the static pressure is calculated by this value and the total pressure for each section is found via the related compressor maps.

Before all calculations, the aerodynamic interface plane (AIP) should be defined just before the inlet of the compressor. In order to calculate the properties there, the compressor design module calculations should be made before.

The static pressure at the inlet of the compressor can be found by the following formula,

$$P = \frac{P_{t2}}{\left(1 + \frac{\gamma - 1}{2} M_2^2\right)^{\frac{\gamma}{\gamma - 1}}} \quad (5.1)$$

where P is the static pressure.

In the compressor design mode calculations, the hub radius, r_h , and the tip radius, r_t , can be found. Using these values, the area at the aerodynamic interface plane, A_{AIP} , can be calculated by

$$A_{AIP} = \pi r_t^2 \quad (5.2)$$

The compressor inlet area is then calculated by

$$A_2 = \pi (r_t^2 - r_h^2) \quad (5.3)$$

The velocity at the inlet of the compressor is then

$$V_2 = M_2 a_2 \quad (5.4)$$

Assuming constant density, the velocity at AIP can be calculated as

$$V_{AIP} = V_2 \frac{A_2}{A_{AIP}} \quad (5.5)$$

5.1.1 Pressure Distortion:

The pressure distortion coefficient is defined to take the inlet distortion into account and it is an input value from the user to calculate the inlet station properties of the compressor and it adjusts the magnitude of the pressure distortion.

$$DC = \frac{P_{mean} - P_{distorted}}{\frac{\rho}{2} V_{AIP}^2} \quad (5.6)$$

where DC is the pressure distortion coefficient. In addition, P_{mean} is the average pressure and $P_{distorted}$ is the pressure at the distorted section.

Using DC, $P_{distorted}$ can be calculated by using Equation (5.6). It is assumed that the total temperature does not change when the pressure distortion is applied. After finding the same static pressures for the exit at the same corrected speeds for each flow rate in the compressor, the average values are set depending on the actual mass flow rates and then the cycle calculation is performed.

5.1.2 Temperature Distortion:

Similar to the pressure distortion coefficient, the temperature distortion coefficient is an input that the user can change the intensity of the temperature distortion. By definition,

$$DT = \frac{T_{distorted} - T_{mean}}{T_{mean}} \quad (5.7)$$

where DT denotes the temperature distortion coefficient.

Additional definition in reference [9] is used in the developed software for the calculation of the temperature with the input of the temperature distortion coefficient,

$$T_{distorted} = \frac{\left(1 - \frac{\alpha}{360}\right) (1 + DT)}{1 - \left(\frac{\alpha}{360}\right) (1 + DT)} T_{t2} \quad (5.8)$$

where α is the circumferential extent of the distortion in degrees.

After finding $T_{\text{distorted}}$, the corrected speed of the distorted section is updated and the iterative process goes on until the same static pressures for the compressor exit is found, as mentioned before. Again, the average values are set depending on the actual mass flow rates.

5.2 Sample Results and Comparison with GasTurb11

For the temperature and pressure distorted inlet, a sample input and output in the developed software is presented in Figure 5.1.

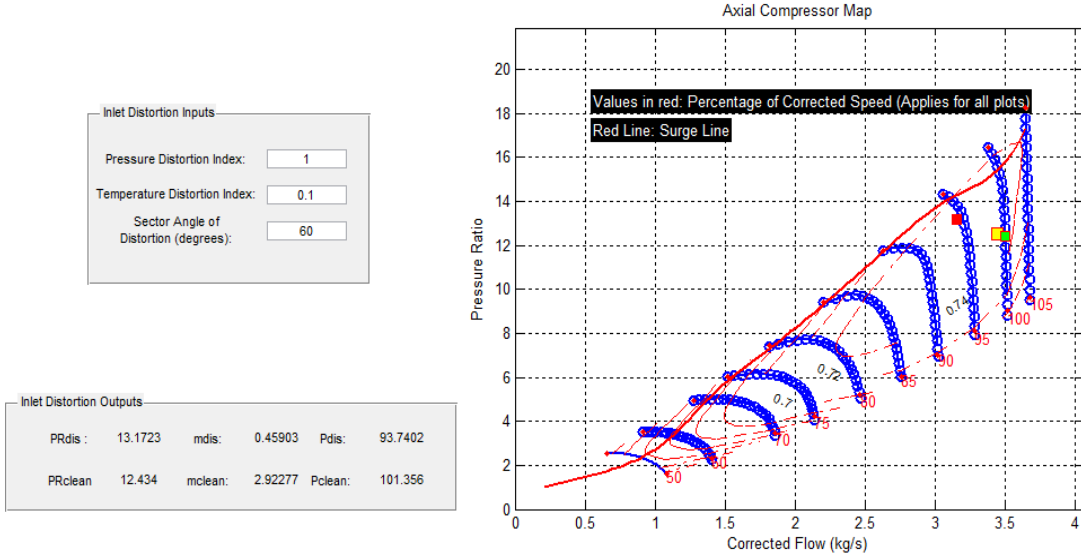


Figure 5.1- Inlet distortion output of the developed software

In this figure, *-dis* affix denotes the distorted section properties whereas *-clean* affix denotes the clean section properties. The darkest point in the compressor map belongs to the distorted section whereas the rightmost dark point shows the operating point of the clean part of the compressor. Furthermore, the point in between is the average working point of the compressor. As expected, the pressure ratio is higher in the distorted section in order to reach the same static pressure at the exit with starting from a much lower pressure value at the inlet.

A sample output of GasTurb11 for the same inputs is shown in Figure 5.2.

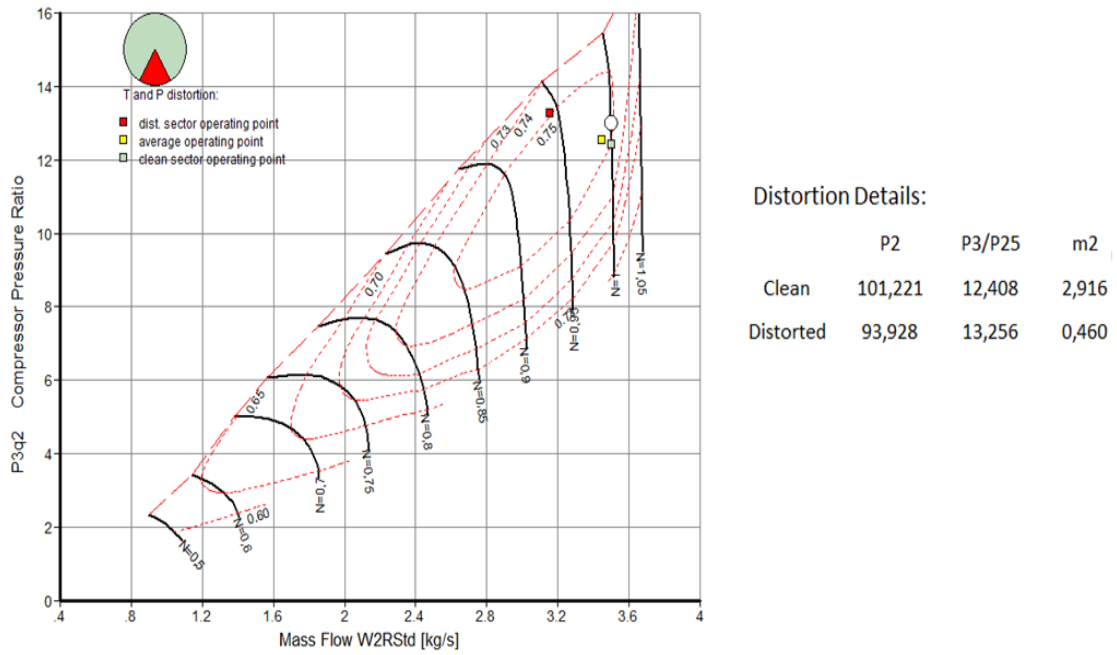


Figure 5.2 - GasTurb11 output with inlet distortion

It is concluded from the results that there is a maximum difference of 0.5 % which is an acceptable value for the inlet disturbance model. The main concern of this inlet distortion model is the effect on the performance of the turboshaft. Because of this, the results of the developed software and GasTurb11 with and without the disturbance shaft powers and specific fuel consumptions are presented in Table 5.1 in order to see the degradation of the performance with inlet distortion.

Table 5.1 - Inlet distortion effect on performance

		Without Distortion	With Distortion
Developed Software	Shaft Power (kW)	879.37	820.13
	SFC (kg/kWh)	0.3002	0.3040
GasTurb 11	Shaft Power (kW)	880.7	817.2
	SFC (kg/kWh)	0.3005	0.3042

It can be seen from the results that, moderate inlet distortion inputs (DT=0.1 and DC=1 taken in sample) result in nearly 7 percent of loss in the shaft power, which can be evaluated as a significant loss.

CHAPTER 6

TRANSIENT PERFORMANCE ESTIMATION

On and off designs of a system can give outputs on state changes. If one needs to determine how the engine and its outputs react to varying inputs (such as fuel input), dynamic analysis of the turboshaft engine is required. This means that a modification is required on the steady state model in order to get the transient model of the engine. This can be accomplished by taking the polar moment of inertia into account while establishing the power balance between the compressors and turbines. It is obvious that more fuel is required during accelerations than that for steady state design point. For decelerations, less fuel is required in the same sense [9].

In accelerations, there is an additional power on the high speed spool due to the increased fuel input. In other words, the power output of the HP turbine exceeds the power that required to drive the compressor, auxiliaries and mechanical losses. Conversely, the power output of the HP turbine decreases and becomes insufficient to drive compressor, auxiliaries and mechanical losses due to the decreased fuel flow rate in decelerations. To take these effects into account, unbalanced power, UP , is introduced to the work compatibility equation of the compressor and the gas generator turbine in order to demonstrate the effect of transients as in the following formula,

$$\eta_{mh} \dot{m}_{4.1} \Delta h_{t45} = \dot{m}_2 \Delta h_{t23} + POT + UP \quad (6.1)$$

It should be noted that the unbalanced power is negative in deceleration type transients. Newton-Raphson Method is used to guess the unbalanced power (UP) in the HP spool. In addition to the off-design matching, the desired fuel flow (WF) is matched with the addition of the guessed unbalanced power in the gas generator spool (similar to the effect of power offtake) at the initial spool speed. The iteration

is completed when the two fuel values are matched and the unbalanced power (results in acceleration or deceleration) is found. After this matching, calculations in the current time step are carried out and the code moves on to the next time step. It should be noted that the fuel pump is modeled with a response with first order time lag.

The spool acceleration is calculated as

$$\frac{dN}{dt} = \frac{UP \text{ (i.e. due to Additional Fuel)}}{\left(\frac{\pi}{30}\right)^2 I N} \quad (6.2)$$

then the new spool speed is obtained by Euler integration as

$$N_{new} = N_{last} + \left(\frac{dN}{dt}\right)_{last} \delta t \quad (6.3)$$

where N is the spool speed in rpm, I is the polar moment of inertia of the HP spool in kgm^2 , dN/dt is the HP spool acceleration rate in rpm/s and dt is the time step.

The algorithm that explains the transient process in the developed code is given in Figure 6.1.

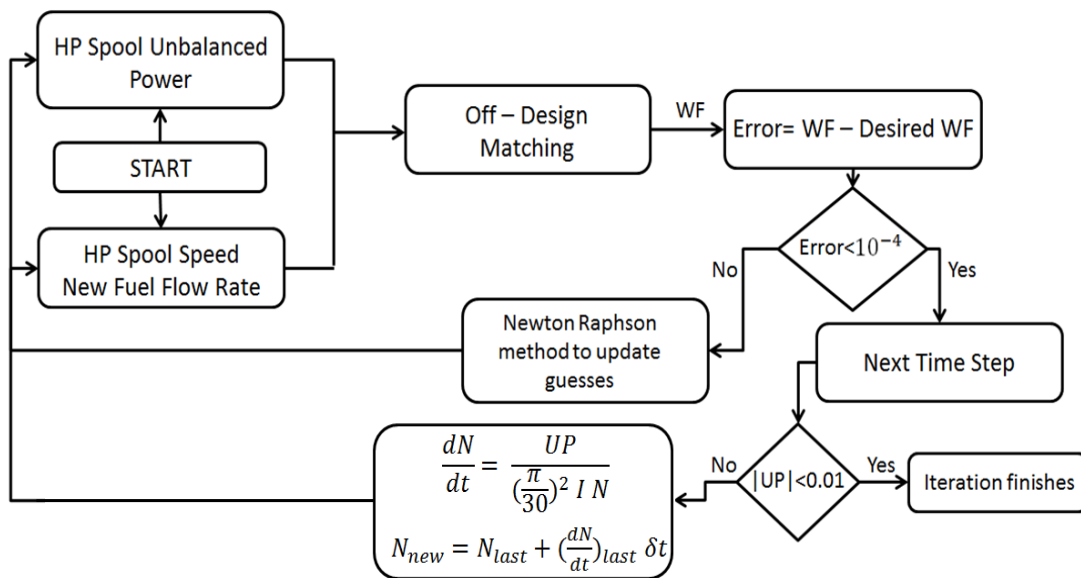


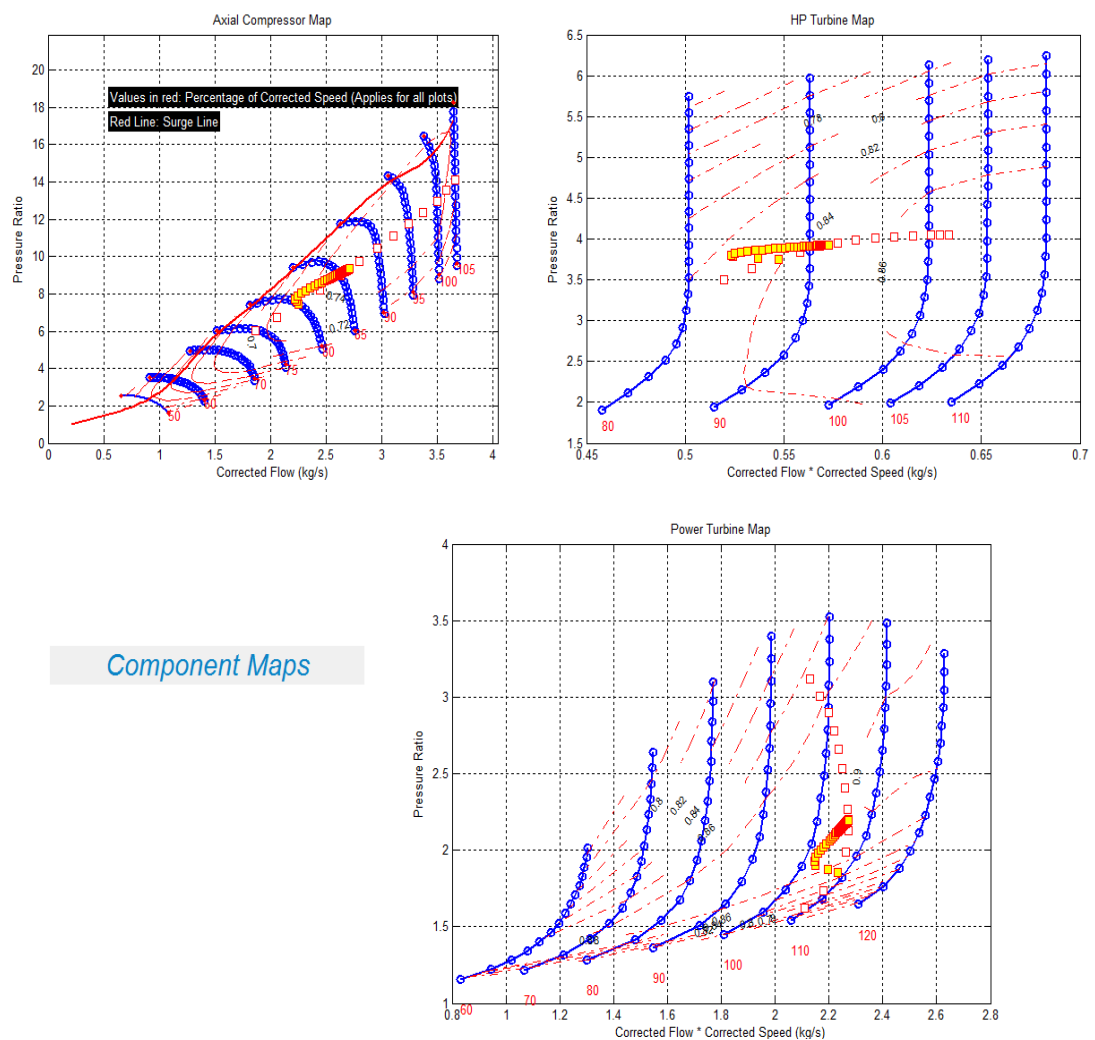
Figure 6.1 - Transient matching algorithm

The iteration process continues until the magnitude of the unbalanced power decreases to 0.01. After that, the new steady state operating point is reached with the

desired fuel value and the operation path of the transient performance estimation is plotted in the component maps. In addition, the following plots are obtained from the developed code:

- i) Burner exit temperature versus time elapsed
- ii) Turbine rotor inlet temperature versus time elapsed
- iii) Power turbine inlet temperature versus time elapsed
- iv) Gas generator spool speed versus time elapsed
- v) Unbalanced power versus time elapsed
- vi) Fuel flow rate versus time elapsed

The sample output is shown in Figure 6.2 and Figure 6.3.



Component Maps

Figure 6.2 - Sample output of transient performance on component maps

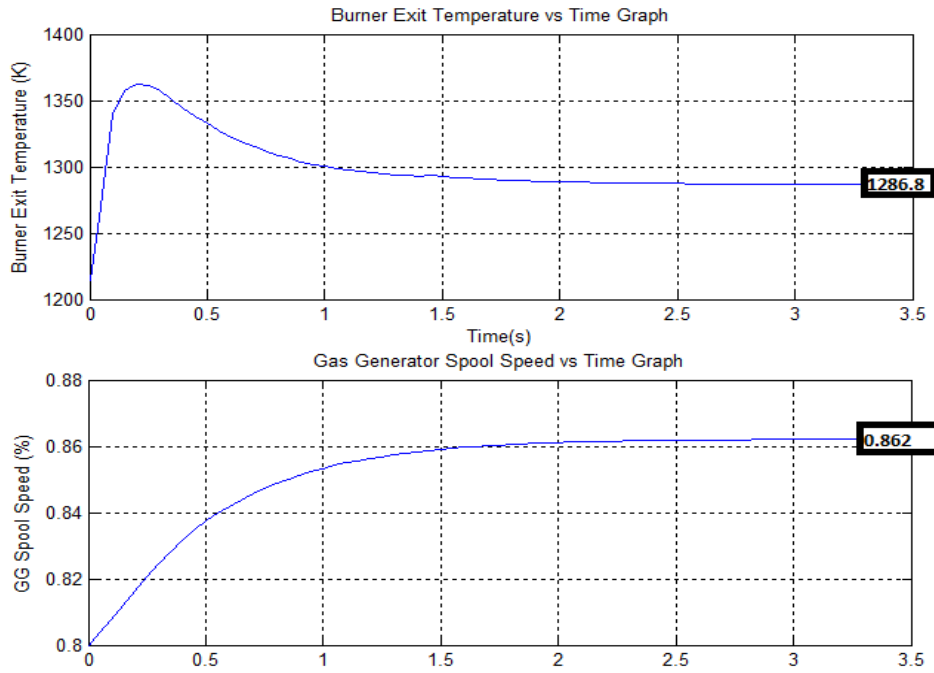


Figure 6.3 - Sample output of transient performance - output figures of Tt4 and Ncorr

There are differences between the results of the developed software and GasTurb 11 which can be seen in Figure 6.4. The difference between the results of these two softwares is mainly due to the different models used for the fuel pump. It can be seen in the temperature versus time elapsed graph given in Figure 6.4 that the increase in the temperature is more rapid in the developed software. This result cannot be interpreted as incorrect since the modeling of the fuel injection may differ from each other.

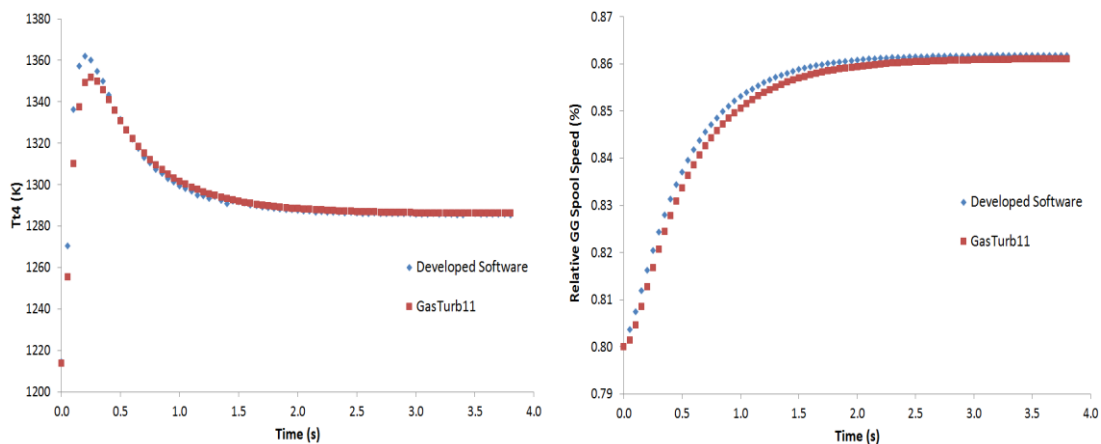


Figure 6.4 - Comparison of Tt4 and GG spool speed of GasTurb11 and the developed software

In the developed software, the formula used in the creation of the first order time lag model for the fuel pump is

$$WF = WF_i + (WF_f - WF_i) (1 - e^{-t/\tau}) \quad (6.4)$$

where WF_i is the fuel flow rate at initial state of transient, WF_f is the fuel flow rate at final state of transient, τ is the fuel pump time constant and t is the elapsed time after initialization of transient.

6.1 Heat Soakage Model

In transient estimations, there are two phenomena that significantly affect the engine performance, namely the heat soakage and volume packing (dynamics). There are large heat fluxes between the operating gas and the metal parts of the engine especially at the inlet of the HP turbine [13]. This results in a considerable variation in the engine performance and the operating gas temperature. The latter effect, volume packing, can be seen in the transient operation of the engine. The reason is that the mass flow at the inlet of a volume (such as a duct) is not equal to that of the exit of that volume during transient operation as the pressure and temperature (hence density) changes with respect to time. However, in order to introduce these effects, detailed geometrical and metallurgical data of the engine of interest or some empirical relationships that fits well to transient behavior of a specific engine are required. According to reference [5], Reynolds and Prandtl numbers dominantly affect the heat transfer coefficients and these coefficients are difficult to evaluate accurately. Hence, empirical correlation factors can be applied to match the model with the engine test data. Since the main interest of this thesis is generating a tool for a generic turboshaft engine, a basic heat soakage model is implemented in the code and the volume dynamics effects are not considered.

The heat transfer between the metal and the gas can be found by the following formula,

$$Q = h_{HT} A (T_{gas} - T_{metal}) \quad (6.5)$$

where h_{HT} is the heat transfer coefficient between the operating gas and the metal part, A is the area of where the heat transfer occurs, T_{gas} is the operating gas temperature and T_{metal} is the temperature of the metal part of the engine in between engine air stations 4 and 4.1.

In the developed software, this effect is modeled with the inputs of:

- Heat Transfer Constant
- Heat Soakage Time Constant

The maximum heat transfer between the gas and the metal is found by the following formula,

$$Q_{max} = HT_{const} \Delta T \quad (6.6)$$

where HT_{const} is used for the approximation of hA of the engine stations 4 and 4.1 and ΔT is the difference between the maximum gas temperature at the initial time and the steady-state gas temperature. The mentioned maximum gas temperature corresponds to the temperature that could be reached if the effects of the fuel pump and the heat soakage models are not included. Then approximation of the heat transfer is calculated by the following 1st order time lag formula,

$$Q = Q_{max} e^{-t/HSTC} \quad (6.7)$$

where t is the time elapsed after initiation of the transient performance and HSTC is the heat soakage time constant which is an input from the user. Sample results with a heat soakage model can be seen in Section 7.2 in Figure 7.1 to Figure 7.2.

CHAPTER 7

COMPARISON OF THE DEVELOPED SOFTWARE RESULTS WITH THE LITERATURE

In addition to the comparison of the results of the developed software with the commercial tool GasTurb 11, comparison with the engine data available in the literature will enhance the reliability of the software. This also shows the progress of the software and the possible applicable improvements in it. The steady state performances are expected to well match with experimental data whereas small variations in the transient performance results may be acceptable due to two main error sources. The first one is the control system that maintains the power turbine speed at 100% relative speed. In the developed software, no control model is defined and it is assumed that the power turbine always operates at a constant relative speed during the transients. The second one is the absence of the volume dynamics and the coarse modelling of the heat soakage effect. The developed software is a generic performance estimation tool and these effects are very much dependent on the specific data of the engine of interest. The consideration of the application of these effects is discussed in the future work section.

7.1 Steady – State Performance Comparison

The steady-state performance estimation results of the software are compared with the available performance data of LHTEC CTS800-4N in FAA Certification in reference [37]. The engine is modeled with the developed software in the design mode with the help of some literature data as in reference [31]. In addition, the compressor map used in the off-design calculations is the digitized version of the compressor map in the same paper [31] whereas the turbine maps are the default maps in the software as mentioned in the map scaling section of this thesis. The

values of the shaft power and power turbine inlet temperature (PTIT) are presented in Table 7.1 with the HP Spool Speeds given in reference [37].

Table 7.1 - Comparison of certification data of LHTEC CTS800-4N with model in the developed software

Engine Ratings	N(rpm)	FAA		Developed Software		Difference (%)	
		Power(kW)	PTIT(K)	Power (kW)	PTIT (K)	Power (kW)	PTIT(K)
30 sec OEI	46681	1208	1251	1197	1249	0.89	0.18
2 min OEI	45556	1108	1201	1104	1206	0.38	0.40
COEI	44576	1014	1158	1008	1163	0.64	0.45
Takeoff	44576	1014	1178	1008	1163	0.64	1.26
Max Cont	43983	955	1134	943	1135	1.32	0.07
AVERAGE						0.78	0.47

Average differences of 0.78 % and 0.47 % in the power and power turbine inlet temperatures respectively, show that the model matches well with the certification data and the software can be used in the estimation of the on and off design performance of the CTS800-4N engine.

7.2 Transient Performance Comparison

The transient performance estimation capability of the developed software is compared with the simulation results of reference [13]. In this reference paper, there is a comparison of a developed real time model of the T700 engine of General Electric with the NASA Lewis simulation. The latter simulation is also validated with the NASA Lewis experimental test engine and referenced in the same paper. The models mentioned in this paper are embedded with the heat sink and volume dynamics approximations with the constants developed specifically for the T700 engine. In reference [38], the digitized T700 engine map is available and this map is used in the transient performance estimation in the developed software. The transient scenario used in this comparison is that the fuel flow of the engine is increased from 400 lbm to 775 lbm per hour (step increase). Resultant turbine inlet temperatures and the relative spool speeds are given in Figure 7.1 and Figure 7.2.

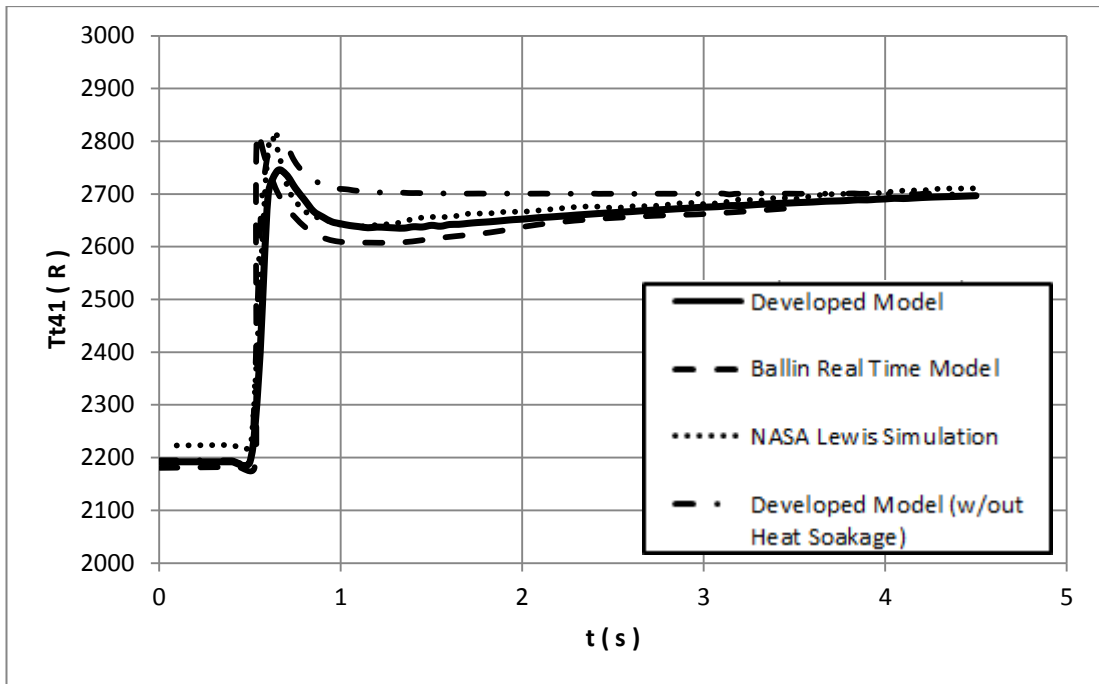


Figure 7.1 - HP turbine inlet temperature versus time elapsed

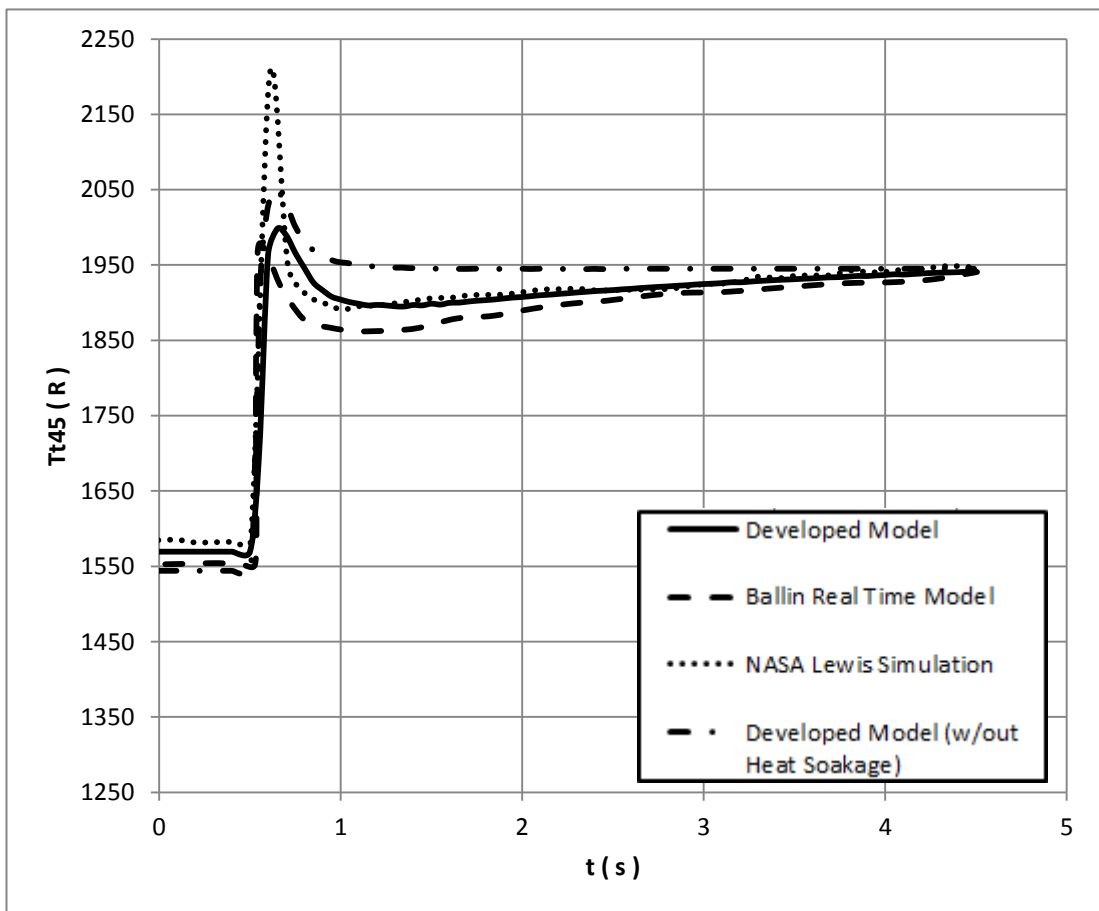


Figure 7.2 - Power turbine inlet temperature versus time elapsed

There are some deviations mainly due to the different heat soakage and volume dynamics approaches in between the simulation models. The constructed models are developed in 100% corrected speed at the developed software, and then gas generator speed values are reduced to nearly 90% of the corrected speed in the off-design calculation module. In this kind of preliminary design calculations, the important examination of the transient applications are the initial and final points of the transient scenario. In other words, if the initial and final parameters (steady-state values with considering the elapsed time after initiation of the transient) of the transient scenario match well with real application results, this software can be categorized as sufficient for preliminary design transient estimations. The difference at the initial part of the transients is caused by the differences in the approximations of the off-design performances of the engine. However, it is seen that there are not any huge differences in these parts in between simulation models. In the two figures above, there are differences in temperature values at some portions of the transients. However, as mentioned before, these variations are due to the different modeling of the heat soakage and volume dynamics in between the models and are not considered in the cycle design phase of the turboshaft engine.

However, as expected, similar trends in transient performances can be seen in Figure 7.1 and Figure 7.2. In addition, properties at steady state performances (i.e. at $t = 0$ s and $t = 5$ s) nearly match with each other, which implies that the developed model matches well with the engine. Furthermore, the effect of the heat transfer to the engine walls can be seen in the models. In the developed model without heat soakage effect, the temperature values are a bit higher at the first part of the transient. After consideration of this effect and the implementation of the model of the heat soakage, the results match more with the available data in the literature as seen in the same figures.

CHAPTER 8

CONCLUSIONS AND FUTURE WORK

8.1 Conclusion

The purpose of this thesis is to develop a computer software to carry out on and off-design performance predictions of a turboshaft engine along with the dynamic analysis. With these abilities of the developed software, the cycle of the engine can be designed in an optimum way to accomplish the previously defined missions for the aircraft.

The design point (on-design) engine performance analysis starts with the design choices. The importance of the preliminary design is usually high because when the calculations proceed further, it may be hard to revive those initial steps in the design of an engine. Therefore, the design point calculations are needed to be carried out carefully and lots of different designs should be compared with each other to find the optimum cycle design of a turboshaft engine. With this aim, firstly the design point and the parametric study modes of the software are developed in order to compare the design points which satisfy the requirements of the engine and select the optimum one. Inside these modes, there are options for efficiency estimations for the components of the turboshaft. These options result in better approximations of real cycles in different pressure ratios, rotational speeds etc. In order to check the accuracy of the developed tool, the results of the software are compared with the results of the commercial product Gasturb11 for the same conditions and inputs. The deviations in results are only 0.1-0.2%, indicating a high accuracy has been obtained.

The software should also carry on the off-design analysis in order to find out whether the designed engine is capable of overcoming every mission in its defined mission profiles or not. The reference compressor and turbine maps have been used in the

off-design performance calculations with the technique of map scaling. Iterations for the component matching are carried out by the Newton-Raphson parameter updating method. The operating line of the engine can be investigated in this mode. In addition, the handling bleed and the inlet distortion effect can be simulated in the off-design mode. These effects are important in application because operating lines differ from each other significantly if these effects are taken into consideration and it should be noted that these effects may result in varying the fundamental parameters of the engine design during the preliminary studies. In addition to the comparison of the results with Gasturb11, the LHTEC CTS800-4N is modeled in the developed software and the off-design results are compared with its certification data. It is seen that the results match well and off-design model is validated satisfactorily.

In the transient model of the turboshaft engine, the fuel pump is modeled with a delay and the heat soakage effect is introduced whereas the power turbine speed is kept constant. With the knowledge of how much additional fuel is exerted and the value of the inertia of the gas generator spool, corresponding behavior of the designed engine can be seen in component maps as an output. In addition, change in some important parameters of the designed engine with time can be seen in the main screen of the transient mode of the developed software. The results are compared with the commercially available tool Gasturb11 and presented in the related chapter. Furthermore, the GE T700 turboshaft model is developed in the software and a sample transient scenario is applied. The results are then compared with the available literature data and it is proved that acceptable levels of accuracy are reached.

To conclude, a computer software that can model the turboshaft engine with features of design, off-design and transient performance estimation is developed for the use of performance engineers. The reliability of the developed software is also validated with comparison to the available literature data and the available commercial software Gasturb 11.

8.2 Future Work

Although the developed software has reached to an agreement with the available engine data, there are some points to be improved.

Firstly, the iteration time may be shortened by improving the Newton – Raphson iteration scheme with the Broyden update model. Since there are small differences in the off-design simulation times, shorter time targets can be reached especially in transient matching.

Secondly, the control algorithm for the power turbine may be embedded into the code. By changing gas generator speeds of the designed turboshaft engine, in real applications, the engine control responses to keep the power turbine speed constant. However, after the initial application of the fuel, there will be fluctuations in the power turbine speed, which is not the case in the model in the software developed.

Another possible improvement is that the mean line analysis may be introduced to the software for a more detailed design of the turboshaft engine. The compressor and turbine 1D mean-line codes will be useful for the determination of the main gas path and the estimation of the pressure ratios in addition to the efficiency levels. However, it is seen in the literature that, instead of using these codes, fundamental efficiency estimation modes as in the developed software may be sufficient for the estimation of the cycle design performance.

Lastly, there may be an additional mode for the detailed modeling of the heat soakage and volume dynamics effects which can be used to update the resulting behavior of the engine in transients as in reference [13]. This can be done by introducing the detailed inputs required for the detailed simulation of the engine transients.

REFERENCES

- [1] "Airliners," [Online]. Available: http://www.airliners.net/aviation-forums/tech_ops/read.main/171102/. [Accessed 22 05 2015].
- [2] H. Saravanamuttoo, H. Cohen and G. Rogers, Gas Turbine Theory, Pearson Education Limited, 2001.
- [3] M. P.Boyce, Gas Turbine Engineering Handbook, Oxford: Gulf Professional Publishing, 2006.
- [4] T. Giampaolo, Gas Turbine Handbook Principles and Practice, Lilburn: The Fairmont Press,Inc., 2009.
- [5] P. Walsh and P. Fletcher, Gas Turbine Performance, Oxford, UK: Blackwell Science Ltd., 2004.
- [6] J. D. Mattingly, W. H. Heiser and D. T. Pratt, Aircraft Engine Design, Reston: American Institute of Aeronautics and Astronautics, Inc., 2002.
- [7] E. Thirunavukarasu, "Modelling and Simulation Study of a Dynamic Gas Turbine System in a Virtual Test Bed Environment (Master's Thesis)," 2013. [Online]. Available: <http://scholarcommons.sc.edu/etd/2254>.
- [8] J. Kurzke, "Advanced User-Friendly Gas Turbine Performance Calculations on the Personal Computer," in *ASME 95-GT-147*, 1995.
- [9] J. Kurzke, "GasTurb11 Program and Manual," Germany, 2007.
- [10] C. Kong and J. Ki, "Performance Simulation of Turboprop Engine for Basic Trainer," in *Proceedings of ASME TURBO EXPO 2001 Land, Sea & Air*, Louisiana, 2001.
- [11] H. Wemming, "Validation and Integration of a Rubber Engine Model into an MDO Environment (Master's Thesis)," *Linköping University*, 2010.

- [12] J. Martinjako, "Low Cost Gas Turbine Off-Design Prediction Technique (Master's Thesis)," *Arizona State University*, 2014.
- [13] M. G. Ballin, "A High Fidelity Real-Time Simulation of a Small Turboshaft Engine," *NASA Technical Memorandum*, 1988.
- [14] G. Koçer, "Aerothermodynamic Modelling and Simulation of Gas Turbines for Transient Operating Conditions (Master's Thesis)," *METU*, 2008.
- [15] Y. Novikov, "Development of a High-Fidelity Transient Aerothermal Model for a Helicopter Turboshaft Engine for Inlet Distortion and Engine Deterioration Simulations (Master's Thesis)," *METU*, 2012.
- [16] A. Alexiou and K. Mathioudakis, "Development of a Turbofan Performance Model Using A Generic Simulation Tool," in *ASME Turbo Expo 2005: Power for Land, Sea and Air*, Nevada, 2005.
- [17] A. Lazzaretto and A. Toffolo, "Analytical and Neural Network Models for Gas Turbine Design and Off-Design Simulation," *Int.J. Applied Thermodynamics*, vol. 4, 2001.
- [18] K. E. Shahroudi, "Development and Validation of a Computer Assisted Design Methodology for Gas-Turbine-Based Aircraft Engines," *Delft University of Technology*, 1994.
- [19] V. Panov, "GasTurboLib - Simulink Library For Gas Turbine Engine Modelling," in *ASME Turbo Expo 2009: Power for Land, Sea and Air*, Orlando, 2009.
- [20] G. D. Garrard, "ATEC: The Aerodynamic Turbine Engine Code for the Analysis of Transient and Dynamic Gas Turbine Engine System Operations (Ph.D Thesis)," *The University of Tennessee*, 1995.
- [21] W. P. J. Visser, "Generic Analysis Methods for Gas Turbine Engine Performance - The development of the gas turbine simulation program GSP," 2014.

- [22] J. Janikovič, "Gas Turbine Transient Performance Modeling for Engine Flight Path Cycle Analysis (PhD Thesis)," *Cranfield University*, 2010.
- [23] J. Kurzke, *Aero-Engine Design: A State of the Art*, Rhode Saint Genese , Belgium: von Karman Institute, 2003.
- [24] U.S Standard Atmosphere, Washington, D.C.: U.S Government Printing Office, 1976.
- [25] A. J. Glassman, "Users Manual for Updated Computer Code for Axial-Flow Compressor Concetpual Design," NASA, Toledo, Ohio, 1992.
- [26] R. H. Aungier, *Centrifugal Compressors - A Strategy for Aerodynamic Design and Analysis*, New York: ASME Press, 2000.
- [27] W. L. Stewart, "A Study of Axial-Flow Turbine Efficiency Characteristics in Terms of Velocity Diagram Parameters," *ASME Publication*, 1962.
- [28] H. G. Münzberg and J. Kurzke, *Gasturbinen-Betriebsverhalten und Optimierung*, Berlin-Heidelberg-New York: Springer-Verlag, 1977.
- [29] S. F. Smith, Afraes and Ma, "A Simple Correlation of Turbine Efficiency," *Journal of the Royal Aeronautical Society*, vol. 69, 1965.
- [30] C. Kong, S. Lim and K. Kim, "A Study on Generation of Gas Turbine Component Maps Using Performance Test Data," in *27th International Congress of the Aeronautical Sciences*, 2010.
- [31] D. L. Palmer and W. F. Waterman, "Design and Development of an Advanced Two-Stage Centrifugal Compressor," *Journal of Turbomachinery, ASME*, 1995.
- [32] R. H. Aungier, *Axial-Flow Compressors - A Strategy for Aerodynamic Design and Analysis*, New York : ASME Press, 2003.
- [33] J. Kurzke, "Effects of Inlet Flow Distortion on the Performance of Aircraft Gas Turbines," *ASME Turbo Expo 2006: Power for Land, Sea and Air*, 2006.
- [34] D. D. Williams, "Review of Current Knowledge on Engine Response to

Distorted Inflow Conditions in: Engine Response to Distorted Inflow Conditions," *AGARD Conference Proceedings*, 1986.

- [35] H. Pearson and A. B. McKenzie, "Wakes in Axial Compressors," *Journal of the Royal Aeronautical Society*, vol. 63, pp. 415-416, 1959.
- [36] W. T. Cousins, "History, Philosophy, Physics and Future Directions of Aircraft Propulsion System/Inlet Integration," *ASME gt2004-53846*, 2004.
- [37] "Administration, Department of Transportation Federal Aviation - TYPE CERTIFICATE DATA SHEET," 2012.
- [38] J. M. Spack, *Linear parameter varying controller for a small turboshaft engine*, Boston: Northeastern University, 2011.
- [39] S. C. Chapra and R. P. Canale, *Numerical Methods for Engineers*, McGraw Hill, 2007.

APPENDIX A

NEWTON-RAPHSON ITERATION METHOD

One of the most widely used root finding methods is the Newton-Raphson iteration method.

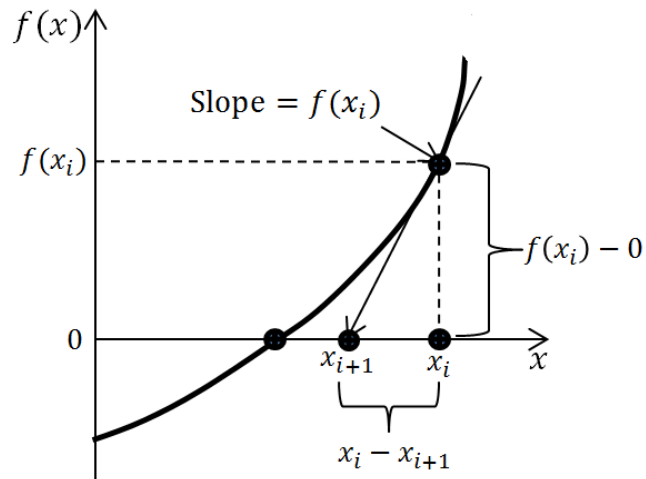


Figure A.1 – Newton-Raphson method

This method is derived from the geometrical interpretation of Figure A.1. The slope at x_i can be found by

$$f'(x_i) = \frac{f(x_i) - 0}{x_i - x_{i+1}} \quad (\text{A.1})$$

After rearranging,

$$x_{i+1} = x_i - \frac{f(x_i)}{f'(x_i)} \quad (\text{A.2})$$

This formula is called the Newton-Raphson formula [39]. In words, this method uses the tangent of the equation at the first point to find the root of the interested equation.

After numbers of iterations, the root can be found as long as the second derivative of the equation at any iteration point is not equal to zero.

In the developed software, since there are many equations linked together, taking the derivative of the equation is not a feasible way to reach a solution. Rather than this, step increases are applied to variables separately and the differences in errors are examined. To illustrate:

At first, assume the beta value of the compressor is equal to 0.5 and the corresponding four errors are 0.2, 0.1, 0.3 and 0.05. It is assumed that the beta value of the compressor is increased to 0.52 and the corresponding errors changes to 0.25, 0.15, 0.25, and 0.03. The new beta value of the compressor is found by the procedure explained below.

At first, Jacobians should be found,

$$A(1) = \frac{0.25 - 0.2}{0.52 - 0.5} = 2.5 \quad (\text{A.3})$$

$$A(2) = \frac{0.15 - 0.1}{0.52 - 0.5} = 2.5 \quad (\text{A.4})$$

$$A(3) = \frac{0.25 - 0.3}{0.52 - 0.5} = -2.5 \quad (\text{A.5})$$

$$A(4) = \frac{0.03 - 0.05}{0.52 - 0.5} = -1 \quad (\text{A.6})$$

The next step is to find how much change is required for beta by (assuming zero errors in other error parameters for only this example)

$$A.X = B \quad (\text{A.7})$$

where A is the matrix of derivatives and the B matrix contains the error values. The X matrix gives how much change in the examined variable is needed.

Different than this sample procedure, all variables affect the errors so that this procedure should be applied simultaneously for all variables by constructing the matrices and all of the variables updated accordingly in one calculation step of the off-design iterations.

APPENDIX B

SCREENSHOTS OF THE DEVELOPED SOFTWARE

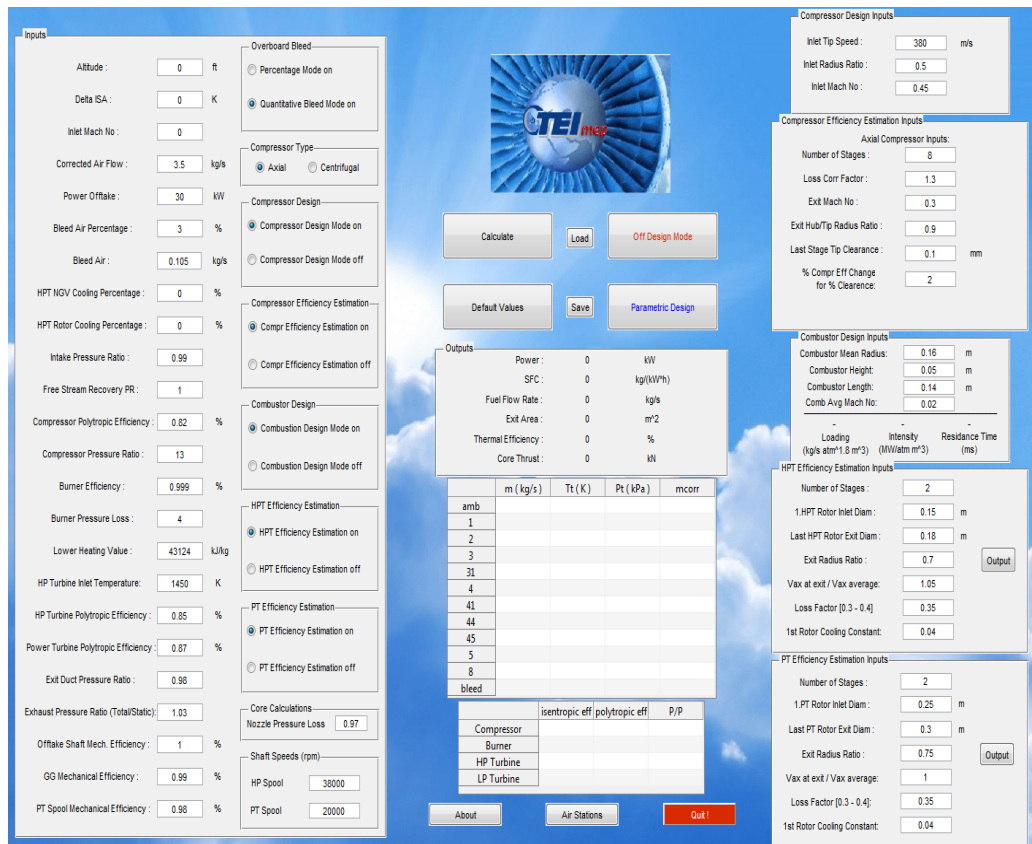


Figure B. 1 - TEImep home page

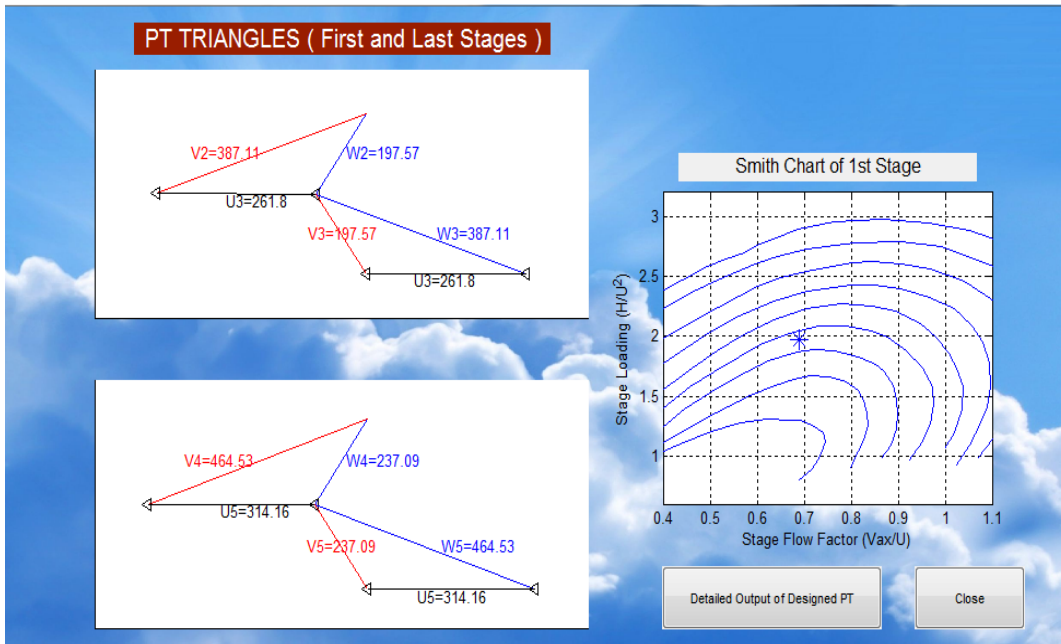


Figure B. 2 - TEImep turbine module

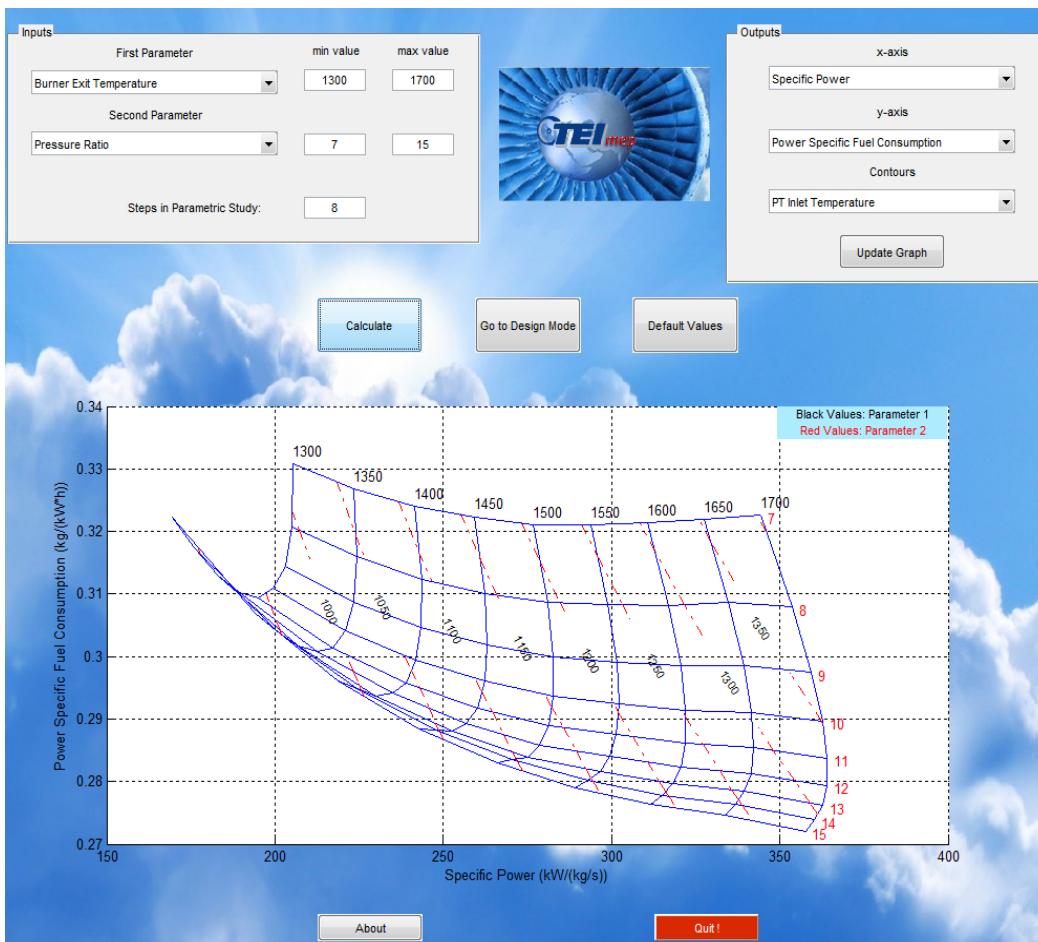


Figure B. 3 - TEImep parametric study

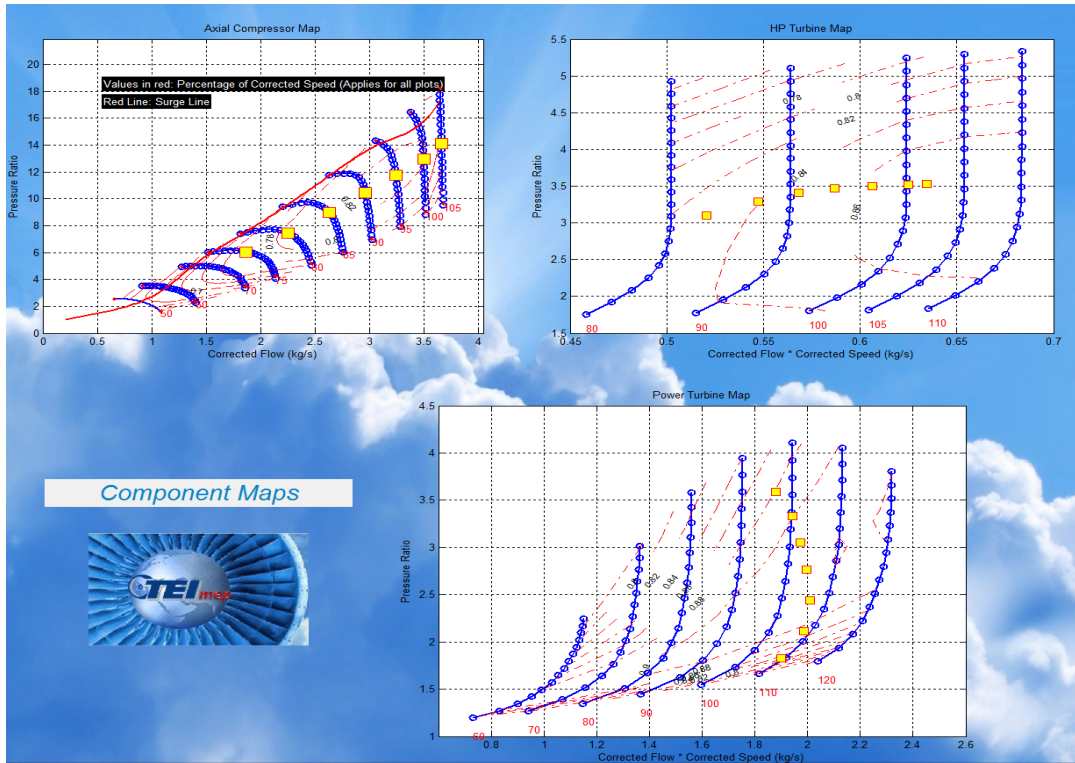


Figure B. 4 - TEImep operating line sample result

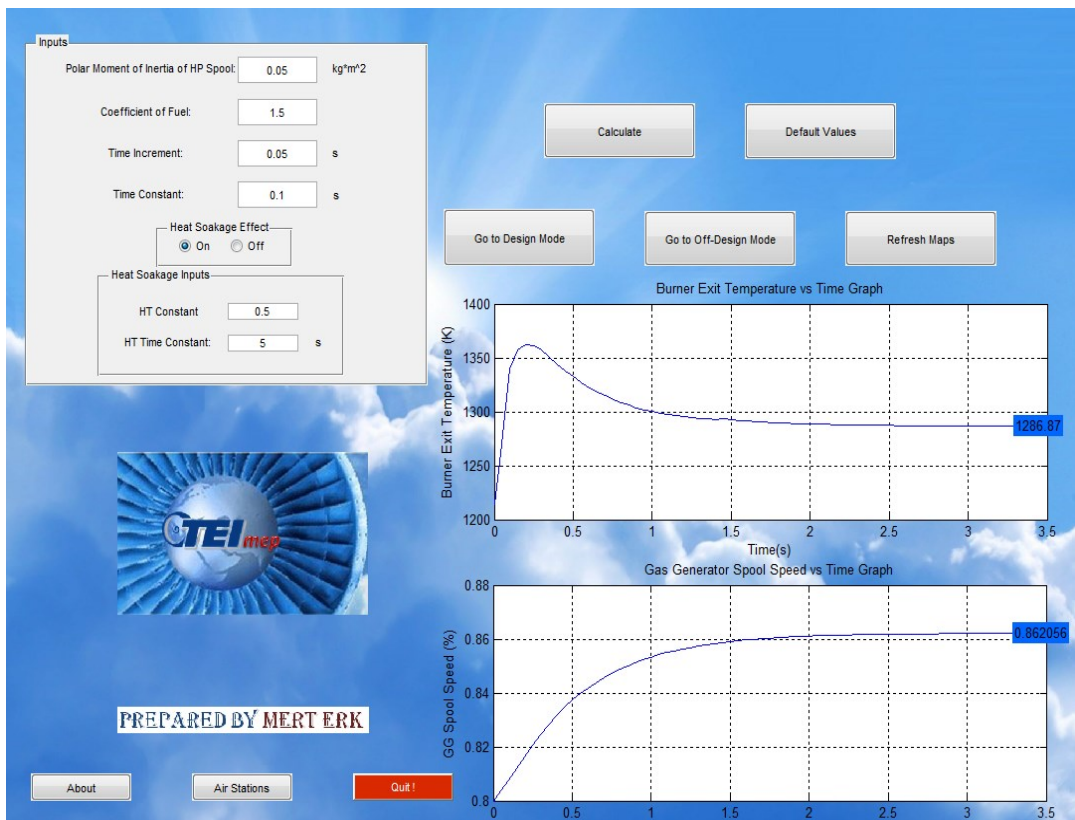


Figure B. 5 - TEImep transient sample screenshot

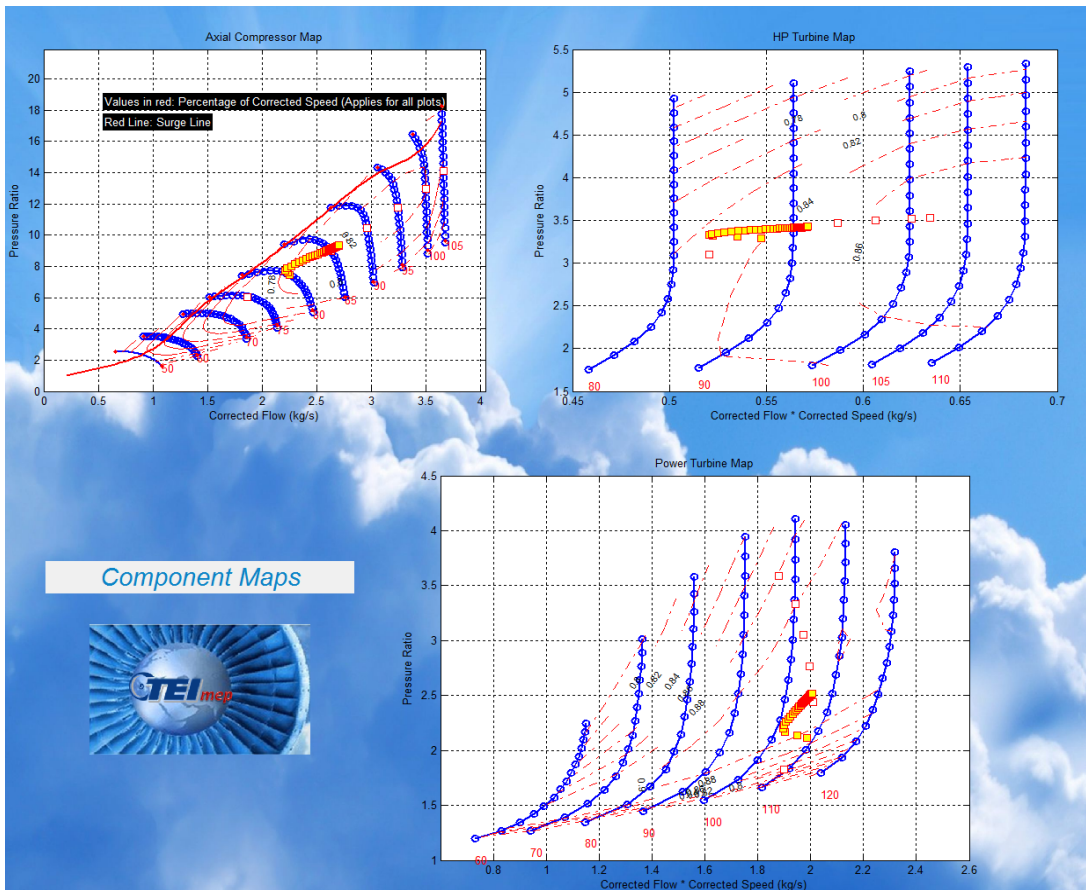


Figure B. 6 - Transient sample map result